

~~ENGINEERING~~

The person charging this material is responsible for its return to the library from which it was withdrawn on or before the **Latest Date** stamped below.

Theft, mutilation, and underlining of books  
are reasons for disciplinary action and may  
result in dismissal from the University.

UNIVERSITY OF ILLINOIS LIBRARY AT URBANA-CHAMPAIGN

APR 18 1976

MAR 28 1976

L161—O-1096





A very faint, light gray watermark-like image of classical architecture is visible in the background. It features four prominent Corinthian columns supporting a horizontal beam or entablature, with a triangular pediment above. The entire structure is set against a dark, textured background.

Digitized by the Internet Archive  
in 2013

<http://archive.org/details/dielectriccoated34week>

ANTENNA LABORATORY

Technical Report No. 34

DIELECTRIC COATED SPHEROIDAL RADIATORS

by

Walter L. Weeks\*

12 September 1958

Contract AF33(616)-3220  
Project No. 6(7-4600) Task 40572

Sponsored by:

WRIGHT AIR DEVELOPMENT CENTER

Electrical Engineering Research Laboratory  
Engineering Experiment Station  
University of Illinois  
Urbana, Illinois

\*Submitted in partial fulfillment of the requirements for the degree of Doctor of Philosophy in Electrical Engineering at the University of Illinois, 1958.



6.21.365

I 6 655te

78,34

14p.2

#### ACKNOWLEDGMENT

The author wishes to thank all of the members of the Antenna Laboratory staff for their help and encouragement, especially his advisor, Professor E.C. Jordan, P.E. Mayes and R.L. Carrel. Mr. T. Lahey also deserves special mention for his help in the preparation of the codes for the ILLIAC. Financial support for the investigations was provided by the Wright Air Development Center, under Contract AF 3220, for which the author is very grateful.



## ABSTRACT

Analytical methods are presented for the determination of the changes in the radiation patterns brought about by dielectric coatings on spheroidal radiators. A description is given of a machine computation system which makes the analytical results useful. This system includes a program for the semiautomatic calculation of the radiation patterns of spherical radiators, a practical method for the determination of the eigenvalues of all of the orders of the spheroidal functions which are needed to obtain convergent representations, and a new method for the calculation of the spheroidal "radial" functions. Numerical results are included for spheres and prolate spheroids, having sizes of the order of several wavelengths, which are excited by axially symmetric slots.

The effects of the dielectric coating are most marked when the excitation is latitudinally asymmetric. One typical effect is an increase in radiation in the general direction of the poles. For spherical radiators, the important effects show a complicated dependence on the size of the radiator and the value of the permittivity. Comparison of the patterns of the coated prolate spheroidal radiators herein calculated with the patterns of spherical radiators indicates that the effects are similar in both cases.



## CONTENTS

	Page
1. Introduction	1
2. Spheroids with Axially Symmetric Excitation	7
2.1 Symmetrically Excited Spheres	11
2.1.1 Boundary Value Problem of the Conducting Sphere (no coating)	14
2.1.2 Boundary Value Problem of the Coated Conducting Sphere	16
2.1.3 Numerical Computations Associated with the Spherical Radiator	22
2.2 Symmetrically Excited Prolate Spheroids	31
2.2.1 Conducting Prolate Spheroid without Dielectric Coating	34
2.2.2 Conducting Prolate Spheroid with Dielectric Coating	37
2.2.3 Numerical Calculations Associated with Prolate Spheroidal Radiators	42
3. Sphere with Arbitrary Source Configuration	59
3.1 The Slot Excited Conducting Sphere in Free Space	62
3.2 The Slot Excited Conducting Sphere Coated with Dielectric	67
4. Summary and Recommendations for Further Work	73
References	136
Appendix A	138
Appendix B	146



## ILLUSTRATIONS

Figure Number		Page
1	Basic Antenna	1
2	Coordinate System	7
3	Spherical Coordinate System	12
4	Spherical Radiator	17
5	Dielectric Coated Spherical Radiator	17
6	Simplified Flow Diagram for Radiation Pattern Calculations (Spherical Radiator)	27
7	Prolate Spheroidal Coordinate System	32
8	Spheroidal Radiator	36
9	Spheroidal Radiator with Dielectric Coating	36
10	Simplified Flow Chart for Machine Calculation of Spheroidal V-Functions	48
11	Simplified Flow Chart for Calculation of the Spheroidal U-Functions	52
12	Slot Excited Spherical Radiator with Dielectric Coating	66
13	Radiation Patterns, $H_\phi$ vs. $\theta$ , of Spherical Antennas with Different Conducting Sphere Radii $r_i$ , Excited by Equatorial Slot. Patterns on Left Are with No Coating. Patterns on Right Are with Coating, Thickness $.05\lambda$ , $\epsilon_r = 3$	84
14	Continuation of Figure 13	85
15	Radiation Patterns, $H_\phi$ vs, $\theta$ of Spherical Antennas with Different Conducting Sphere Radii, $r_i$ , Excited by Slot at $160^\circ$ Latitude. Patterns on Left Are with No Coating, Patterns on Right Are with Coating. Thickness $.1\lambda$ , $\epsilon = 2.25$	86
16	Radiation Patterns, $H_\phi$ vs $\theta$ , of Spherical Antennas with Different Conducting Sphere Radii, $r_i$ , Excited by Slot at $160^\circ$ Latitude. Patterns on Left Are With no Coating. Patterns on Right Are With Coating. Thickness $.1\lambda$ , $\epsilon = 2.25$	87



## ILLUSTRATIONS (CONTINUED)

iv

17	Radiation Patterns, $H_\phi$ vs $\theta$ , of Coated Spherical Antenna, $r/\lambda = 1.51$ , Coating Thickness $.1\lambda$ , for Different Values of Dielectric Constant Slot at $160^\circ$ .	88
18	Radiation Patterns, $H_\phi$ vs $\theta$ , of Coated Spherical Antenna, $r/\lambda = 1.51$ , Coating Thickness $.1\lambda$ , for Different Values of Dielectric Constant Slot at $160^\circ$ .	89
19	Radiation Patterns, $H_\phi$ vs. $\theta$ , of Coated Spherical Antennas, $r/\lambda = 1.51$ , Dielectric Constant $\epsilon = 2.56$ , for Different Coating Thicknesses. Slot at $160^\circ$ .	90
20	Radiation Patterns, $H_\phi$ vs. $\theta$ , of Coated Spherical Antennas, $r/\lambda = 1.51$ , Dielectric Constant $\epsilon = 2.56$ , for Different Coating Thicknesses. Slot at $160^\circ$ .	91
21	Prolate Spheroid Radiation Patterns (One Half Symmetric Patterns) $\beta_0 \ell = 3, \epsilon = \sqrt{4/3}$ , $H_\phi$ vs. $\theta$	92
22	Prolate Spheroid Radiation Patterns $\beta_0 \ell = 5, \epsilon_r = \sqrt{8/3}$ for Different Slot Patterns, $H_\phi$ vs. $\theta$	93
23	Prolate Spheroid Radiation Patterns $\beta_0 \ell = 5, \epsilon_r = \sqrt{8/3}$ for Different Slot Patterns, $H_\phi$ vs. $\theta$	94
24	Prolate Spheroidal Radiation Patterns, $\beta_0 \ell = 8, H_\phi$ vs. $\theta$	95
25	Prolate Spheroidal Radiation Patterns, $\beta_0 \ell = 8, H_\phi$ vs. $\theta$	96
26	Prolate Spheroidal Radiation Patterns, $\beta_0 \ell = 5, 12,$ $H_\phi$ vs. $\theta$	97
27	Prolate Spheroidal Radiation Patterns, $\beta_0 \ell = 5, 12,$ $H_\phi$ vs. $\theta$	98
28	A Graph of the Quantity $\frac{1}{\hat{H}_n'(2\pi r/\lambda)^2}$ , which Indicates Quasi-Resonances and Sets the Rate of Convergence in the Field Expansions in Spherical Coordinates.	99
29	$[\hat{H}_n'(2\pi r/\lambda)]^{-1}$ as a Function of $n$ .	100
30	$[\hat{H}_n'(2\pi r/\lambda)]^{-1}$ as a Function of $n$ .	101
31	$[\hat{H}_n'(2\pi r/\lambda)]^{-1}$ as a Function of $n$ .	102
32	$[\hat{H}_n'(2\pi r/\lambda)]^{-1}$ as a Function of $n$ .	103



## ILLUSTRATIONS (CONTINUED)

33	$[\hat{H}_n'(2\pi r/\lambda)]^{-1}$ as a Function of n.	104
34	$[\hat{H}_n'(2\pi r/\lambda)]^{-1}$ as a Function of n.	105
35	$[\hat{H}_n'(2\pi r/\lambda)]^{-1}$ as a Function of n.	106
36	$[\hat{H}_n'(2\pi r/\lambda)]^{-1}$ as a Function of n.	107
37	$[\hat{H}_n'(2\pi r/\lambda)]^{-1}$ as a Function of n.	108
38	$[\hat{H}_n'(2\pi r/\lambda)]^{-1}$ as a Function of n.	109
39	$[\hat{H}_n'(2\pi r/\lambda)]^{-1}$ as a Function of n.	110
40	Ratio of Coefficients, $c_n$ , in the Field Expansion for the Coated Spherical Radiator to the Coefficients $a_n$ in the Expansion for the Uncoated Spherical Radiator with the Same Excitation ( $g = r/\lambda$ ) Coating Thickness $.1\lambda \epsilon = 2.25$	111
41	Ratio of Coefficients, $c_n$ , in the Field Expansion for the Coated Spherical Radiator to the Coefficients $a_n$ in the Expansion for the Uncoated Spherical Radiator with the Same Excitation ( $g = r/\lambda$ ) Coating Thickness $.1\lambda \epsilon = 2.25$	112
42	Ratio of Coefficients, $c_n$ , in the Field Expansion for the Coated Spherical Radiator to the Coefficients $a_n$ in the Expansion for the Uncoated Spherical Radiator with the Same Excitation, ( $g = r/\lambda$ ) Coating Thickness $.1\lambda \epsilon = 2.25$	113
43	Ratio of Coefficients, $c_n$ , in the Field Expansion for the Coated Spherical Radiator to the Coefficients $a_n$ in the Expansion for the Uncoated Spherical Radiator with the Same Excitation, ( $g = r/\lambda$ ). Coating Thickness $.1\lambda \epsilon = 2.25$	114
44	Ratio of Coefficients, $c_n$ , in the Field Expansion for the Coated Spherical Radiator to the Coefficients $a_n$ in the Expansion for the Uncoated Spherical Radiator with the Same Excitation, ( $g = r/\lambda$ ). Coating Thickness $.1\lambda \epsilon = 2.5$	115
45	Ratio of Coefficients, $c_n$ , in the Field Expansion for the Coated Spherical Radiator to the Coefficients $a_n$ in the Expansion for the Uncoated Spherical Radiator with the Same Excitation, ( $g = r/\lambda$ ). Coating Thickness $.1\lambda \epsilon = 2.25$	116



## ILLUSTRATIONS (CONTINUED)

- 46 Ratio of Coefficients,  $c_n$ , in the Field Expansion for the Coated Spherical Radiator to the Coefficients,  $a_n$ , in the Expansion for the Uncoated Spherical Radiator with the Same Excitation, ( $g = r/\lambda$ ). Coating Thickness  $.1\lambda \epsilon = 2.25$  117
- 47 Ratio of Coefficients,  $c_n$ , in the Field Expansion for the Coated Spherical Radiator to the Coefficients,  $a_n$ , in the Expansion for the Uncoated Spherical Radiator with the Same Excitation, ( $g = r/\lambda$ ). Coating Thickness  $.1\lambda \epsilon = 2.25$  118
- 48 Ratio of Coefficients,  $c_n$ , in the Field Expansion for the Coated Spherical Radiator to the Coefficients,  $a_n$ , in the Expansion for the Uncoated Spherical Radiator with the Same Excitation, ( $g = r/\lambda$ ). Coating Thickness  $.1\lambda \epsilon = 2.25$  119
- 49 Ratio of Coefficients,  $c_n$ , in the Field Expansion for the Coated Spherical Radiator to the Coefficients,  $a_n$ , in the Expansion for the Uncoated Spherical Radiator with the Same Excitation, ( $g = r/\lambda$ ). Coating Thickness  $.1\lambda \epsilon = 4$  120
- 50 Ratio of Coefficients,  $c_n$ , in the Field Expansion for the Coated Spherical Radiator to the Coefficients,  $a_n$ , in the Expansion for the Uncoated Spherical Radiator with the Same Excitation, ( $g = r/\lambda$ ). Coating Thickness  $.1\lambda \epsilon = 4$  121
- 51 Ratio of Coefficients,  $c_n$ , in the Field Expansion for the Coated Spherical Radiator to the Coefficients,  $a_n$ , in the Expansion for the Uncoated Spherical Radiator with the Same Excitation, ( $g = r/\lambda$ ). Coating Thickness  $.1\lambda \epsilon = 4$  122
- 52 Ratio of Coefficients,  $c_n$ , in the Field Expansion for the Coated Spherical Radiator to the Coefficients,  $a_n$ , in the Expansion for the Uncoated Spherical Radiator with the Same Excitation, ( $g = r/\lambda$ ). Coating Thickness  $.1\lambda \epsilon = 4$  123
- 53 Ratio of Coefficients,  $c_n$ , in the Field Expansion for the Coated Spherical Radiator to the Coefficients,  $a_n$ , in the Expansion for the Uncoated Spherical Radiator with the Same Excitation, ( $g = r/\lambda$ ). Coating Thickness  $.1\lambda \epsilon = 4$  124



## ILLUSTRATIONS (CONTINUED)

54	Ratio of Coefficients, $c_n$ , in the Field Expansion for the Coated Spherical Radiator to the Coefficients, $a_n$ , in the Expansion for the Uncoated Spherical Radiator with the Same Excitation, ( $g = r/\lambda$ ). Coating Thickness $.1\lambda \epsilon = 6.25$	125
55	Ratio of Coefficients, $c_n$ , in the Field Expansion for the Coated Spherical Radiator to the Coefficients, $a_n$ , in the Expansion for the Uncoated Spherical Radiator with the Same Excitation, ( $g = r/\lambda$ ). Coating Thickness $.1\lambda \epsilon = 6.25$	126
56	Ratio of Coefficients, $c_n$ , in the Field Expansion for the Coated Spherical Radiator to the Coefficients, $a_n$ , in the Expansion for the Uncoated Spherical Radiator with the Same Excitation, ( $g = r/\lambda$ ). Coating Thickness $.1\lambda \epsilon = 6.25$	127
57	Ratio of Coefficients, $c_n$ , in the Field Expansion for the Coated Spherical Radiator to the Coefficients, $a_n$ , in the Expansion for the Uncoated Spherical Radiator with the Same Excitation, ( $g = r/\lambda$ ). Coating Thickness $.1\lambda \epsilon = 6.25$	128
58	Ratio of Coefficients, $c_n$ , in the Field Expansion for the Coated Spherical Radiator to the Coefficients, $a_n$ , in the Expansion for the Uncoated Spherical Radiator with the Same Excitation, ( $g = r/\lambda$ ). Coating Thickness $.1\lambda \epsilon = 6.25$	129
59	Ratio of Coefficients, $c_n$ , in the Field Expansion for the Coated Spherical Radiator to the Coefficients, $a_n$ , in the Expansion for the Uncoated Spherical Radiator with the Same Excitation. $\epsilon = 2.25$ , $r = 1.6$ . Thickness $t/\lambda$ Varied in Successive Graphs	130
60	Ratio of Coefficients, $c_n$ , in the Field Expansion for the Coated Spherical Radiator to the Coefficients, $a_n$ , in the Expansion for the Uncoated Spherical Radiator with the Same Excitation. $\epsilon = 2.25$ , $r = 1.6$ . Thickness $t/\lambda$ Varied in Successive Graphs	131
61	Ratio of Coefficients, $c_n$ , in the Field Expansion for the Coated Spherical Radiator to the Coefficients, $a_n$ , in the Expansion for the Uncoated Spherical Radiator with the Same Excitation. $\epsilon = 2.25$ , $r = 1.6$ . Thickness $t/\lambda$ Varied in Successive Graphs	132



## ILLUSTRATIONS (CONTINUED)

- 62 Ratio of Coefficients,  $c_n$ , in the Field Expansion for  
the Coated Spherical Radiator to the Coefficients,  $a_n$ ,  
in the Expansion for the Uncoated Spherical Radiator  
with the Same Excitation.  $\epsilon = 2.25$ ,  $r = 1.6$ . Thickness  
 $t/\lambda$  Varied in Successive Graphs  $\frac{t}{\lambda}$  133
- 63 Ratio of Coefficients,  $c_n$ , in the Field Expansion for  
the Coated Spherical Radiator to the Coefficients,  $a_n$ ,  
in the Expansion for the Uncoated Spherical Radiator  
with the Same Excitation.  $\epsilon = 2.25$ ,  $r = 1.6$ . Thickness  
 $t/\lambda$  Varied in Successive Graphs  $\frac{t}{\lambda}$  134



## LIST OF TABLES

Table Number		Page
1.	Scale Factors for Spheroidal Coordinate Systems	8
2.	Facsimile of a Typical ILLIAC Print Out of the Spheroidal Functions, U	55
3.	Comparison of the Coefficients Calculated from Different Numbers of Equations in the Coated Prolate Spheroid Problem	58
4.	Excitation Coefficients for an Axially Symmetric Slot in a Spherical Radiator	77
5.	Resonance and Convergence Factors for Spherical Radiators	78
6.	Numbers Which Indicate the Relative Importance of Dielectric Coatings on Spherical Radiators	79
7.	Eigenvalues of the Spheroidal Wave Function	80



LIST OF SYMBOLS

$A$	In section 2, introduction, auxiliary wave function, $A = h_\phi H_\phi$
$A_n$	Section 2.1.3, expansion coefficient in field expansions for spherical radiators
$B_k$	Symbol introduced to save writing, see definition pg. 40
$B'_k$	Symbol introduced to save writing, see definition pg. 40
$E$	Electric field intensity
$E_a$	Applied field, presumed to be known on the slot, zero elsewhere
$\bar{E}_r$	Electric field vector transverse to the radial coordinate in spherical coordinates
$\bar{E}_{ra}$	Applied field (known in the slot, zero elsewhere)
$E_u$	$u$ - component of electric field intensity
$E_v$	$v$ - component of electric field intensity
$E_{vr}$	$E_v$ in dielectric region
$E_{vf}$	$E_v$ in free space region
$H$	Magnetic field intensity
$\mathcal{H}$	Quantity which shows the distant field variation with angle
$H_\phi$	$\phi$ - component of magnetic field intensity
$H_{\phi I}$	$H_\phi$ in dielectric region
$H_{\phi II}$	$H_\phi$ in free space region
$\bar{H}_r$	Magnetic field vector transverse to the radial coordinate in spherical coordinates
$\hat{H}_n$	$(\frac{\pi z}{a})^{\frac{1}{2}} H_{n+\frac{1}{2}}(z) = \hat{J}_n(z) - j \hat{N}_n(z)$
$J_n$	Symbol in coated sphere calculation, defined pg. 26
$I_m$	Imaginary part of
$J_{n+\frac{1}{2}}$	Bessel function of the first kind, half integral order
$\hat{J}_n$	$(\frac{\pi z}{a})^{\frac{1}{2}} J_{n+\frac{1}{2}}$
$\hat{J}'_n$	$\frac{d \hat{J}_n(\beta r)}{d r}$ except in formulas, pg. 26
$L$	Symbol for matrix in spheroidal function eigenvalue calculation



LIST OF SYMBOLS (continued)

$L_{nm}$	Elements of the matrix $\mathcal{L}$ . The determinant of the matrix of these elements is equal to zero for the consistency of the set of equations for the expansion coefficients for the spheroidal functions
$N_{n+\frac{1}{2}}$	Bessel function of the second kind, half integral order
$\hat{N}_n$	$(\frac{\pi z}{2})^{\frac{1}{2}} N_{n+\frac{1}{2}}$
$\hat{N}'_n$	$\frac{\partial \hat{N}_n(\beta r)}{\partial r}$ except in formulas, pg. 26
$P_n^1$	Associated Legendre polynomial of order, $n$ , degree one
$P_n^m$	Associated Legendre function of the first kind
$Q_n^m$	Associated Legendre function of the second kind
$R$	Solution to radial differential equation in spherical coordinates
$R_e$	Real part of
$R_n$	Symbol in coated sphere calculation, defined pg. 26
$S$	$dS$ is element of area on the surface of a sphere
$T_{k_0}^m$	$P_n^m \times \left\{ \begin{array}{l} \cos m\phi \\ \sin m\phi \end{array} \right\}$ where upper subscript means even and goes with the $\cos m\phi$ in brackets, and lower subscript means odd and goes with the $\sin m\phi$ in brackets. When both are present, the symbol implies that both even and odd solutions are being considered
$U$	Solutions to differential equation involving the coordinate $u$
$U_{k_1}$	One independent solution to the differential equation in prolate spheroidal coordinate, $u$ (analogous to $J_n$ )
$U_{k_2}$	Second independent solution to the differential equation in the prolate spheroidal coordinate, $u$ (analogous to $\hat{N}_n$ )
$U_{k_3}$	Solution to the differential equation in the prolate spheroidal coordinate, $u$ , which satisfies the radiation condition (analogous to $\hat{H}_n$ )
$V$	Solution to the differential equation which involves the coordinate $v$
$V_k$	Characteristic solution to the differential equation in the coordinate, $v$ , which satisfies the boundary conditions



LIST OF SYMBOLS (continued)

$\mathcal{U}_{\zeta}$	Excitation coefficients in the vector mode function expansions in spherical coordinates
$W$	Wronskian determinant of radial functions
$Z_{n+\frac{1}{2}}$	Bessel function of first, second or third kind, of half integral order
$\hat{Z}_n$	$(\frac{\pi \zeta}{2})^{\frac{1}{2}} Z_{n+\frac{1}{2}}$
$a$	A constant in the field expansions, to be determined
$a_n$	Constant in the field expansion in the problem of the uncoated sphere with axially symmetric excitation
$a_k$	Constant in the field expansion in coated spheroid problem
$a_{2n}$	Section 2.2.3, expansion coefficient for the spheroidal radial function
$a_{nm\pm}$	Constant in the expansion for the field of a sphere with arbitrary slot excitation; used in both coated problem (dielectric region) and uncoated problem
$b$	A constant in the field expansions, to be determined
$c$	Constant in the field expansions, to be determined
$C_n$	Constant in the distant field expansion in the problem of the coated sphere with axially symmetric excitation
$C_{nm\pm}$	Constant in the expansion for the field of a sphere with arbitrary slot excitation; used as is $a_{nm\pm}$ described above
$d_n$	Expansion coefficient for spheroidal angular functions
$d_{nm\pm}$	Constant in dielectric region field representation in coated sphere problem, arbitrary slot excitation
$\pm$	As subscript, means even and odd. When both appear on a quantity in an equation, this indicates that the equation actually represents two equations, one for the even solutions and one for the odd solutions
$\bar{E}_{\zeta}$	Vector mode function $= \nabla T_{\zeta}$ see pg. 64
$\bar{E}_{\zeta}''$	Vector mode function $= \nabla T_{\zeta} \times \hat{r}$ see pg. 64
$f_{nm\pm}$	Constants in the distant field expansions in the problem of the coated sphere with arbitrary slot excitation



LIST OF SYMBOLS (continued)

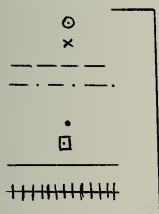
$h_u$	Scale factor corresponding to the coordinate $u$
$h_v$	Scale factor corresponding to the coordinate $v$
$h_\phi$	Scale factor corresponding to the coordinate $\phi$
$j$	Imaginary unit
$J_n$	Spherical Bessel function of first kind as used by Stratton, and Morse and Feshbach
$k$	Eigenvalue symbol
$k_s$	Eigenvalue symbol in spherical coordinates
$n_n$	Spherical Bessel function of second kind as used by Stratton, and Morse and Feshbach
$l$	Semi-focal distance in prolate spheroidal coordinates
$r_1$	Radius of conducting sphere
$r_2$	Outside radius of spherical shell of dielectric
$\hat{r}$	Unit vector in $r$ direction in spherical coordinates
$u$	Coordinate symbol. In prolate spheroidal coordinates, it is the reciprocal of the eccentricity of the generating ellipse.
$u_1$	$u$ -surface which coincides with the conducting spheroid
$u_2$	$u$ -surface which coincides with the outside of the spheroidal shell of dielectric
$v$	Coordinate surface symbol. In prolate spheroidal coordinates, it is the reciprocal of the eccentricity of the generating hyperboloid
$z_n$	Any of the spherical Bessel functions as used by Stratton, and Morse and Feshbach
$\alpha_n$	Excitation coefficient in spherical problems
$\alpha_k$	Excitation coefficient in spheroid problems
$\beta$	Phase constant, $\frac{2\pi}{\lambda}$ or $\omega(\epsilon\mu)^{\frac{1}{2}}$
$\beta_1$	$\beta$ for dielectric region
$\beta_2$	$\beta$ for free space region



LIST OF SYMBOLS (continued)

- $\delta_{ij}$  Kronecker delta; equals one if  $i = j$ , zero otherwise
- $\epsilon$  Permittivity or dielectric constant
- $\epsilon_1$   $\epsilon$  for dielectric region
- $\epsilon_0$   $\epsilon$  for free space
- $\lambda$  Wavelength
- $\mu$  Permeability
- $\sqrt{k}$  Constant in the field expansion for uncoated prolate spheroid
- $\omega$  Frequency times  $2\pi$

Note: In section 3, the quantities associated with TM fields are denoted by single primes; the quantities associated with TE fields are denoted by double primes.



See note page 100



## 1. INTRODUCTION

The object of this work is to provide at least a partial answer to the following question: What changes in the radiation pattern of a moderately large antenna are brought about in the event that for some reason, either within or beyond the control of the designer, the structure is given a coating of dielectric material? The specific antennas considered are conducting bodies of the spheroid family, excited by slots or gaps. In the pages which follow, an analytical method is presented for the determination of the changes in the radiation patterns brought about by spheroidal dielectric casings on spheroidal radiators. The basic geometry is indicated in Fig. 1.

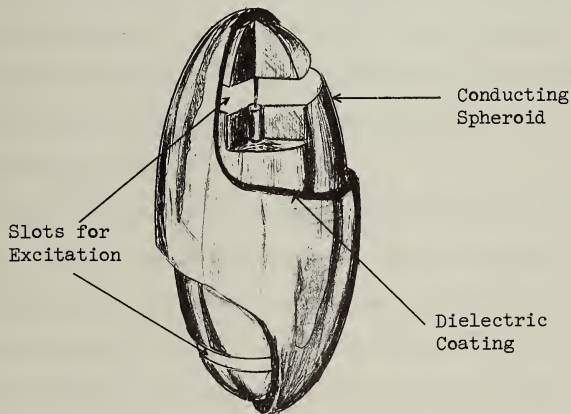


FIGURE 1. BASIC ANTENNA

It is shown herein that numerical results can be obtained, in some cases rather easily, with the aid of a digital computer, and some numerical and graphical results so obtained are included.



The impetus for the study was provided by the fact that the shapes included in the spheroid family provide reasonable approximations to certain space vehicles or missiles, some of which may be given coatings of (nonconducting) refractory material in order to withstand the temperatures developed by tremendous speeds through the atmosphere. But this is by no means the only interesting aspect to the problem. The effects of dielectric coatings on cylinders and planes have been the subject of much study in recent years in connection with the propagation and launching of surface waves, and there is the interesting question of a possible connection or relationship between the effects in spheroidal geometries and those in plane and cylindrical geometries. Moreover, the general problem is of interest to the antenna engineer, since the effects of dielectric coatings on the one hand introduce new possibilities for the control of radiation and on the other hand may present difficulties to him when the coatings (such as ice or radomes) are beyond his control.

The spheroidal radiators are particularly attractive for a study of this kind since they are the only antennas of finite dimensions for which exact analytical formulations of the electromagnetic boundary value problems are possible (at least at the present state of knowledge). In spite of this, there has been surprisingly little published work concerning dielectric coated spheroids. The problem of the scattering of a plane wave by a dielectric coated sphere having a size near that of the first resonance has been studied by Scharfman<sup>1</sup> and Aden and Kerker.<sup>2</sup> Elliot<sup>3</sup> has discussed the possibility of surface waves on



a dielectric coated hemisphere set on a perfectly absorbing pad.

As far as is known to the author, there are no previous publications on the subject of the dielectric coated prolate (or oblate) spheroids.

The method employed in the present work is the classical method for the solution of electromagnetic boundary value problems. The fundamental idea is that an electromagnetic field is uniquely determined in a source free interior region by the values of the tangential components of electric (or magnetic) fields on the bounding surfaces of that region. In the antenna problem, the space exterior to the antenna is effectively converted into an interior region by the device of regarding space as bounded at one extreme by the antenna surface and at the other extreme by a large enclosing surface located at a distance from the antenna which is so great that the fields can safely be assumed to be those of outward traveling waves. In the present problem, this exterior (rendered interior) space is not homogeneous (viz., it is partly filled with dielectric material). As a result, since solutions are easily obtained only in homogeneous regions, the problem is handled by splitting the complete region into two homogeneous regions and obtaining solutions for each of these regions by requiring that the tangential components of the electric and magnetic fields be continuous at the boundary between the homogeneous regions. In outline the solution proceeds as follows: Maxwell's equations for the electromagnetic field are first postulated. These vector partial differential equations are transformed to ordinary scalar differential equations by introducing suitable potential functions and/or by taking advantage of



known symmetries. The ordinary differential equations so obtained are of the Sturm-Liouville type, and as such, with the appropriate boundary conditions, define characteristic functions and characteristic numbers (eigenvalues) in terms of which the solutions can be expressed. The fields are expressed in terms of these functions multiplied by (at first) unknown constants. Fortunately, in the boundary value problems, the number of independent boundary conditions which can be applied is exactly equal to the number of linear equations which is required for the determination of the unknown constants. Unfortunately, however, the number of equations which must be solved is seldom small.

In the sections which follow, the foregoing outline is developed in detail. The organization is such that the problems are separated first according to whether or not the fields have rotational symmetry, and then into the specific coordinate systems. In Chapter 2, the Maxwell field equations in a general coordinate system having rotational symmetry are considered, and it is shown that the partial differential equations can be separated in spheroidal coordinate systems. The conditions for separability are exhibited. Following this, general expressions for the field components in such systems are developed and, in Section 2.1, these expressions are applied to spheres with rotationally symmetric excitation (latitudinal slots). Section 2.1.1 includes a review of the solution for the radiated field of a spherical antenna in order to standardize the notation. The solutions for a dielectric coated spherical radiator are presented in Section 2.1.2. Also in that section, an expression is developed which makes it possible to



evaluate the effect of a dielectric coating, independent of the type of (rotationally symmetric) excitation. It is interesting to note that because of the ease with which the different orders of the characteristic functions of spherical coordinates (spherical Bessel functions and associated Legendre functions) can be generated, the sphere calculation is almost ideally suited for a digital computer. Almost all of the results included herein were obtained with the aid of the University of Illinois Digital Computer (ILLIAC). The system of calculation is discussed in Section 2.1.3.

In Section 2.2, the general equations which are developed in the first part of Chapter 2 are applied to the prolate spheroid. The problem of the uncoated prolate spheroid is reviewed for the purpose of standardizing the notation. In Section 2.2.2, the solutions for the dielectric coated prolate spheroid are presented. A description of a way in which the spheroid calculations can be programmed for a digital computer is included in Section 2.2.3, together with the radiation patterns for a few specific spheroids. Most of the results are new in that they are based on function values which heretofore had not been tabulated. The system of calculation for the spheroidal functions is different from that which has been reported before and it appears to have some advantages.

Chapter 3 is devoted to the development of the equations for spherical antennas with arbitrary (known) excitation — that is, the restriction of rotational symmetry is removed. The equations for both coated and uncoated spheres are developed, and it is shown that the ratio of the coefficients in the series expansions for the TM fields is the same as that developed in Section 2 for the case of rotationally symmetric excitation.



The results included in the following pages show that the effect of a dielectric coating on a spherical radiator follows a rather typical pattern, the net result usually being an enhancement of the relative magnitudes of the higher order Legendre polynomials in the representations. One effect then is the introduction into the patterns of coated spherical antenna of a given size some of the characteristics of the patterns of an uncoated antenna of somewhat larger size, but there are other more interesting effects. The solutions for the prolate spheroid are somewhat less satisfactory in that the calculations require a relatively large amount of computer time, but more than this, they seem to be too involved to provide insight into the physical processes involved. The results indicate, however, that the behavior is similar to that of spherical antennas.

We now turn to the task of developing the equations which apply to general orthogonal coordinate systems in the special case that the fields have rotational symmetry.



## 2. SPHEROIDS WITH AXIALLY SYMMETRIC EXCITATION

In the special case that the sources of the field (and therefore the field itself) have no variation with the coordinate  $\phi$  (see Fig. 2), Maxwell's equations<sup>4</sup> expressed in rotationally symmetric coordinate systems ( $u, v, \phi$ ) reduce to (assuming  $e^{j\omega t}$  time variation) the equations

$$\frac{\partial(h_\phi H_\phi)}{\partial v} = j\omega\epsilon h_v h_\phi E_u \quad (1)$$

$$\frac{\partial(h_\phi H_\phi)}{\partial u} = -j\omega\epsilon h_\phi h_u E_v \quad (2)$$

$$\frac{\partial(h_v E_v)}{\partial u} - \frac{\partial(h_u E_u)}{\partial v} = -j\omega\mu h_u h_v H_\phi \quad (3)$$

together with a similar independent set which can be written down by interchanging  $E$  and  $H$  while exchanging the permittivity and permeability

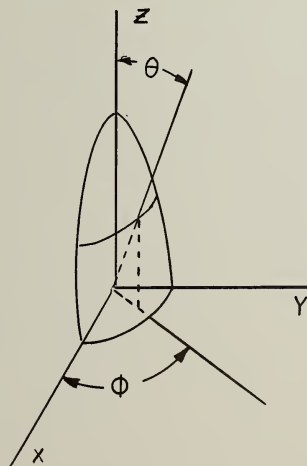


FIGURE 2 COORDINATE SYSTEM



TABLE 1. SCALE FACTORS FOR SPHEROIDAL COORDINATE SYSTEMS  $(u, v, \phi)$ 

Scale factors and related quantities	Coordinate System		
	spherical $(r, (-\cos \theta), \phi)$	prolate spheroidal	oblate spheroidal
$h_u$	1	$\ell \left( \frac{u^2 - v^2}{u^2 - 1} \right)^{1/2}$	$\ell \left( \frac{u^2 + v^2}{u^2 + 1} \right)^{1/2}$
$h_v$	$\frac{r}{(1-v^2)^{1/2}}$	$\ell \left( \frac{u^2 - v^2}{1 - v^2} \right)$	$\ell \left( \frac{u^2 + v^2}{1 - v^2} \right)^{1/2}$
$h_\phi$	$r(1 - v^2)^{1/2}$	$\ell \left( (u^2 - 1)(1 - v^2) \right)^{1/2}$	$\ell \left( (u^2 + 1)(1 - v^2) \right)^{1/2}$
$\frac{h_v}{h_\phi h_u}$	$\frac{1}{1 - v^2}$	$\frac{1}{\ell(1 - v^2)}$	$\frac{1}{\ell(1 - v^2)}$
$\frac{h_u}{h_\phi h_v}$	$\frac{1}{r^2}$	$\frac{1}{\ell(u^2 - 1)}$	$\frac{1}{\ell(u^2 + 1)}$
$h_u h_v h_\phi$	$r^2$	$\ell^3 (u^2 - v^2)$	$\ell^3 (u^2 + v^2)$
$f_1(u)$	$r^2$	$\ell^3 u^2$	$\ell^3 u^2$
$f_2(v)$	0	$-\ell^3 v^2$	$\ell^3 v^2$



symbols according to the rule  $\varepsilon = -4$ . The  $h_i$ 's are scale factors of the coordinate system and  $E_i$  and  $H_i$  represent the components of electric and magnetic fields in the coordinate system  $(u, v, \phi)$ .

If a new variable,  $A = h_\phi H_\phi$ , is introduced, the Eqs. 1, 2, and 3 can be combined into the equation

$$\frac{\partial}{\partial u} \left( \frac{h_v}{h_\phi h_u} \frac{\partial A}{\partial u} \right) + \frac{\partial}{\partial v} \left( \frac{h_u}{h_\phi h_v} \frac{\partial A}{\partial v} \right) + \omega^2 \mu \varepsilon \frac{h_u h_v}{h_\phi} A = 0 \quad (4)$$

Inspection of the table of scale factors (Table I) discloses that in all of the spheroidal coordinate systems, the quantity  $(\frac{h_v}{h_\phi h_u})$  is independent of  $u$ , while the quantity  $(\frac{h_u}{h_\phi h_v})$  is independent of  $v$ , so that Eq. 4 can be written

$$\frac{h_v}{h_u} \frac{\partial^2 A}{\partial u^2} + \frac{h_u}{h_v} \frac{\partial^2 A}{\partial v^2} + h_u h_v \omega^2 \mu \varepsilon A = 0$$

Assuming that  $A$  has the separable form  $A = U(u)V(v)$ , it is possible to write the equation in the form

$$\frac{h_v h_\phi}{h_u} \frac{U''}{U} + \frac{h_u h_\phi}{h_v} \frac{V''}{V} + h_u h_v h_\phi \omega^2 \mu \varepsilon = 0 \quad (5)$$

As before, a glance at Table I shows that the scale factors depend on the coordinates in such a way that  $h_u h_v h_\phi = f_1(u) + f_2(v)$  (and as before  $(\frac{h_v h_\phi}{h_u})$  is a function of  $u$  only while  $(\frac{h_u h_\phi}{h_v})$  is a function of  $v$  only) so that the partial differential equation separates into the two ordinary differential equations:



$$\frac{h_v h_\phi}{h_u} U'' + (f_1(u) \omega^2 u \epsilon - k) U = 0 \quad (6)$$

$$\frac{h_u h_\phi}{h_v} V'' + (f_2(v) \omega^2 v \epsilon + k) V = 0 \quad (7)$$

where  $k$  is the separation constant. Because of the symmetry of the source distributions which have been postulated, the  $v$ - and  $\phi$ -components of the fields must be zero on the  $z$ -axis. For spheroids, these field components are therefore zero at  $v = \pm 1$ , independent of  $u$ . It follows from the identity

$$H_\phi = \frac{A}{h_\phi} = \frac{U(u) V(v)}{h_\phi},$$

with Eq. 2, that these field components involve the  $V$ -functions directly, and therefore the following conditions on the functions are implied:

$$V_k = 0, v = \pm 1.$$

Equation 7 with these boundary conditions constitutes a Sturm-Liouville system, for which it is known<sup>5,6</sup> that the solutions can be represented by characteristic functions having eigenvalues  $k_i$  which give non-zero solutions of Eq. 7. The general solution to Eq. 6 can be written

$$U_k = a_{k_1} U_{k_1} + b_{k_2} U_{k_2}$$

where  $U_{k_1}$  and  $U_{k_2}$  are the two linearly independent solutions. It follows therefore that any solutions to the field equations which meet the specified conditions of symmetry and continuity can be written as follows:



$$H_\phi = \frac{A}{h_\phi} = \frac{1}{h_\phi} \sum_k (a_k U_{k1} + b_k U_{k2}) V_k \quad (8)$$

The electric field components can be found by substituting Eq. 8 in Eqs.

1 and 2. The result is

$$E_u = \frac{1}{j\omega \epsilon h_v h_\phi} \frac{\partial}{\partial v} \sum_k (a_k U_{k1} + b_k U_{k2}) V_k \quad (9)$$

$$E_v = -\frac{1}{j\omega \epsilon h_u h_\phi} \sum_k (a_k \frac{\partial U_{k1}}{\partial u} + b_k \frac{\partial U_{k2}}{\partial u}) V_k. \quad (10)$$

Having thus derived the expressions for the field components in the general spheroidal system, we can now proceed to the formulation of the boundary value problems for particular classes of spheroids.

## 2.1 Symmetrically Excited Spheres

Among the spheroids, the sphere is usually the easiest to study because of the familiarity of the functions which are involved. This study will therefore begin with the sphere and, in fact, will present more numerical details for it than for the other spheroids. The coordinate system selected is that one in which  $u = r$ ,  $v = -\cos \theta$ , i.e.  $(r, -\cos \theta, \phi)$ . This selection, in place of the usual  $(r, \theta, \phi)$  system, makes the sphere a more typical member of the family of spheroids (the negative sign in  $v = -\cos \theta$  makes a right handed coordinate system).



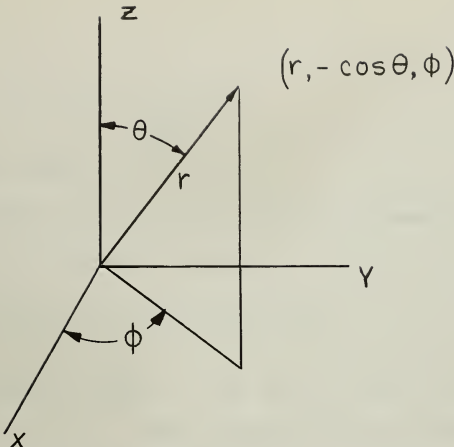


FIGURE 3 SPHERICAL COORDINATE SYSTEM

With the scale factors for this coordinate system taken from Table I, the differential Eqs. 6 and 7 become, after replacing  $\nabla(\omega)$  by  $R(r)$ ,

$$r^2 R'' + (r^2 \omega^2 \mu \varepsilon - k_s) R = 0 \quad (11)$$

and

$$(1-v^2) V_s'' + k_s V_s = 0 \quad . \quad (12)$$

Although it seems a pity to do so, Eq. 12 will be transformed into the more complicated but more familiar associated Legendre equation by means of the substitution  $V_s = (1-v^2)^{\frac{1}{2}} P$ , as follows:

$$(1-v^2) P'' - 2v P' + \left( k_s - \frac{1}{(1-v^2)} \right) P = 0$$

The functions which satisfy the differential equation, plus the condition  $V_s(\pm 1) = 0$ , are therefore the associated Legendre function of degree one,



$$P_n^1 = (1 - v^2)^{\frac{1}{2}} \frac{d P_n(v)}{d v}$$

with the eigenvalues  $k_s$  equal to  $n(n+1)$ .

With these eigenvalues, Eq. 11 is recognized to be a Bessel-type differential equation<sup>7</sup> which has solutions of the form

$$R = a r^{\frac{1}{2}} J_{n+\frac{1}{2}}(\beta r) + b r^{\frac{1}{2}} N_{n+\frac{1}{2}}(\beta r)$$

( $k_s = n(n+1)$  identified as  $\frac{4p^2 - 1}{4}$ , so  $p = \pm n + \frac{1}{2}$ , where  $p$  is the function order)  $\beta^2 = \omega^2 \mu \epsilon$ . These functions can now be inserted into the general Eqs. 8 and 10 for the field components which are tangent to the spherical surfaces. In doing so, it is convenient to use the notation of Schelkunoff and introduce a radial function

$$\hat{Z}_n(x) = (\frac{\pi x}{2})^{\frac{1}{2}} Z_{n+\frac{1}{2}}(x)$$

where  $Z_{n+\frac{1}{2}}(x)$  is any one of the three kinds of Bessel functions. In terms of these functions, the equations for the tangential field components become

$$H_\phi = \frac{1}{r} \sum_n (a_n \hat{J}_n(\beta r) + b_n \hat{N}_n(\beta r)) P_n^1(r) \quad (13)$$

and from Eq. 2

$$E_r = -\frac{1}{j\omega \epsilon r} \sum_n (a_n \hat{J}'_n(\beta r) + b_n \hat{N}'_n(\beta r)) P_n^1(r) \quad (14)$$

where

$$\hat{Z}' = \frac{d \hat{Z}}{d r} .$$



### 2.1.1 Boundary Value Problem of the Conducting Sphere (no coating)

Unique solutions of boundary value problems in regions exterior to a spherical surface are obtained from the values of tangential  $E$  (or  $H$ ) over the spherical surface, together with the radiation condition at a larger spherical surface whose radius tends to infinity. Since the radiation condition implies that the fields are propagating in the direction of increasing  $\tau$ , we note from Eq. 13 that the coefficients  $a_n$  and  $b_n$  must be related so that  $b_n = -j a_n$ , in order to give the proper function to represent the outward traveling waves,

$$\hat{H}_n(\beta\tau) = \hat{J}_n(\beta\tau) - j \hat{N}_n(\beta\tau).$$

Thus the expressions for the fields exterior to a conducting sphere can be written in the form

$$H_\phi = \frac{1}{r} \sum_n a_n \hat{H}_n(\beta\tau) P_n^1(v) \quad (15)$$

$$E_v = -\frac{1}{j\omega\epsilon r} \sum_n a_n \hat{H}'_n(\beta\tau) P_n^1(v). \quad (16)$$

The coefficients in these expansion are determined by requiring that the series expansion Eq. 16 represent the electric field at the surface of the conducting sphere ( $\tau = \tau_i$ ). This latter electric field is of course zero except over the axially symmetric slots. The field in the slot is presumed to be known, and if it is represented in the form



$$\left[ E_v \right]_{r=r_i} = \sum_n \alpha_n P_n^1(v) , \quad (17)$$

the orthogonality properties of the Legendre functions make it possible to obtain the following equation for the coefficients:

$$\alpha_n = \frac{\int_{-1}^1 E_a P_n^1 dv}{\int_{-1}^1 (P_n^1)^2 dv} \quad (18)$$

where

$$\int_{-1}^1 (P_n^1)^2 dv = \frac{2n(n+1)}{2n+1} \quad (19)$$

The expansion Eq. 16 evaluated at  $r = r_i$  must be identical to the expansion, Eq. 17; this implies that the coefficients must be equal term by term. Thus the unknown coefficients in Eq. 16 can be found in terms of the excitation coefficients  $\alpha_n$  from the equation

$$\alpha_n = - \frac{j \omega \epsilon r_i \alpha_n}{\hat{H}'_n(\beta_0 r_i)} \quad (20)$$

The formula for the computation of the fields reads therefore

$$H_\phi = - \frac{j \omega \epsilon r_i}{r} \sum_n \frac{1}{\hat{H}'_n(\beta_0 r_i)} \left( \int_{r_i}^{r_0} E_a P_n^1(v) dv \right) \hat{H}_n(\beta_0 r) P_n^1(r) \quad (21)$$

In the calculation of the distant field, the asymptotic form for  $\hat{H}_n(\beta r)$  can be used:

$$\hat{H}_n(x) \xrightarrow{x \rightarrow \infty} j^{n+1} e^{-jx}$$



Thus, the expression for the calculation of the radiated field is

$$H_{\phi} = -j \frac{\omega \epsilon_0 r}{\tau} e^{-j\beta_0 r} \sum_{n=1}^{\infty} j^{n+1} \frac{\alpha_n P_n^1(r)}{H_n'(\beta_0 r)} . \quad (22)$$

To display the variation of the field with angle  $\theta$  (the pattern),

only the quantities to the right of the summation sign are of interest

This much of equation (22) was programmed for calculation by the ILLIAC.

Some of the details of the solution by the digital computer are presented in Section 2.1.3.

In a desk calculation, the book Tables of Spherical Bessel Functions can be used to advantage. Therein, the function  $Z_n(x) = (\frac{\pi}{2x})^{\frac{1}{2}} Z_{n+\frac{1}{2}}(x)$  is tabulated. With these tables, the following relationships are helpful:

$$\begin{aligned} \hat{Z}_n(\beta r) &= \beta + z_n(\beta r) \\ \frac{d \hat{Z}_n(\beta r)}{dr} &= \beta [ z_n(\beta r) + r \frac{dz_n(\beta r)}{dr} ] \\ &= \beta [ \frac{\beta r}{2n+1} ((n+1)z_{n-1} - nz_{n+1}) ] . \end{aligned}$$

### 2.1.2 Boundary Value Problem of the Coated Conducting Sphere

The equation for the distant field intensity is basically the same whether or not the radiator is dielectric coated. However, the coefficients in the field expansions are of course different and these are obtained from the solution of the boundary value problem. One measure of the effect of a



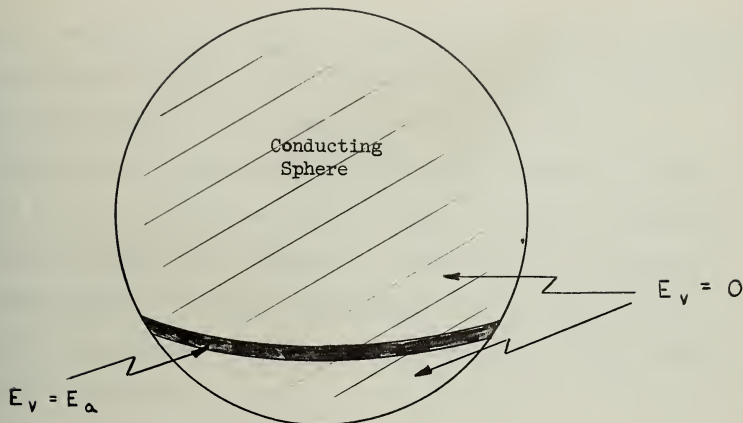


FIGURE 4 SPHERICAL RADIATOR

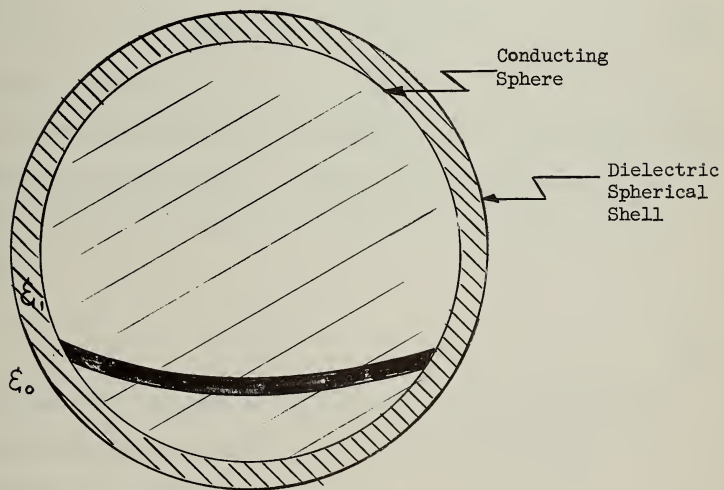


FIGURE 5 DIELECTRIC COATED SPHERICAL RADIATOR



dielectric coating on the surface of a sphere can be obtained by comparing the coefficients, as given by Eq. 20 with the corresponding coefficients in the coated problem. This is done in the present section.

When the sphere is dielectric coated, we must recognize two regions: a region (I) consisting of the spherical shell of dielectric surrounding the conducting sphere, and a region (II) consisting of the remainder of the exterior space. In region (I), the Eqs. 13 and 14 apply directly. In region (II), the equations have the same form as Eqs. 15 and 16, which can be rewritten as follows:

$$H_{\phi \text{ II}} = \frac{1}{r} \sum_n c_n \hat{H}_n^{(\beta_0, r)} P_n^1(r) \quad (23)$$

$$E_{v \text{ II}} = - \frac{1}{j \omega \epsilon_0 r} \sum_n c_n \hat{H}'_n^{(\beta_0, r)} P_n^1(r) . \quad (24)$$

Again, the series expansion for  $E_{v \text{ II}}$ , evaluated at  $r = r_1$ , must be equal to the series expansion for the applied field at that surface, which latter is taken to be that of Eq. 17. Equating the coefficients in these two expansions, term by term, gives the following relationship among the coefficients:

$$a_n \hat{J}'_n(\beta, r_1) + b_n \hat{N}'_n(\beta, r_1) = - j \omega \epsilon_0 r_1 \alpha_n . \quad (25)$$

Equating the tangential component of the magnetic fields at the surface  $r = r_2$ , by equating (13) evaluated at  $r_2$  to (23) evaluated at  $r_2$ , gives the following relationship:



$$a_n \hat{J}_n(\beta, \tau_2) + b_n \hat{N}_n(\beta, \tau_2) = c_n \hat{H}_n(\beta, \tau_2) . \quad (26)$$

The corresponding condition on the tangential component of the electric fields, applied by equating (14) and (24) evaluated at  $\tau = \tau_2$ , gives the following relationship:

$$a_n \hat{J}'_n(\beta, \tau_2) + b_n \hat{N}'_n(\beta, \tau_2) = \frac{\epsilon_i}{\epsilon_o} c_n \hat{H}'_n(\beta, \tau_2) . \quad (27)$$

Equations 25, 26, and 27 constitute sets of three equations in the three sets of unknown expansion coefficients. The augmented matrix for this system of equations is

$$\left[ \begin{array}{ccc|c} \hat{J}'_n(\beta, \tau_1) & \hat{N}'_n(\beta, \tau_1) & 0 & -j\omega \epsilon_i \tau_1 \alpha_n \\ \hat{J}'_n(\beta, \tau_2) & \hat{N}'_n(\beta, \tau_2) & -\hat{H}_n(\beta, \tau_2) & 0 \\ \hat{J}'_n(\beta, \tau_2) & \hat{N}'_n(\beta, \tau_2) & -\frac{\epsilon_i}{\epsilon_o} \hat{H}'_n(\beta, \tau_2) & 0 \end{array} \right] .$$

Thus, we find an equation for the expansion coefficients in region (II) as follows:

$$c_n = -j\omega \epsilon_i \tau_1 \alpha_n \frac{[\hat{J}_n(\beta, \tau_2) \hat{N}'_n(\beta, \tau_2) - \hat{J}'_n(\beta, \tau_2) \hat{N}_n(\beta, \tau_2)]}{\Delta_n} \quad (28)$$



where

$$\Delta_n = \begin{vmatrix} \hat{J}'_n(\beta, r_i) & \hat{N}'_n(\beta, r_i) & 0 \\ \hat{J}'_n(\beta, r_2) & \hat{N}'_n(\beta, r_2) & -\hat{H}'_n(\beta, r_2) \\ \hat{J}'_n(\beta, r_2) & \hat{N}'_n(\beta, r_2) & -\frac{\epsilon_r}{\epsilon_0} \hat{H}'_n(\beta, r_2) \end{vmatrix}. \quad (29)$$

The quantity in braces in Eq. 28 is the Wronskian determinant of  $(\hat{J}_n, \hat{N}_n)$ . This quantity can be determined from the asymptotic solutions of Eq. 11. The result is

$$W(\hat{J}_n, \hat{N}_n) = \beta_i.$$

With this result, the equation for the distant field coefficients takes a simpler form as follows:

$$C_n = -j \frac{\omega \epsilon_i r_i \alpha_n \beta_i}{\Delta_n}. \quad (30)$$

Now a measure of the effect on the radiation pattern of the dielectric layer on a conducting sphere may be found from studying the ratio of the coefficients,  $\alpha_n$  (Eq. 20), which apply to the uncoated sphere to the coefficients,  $C_n$  (Eq. 30), in the situation that the conducting sphere has the same size and the same excitation but has a dielectric layer. The ratio is as follows:

$$\frac{\alpha_n}{C_n} = \frac{\epsilon_r}{\epsilon_0} \frac{\Delta_n}{\beta_i \hat{H}'_n(\beta, r_i)} \quad (31)$$

or

$$\frac{C_n}{\alpha_n} = \beta_i \frac{\epsilon_r}{\epsilon_0} \frac{\hat{H}'_n(\beta, r_i)}{\Delta_n}. \quad (32)$$



It is interesting to study these ratios in limiting cases. For example, if both spherical surfaces are large enough so that the Bessel functions can be replaced by their asymptotic forms for large arguments, i.e.,

$$\begin{aligned}\hat{J}_n &\longrightarrow \cos(\beta r - \frac{\pi}{2}(n+1)) \\ \cdot \hat{N}_n &\longrightarrow \sin(\beta r - \frac{\pi}{2}(n+1)) \\ \hat{H}_n &\longrightarrow j^{n+1} e^{-j\beta r}\end{aligned}$$

the result, after a fair amount of rearrangement, can be put into the following form:

$$\frac{C_n}{a_n} \longrightarrow -j \varepsilon_r^{\frac{1}{2}} \frac{e^{-j\beta(r_2-r_1)}}{\sin \beta(r_2-r_1) - j \varepsilon_r^{\frac{1}{2}} \cos \beta(r_2-r_1)} \quad r_1, r_2 \rightarrow \infty.$$

It is noteworthy that this ratio is independent of  $n$ . This indicates that for such large spheres, the dielectric coating will not influence the pattern variation with angle, but the approximations may not be valid for the highest orders needed in this representation.

On the other hand, if  $(\beta r)$  is very small, we can take as approximations the first terms in the power series representations:

$$\hat{J}_n(x) \doteq \frac{x^n n! x^{n+1}}{(2n+1)!}$$

$$\hat{N}_n(x) \doteq -\frac{(2n)! x^n}{2^n n!}$$



Then, after a fair amount of algebra, the ratio of coefficients becomes

$$\frac{a_n}{c_n} \doteq \frac{-(n+1)}{(2n+1)\epsilon_r} \left[ \left( \frac{r_1}{r_2} \right)^{n(n+1)} - 1 - \epsilon_r \left\{ \left( \frac{r_1}{r_2} \right)^{n(n+1)} + \frac{n}{n+1} \right\} \right].$$

For such small spheres, only the term having  $n$  equal to unity is important:

$$\frac{a_1}{c_1} \doteq \frac{2}{3\epsilon_r} \left[ \epsilon_r \left\{ \left( \frac{r_1}{r_2} \right)^2 + \frac{1}{2} \right\} + 1 - \left( \frac{r_1}{r_2} \right)^2 \right] .$$

It should be mentioned here that there is a danger of making an invalid observation based on the latter equation. This equation applies in the event that the electric field is the same in both the coated and uncoated state. Normally in practice the constant would be the voltage across the gap, in which case the electric field would be less with the dielectric present.

For the intermediate (and more interesting) range of values of  $\beta r$ , the ratio must be studied numerically. This was done and the results are discussed in Section 2.1.3.

### 2.1.3 Numerical Computations Associated with the Spherical Radiator

Because of the relative ease with which different orders of the spherical functions can be generated, the sphere calculation is almost ideally suited to a digital computer. The functions which are involved (spherical Bessel functions and associated Legendre polynomials) satisfy very convenient recurrence relationships as follows:



$$\hat{\sum}_{n+1}(x) = \frac{2n+1}{x} \hat{\sum}_n(x) - \hat{\sum}_{n-1}(x)$$

$$\hat{\sum}'_n(x) = \frac{n+1}{x} \hat{\sum}_n(x) - \hat{\sum}_{n+1}(x) = \frac{1}{2n+1} [(n+1)\hat{\sum}_n(x) - n\hat{\sum}_{n+1}(x)]$$

and

$$\hat{P}_{n+1}^1(x) = \frac{1}{n} [(2n+1)x \hat{P}_n^1(x) - (n+1)\hat{P}_{n-1}^1(x)] .$$

Thus, given the two lowest orders of the functions (which involve only sines and cosines), the higher orders are easily generated in a digital computer "loop". The calculations described herein were based on these recurrence relationships - Generation of the functions was done entirely by the machine.

With Legendre polynomials and the spherical Bessel functions of the second kind ( $\hat{N}_n$ ) this upward recurrence process can apparently be carried out to almost indefinitely high orders of the functions without serious loss of accuracy. However, in the calculation of the spherical Bessel functions of the first kind  $\hat{J}_n$ , there is a serious loss of accuracy if carried out in a straightforward upward recurrence process. In fact, the figures begin to lose significance for those orders ( $n$ ) which exceed approximately twice the argument -- and this is approximately the number of terms required for the series expansions for the fields to converge satisfactorily. Hence, an alternative system is employed for these functions. The relationship,

$$\hat{J}_{n+1} = \frac{2n+1}{x} \hat{J}_n - \hat{J}_{n-1}$$



is transformed into a continued fraction form for use in a downward scheme as follows:

$$\frac{\hat{J}_{n+1}}{\hat{J}_{n-1}} = \frac{2n+1}{x} \frac{\hat{J}_n}{\hat{J}_{n-1}} - 1$$

or

$$\frac{\hat{J}_n}{\hat{J}_{n-1}} = \frac{1}{\left[ \frac{2n+1}{x} - \frac{\hat{J}_{n+1}}{\hat{J}_n} \right]}$$

or

$$\frac{\hat{J}_n}{\hat{J}_{n-1}} = \frac{1}{\left[ \frac{2n+1}{x} - \left[ \frac{2n+3}{x} - \left[ \frac{2n+5}{x} - \left[ \dots \right] \right] \right] \right]}$$

$$\frac{1}{\left[ \frac{2(n+m)-1}{x} - \frac{\hat{J}_{n+m}}{\hat{J}_{n+m-1}} \right]}$$

Now if  $m$  is taken sufficiently large, the ratio  $\hat{J}_{n+m}/\hat{J}_{n+m-1}$  is negligible in comparison to the term  $2(n+m-1)/x$  (because of the nature of the functions of high order and relatively small argument), and hence a good approximation for this ratio is zero. With this approximation, the ratio  $\hat{J}_{n+m-1}/\hat{J}_{n+m-2}$  is first calculated and then employed to calculate the lower order ratio. This process is continued so as to calculate



and store the ratios of successive orders of functions from some high order to some low order (say  $n = 1$ ) for which the value of the function in the denominator is readily obtained ( $\hat{J}_0(x) = \sin x$ ). The functions themselves are obtained from the ratios by successive multiplications. When generated in this way, all except the highest several orders calculated can have full machine accuracy. However, the method breaks down if the argument coincides exactly with a zero in one of the (lower) orders. Thus, it is safest to use the upward recurrence form in the oscillating region of the functions and the continued fractions scheme in the monotone region. An alternative is the use of the recurrence form in the downward sense. This latter method is satisfactory except for the arguments which correspond to the zeros of the lowest order function computed (integral multiples of  $2\pi$  if the process is carried to  $\hat{J}_0(x)$ ).

Except for this difficulty with the  $\hat{J}_n$  functions, a completely automatic digital computer program could easily be written, in that the decision as to the number of terms to be computed could be made by the machine (by a convergence test). The actual program, described below, which was written for the ILLIAC is semi-automatic in the sense that the programmer makes a guess concerning the number of terms required for convergence, and on this basis, a sufficient number of  $\hat{J}_n$  functions is made available. If the guess which is made is too low, the program stops on a special stop order. (The number of terms required appears to be of the order of twice the argument of the Bessel functions ( $\beta_0$ ) or perhaps ten times the radius in wavelengths. Actually, orders of the functions as high as sixteen times the radius in wavelengths were computed in the program, and this number never



failed to provide a safe margin).

In the calculation of the radiation patterns, the constants and the variation in Eqs. 22 and 23 are suppressed and an expression having the form

$$\mathcal{H} = \sum j^{n+1} A_n P_n^1(v)$$

is evaluated. The quantity  $A_n$  is of course a complex number which is evaluated as follows, in the uncoated and coated problems respectively:

$$A_n = \frac{\alpha_n}{\hat{J}_n^2 + \hat{N}_n^2} \left[ \hat{J}'_n(\beta_r r_i) + j \hat{N}'_n(\beta_r r_i) \right]$$

$$A_n = \frac{\alpha_n}{R_n^2 + d_n^2} \left( R_n + j d_n \right) \text{ (coated)}$$

where

$$R_n = \hat{J}_n(\beta_r r_2) \{ \} _1 - \varepsilon_r^{\frac{1}{2}} \hat{J}'_n(\beta_r r_2) \{ \} _2$$

$$d_n = \hat{N}_n(\beta_r r_2) \{ \} _1 - \varepsilon_r^{\frac{1}{2}} \hat{N}'_n(\beta_r r_2) \{ \} _2$$

and

$$\{ \} _1 = \{ \hat{J}'_n(\beta_r r_i) \hat{N}'_n(\beta_r r_2) - \hat{J}'_n(\beta_r r_2) \hat{N}'_n(\beta_r r_i) \}$$

$$\{ \} _2 = \{ \hat{J}'_n(\beta_r r_i) \hat{N}_n(\beta_r r_2) - \hat{J}_n(\beta_r r_2) \hat{N}'_n(\beta_r r_i) \}$$

in which

$$\hat{Z}'_n = \frac{d \hat{Z}(\beta r)}{d(\beta r)} .$$



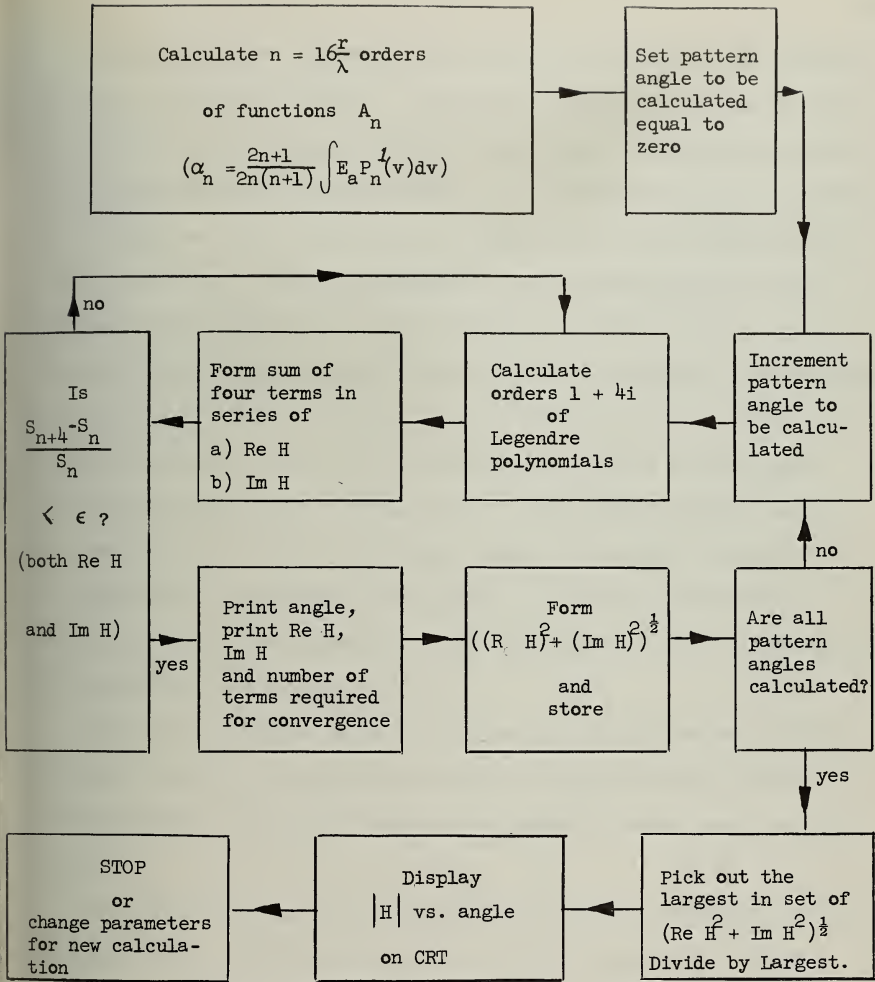


FIGURE 6 SIMPLIFIED FLOW DIAGRAM FOR RADIATION PATTERN CALCULATIONS (SPHERICAL RADIATOR)



A simplified flow diagram for the machine calculation of the radiation patterns is presented in Fig. 6. The computer program is written in such a way that for a given angle in the field, additional terms in the summation (on  $n$ ) are obtained in groups of four. This summation process is carried on to higher and higher orders until a comparison with the cumulative sum shows that the last four terms computed is satisfactorily small in comparison to the cumulative sum. The excitation coefficients ( $\alpha_n$ ) are obtained by a five point Simpson's rule integration process on the assumption that the electric field is constant over a slot whose width subtends two degrees of latitude. The machine time required (using a floating point interpretive routine) for a single pattern calculation involving thirty-five points in the field is about five minutes (for greater accuracy than is required for a cathode ray tube display). If several patterns are computed by varying the parameters while the program is still in the machine, the average time per pattern is less.

Some of the radiation patterns which were so calculated are displayed in Figs. 13 to 20. The radiation patterns of a given spherical radiator with and without a dielectric coating are presented side by side for contrast.

The number of radiation patterns included herein is not large, since it appears to be ultimately more useful and more economical to present certain key data pertaining to spherical radiators, from which additional calculations can be made with a minimum of effort. Thus, Table 4 gives the excitation coefficients (calculated as mentioned above in the hope that they will be useful in future impedance calculations) for slots whose position varies from ten to ninety degrees latitude. Another quantity of



interest is  $\left| \hat{H}'_n(\beta_0 r) \right|^{-1}$ , for the uncoated radiator. The square of this quantity is plotted as a function of  $r/\lambda$  for a given  $n$  in Fig. 28. The maxima in these curves show the sizes for which the sphere becomes quasi-resonant for the various orders of the functions. The same quantity as a function of  $n$ , for different values of  $\beta_0 r$  is given in Figs. 29 to 39, and in Table 5 with the quantities  $\hat{J}_n / |\hat{H}'_n|^2$  and  $\hat{N}_n / |\hat{H}'_n|^2$  which are needed in any pattern calculations. Thus, with these data, and a good table of Legendre polynomials, a radiation pattern calculation can be made relatively easily with a desk calculator.

Similarly, some key data are included for the dielectric coated spherical radiator. As was mentioned earlier, the ratio of coefficients (coated to uncoated) given by Eq. 32 is studied in some detail. However, it appears to be ultimately more useful to present the data for the real parts and the imaginary parts separately, since with this done, given the coefficients in the expansion for the uncoated case, one can immediately find those for the coated sphere from the Tables. Thus, in Figs. 40 to 63, and Table 6, the results of a study of the equations

$$\frac{\operatorname{Re} c_n}{\operatorname{Re} a_n} = \varepsilon_r^{\frac{1}{2}} \frac{\left| \hat{H}'_n(\beta_0 r) \right|^2 R_n}{(R_n^2 + d_n^2) \hat{J}'_n(\beta_0 r)}$$

$$\frac{\operatorname{Im} c_n}{\operatorname{Im} a_n} = \varepsilon_r^{\frac{1}{2}} \frac{\left| \hat{H}'_n(\beta_0 r) \right|^2 d_n}{(R_n^2 + d_n^2) \hat{N}'_n(\beta_0 r)}$$

are presented. These ratios were evaluated as a function of the size of the conducting sphere, the dielectric constant, and the thickness of the coating.



Three sets of calculations were carried out, in each of which one of the above quantities was varied while the other two were held constant. Note that there is a rather characteristic pattern, which is best exemplified by Fig. 42. The characteristic peak which appears always indicates an enhancement of the magnitudes of the higher order Legendre polynomials in the field expansion. The peaks (orders of greatest enhancement) grow higher and move to higher orders as either the value of the permittivity or the thickness of the coating is increased (for a given size of conducting sphere). There are other interesting features in the graphs, some of which can be misleading. It hardly needs to be pointed out that the curves will exhibit peaks in the vicinity of the zeros of  $\sum_n^{\infty} (\beta_n)^t$ , but the peaks may not be significant as far as the patterns are concerned since the contribution of those orders to the uncoated radiation pattern may be negligible. The peaks are generally higher in the curves of  $\text{Re } c_n / \text{Re } a_n$ , but again the effect in the patterns may be less marked if  $\text{Re } a_n$  does not itself make an appreciable contribution to the uncoated pattern. It can also be seen that the extent of the effect depends upon the nature of the excitation. For example, suppose that there is a rather sharp peak at a particular odd (even) order of the functions; then, there will be a marked effect if the odd (even) orders are excited but practically none if the odd (even) orders are not excited. (Even orders are not excited by slot fields which are symmetric about the equator; odd orders are not excited by excitations which are anti-symmetric about the equator, such as a pair of slots having the same latitude, one in the northern hemisphere and one in the southern hemisphere, excited one hundred and eighty degrees out of phase.) In general,



the effects are greater when the excitation is such that all orders are present, and one typical result is an increase in the radiated field in the general direction of the poles (z-axis). This effect arises because of the enhancement of the higher orders of the Legendre polynomials. If, however, certain of the adjacent higher order ratios have comparable magnitudes but opposite signs, some surprising results may arise as may be seen in some of the radiation patterns.

We next turn our attention from spherical radiators to prolate spheroidal radiators, excited by axially symmetric slots.

## 2.2 Symmetrically Excited Prolate Spheroids

The dielectric clad spheroid which is probably of most practical interest at the present time is the prolate spheroid. In the prolate spheroidal coordinate system, the values of the coordinate  $u$  are the reciprocals of the eccentricities of the ellipses which generate the prolate spheroids (so  $1 \leq u \leq \infty$ ). The orthogonal  $v$  surfaces are hyperboloids of two sheets and the values of the coordinate  $v$  correspond to the reciprocals of the eccentricities of the generating hyperbolas ( $-1 \leq v \leq 1$ ). The relationship of this coordinate system to the spherical system can be illustrated by writing  $v = -\cos \theta$ , where  $\theta$  is the (polar) angle which is defined by the asymptotic cones: thus, as  $u \rightarrow \infty$  so that the surfaces  $u = \text{constant}$  become spherical, the angle  $\theta$  becomes the usual polar angle of spherical coordinates. The quantity  $l$  is the semi-focal distance.



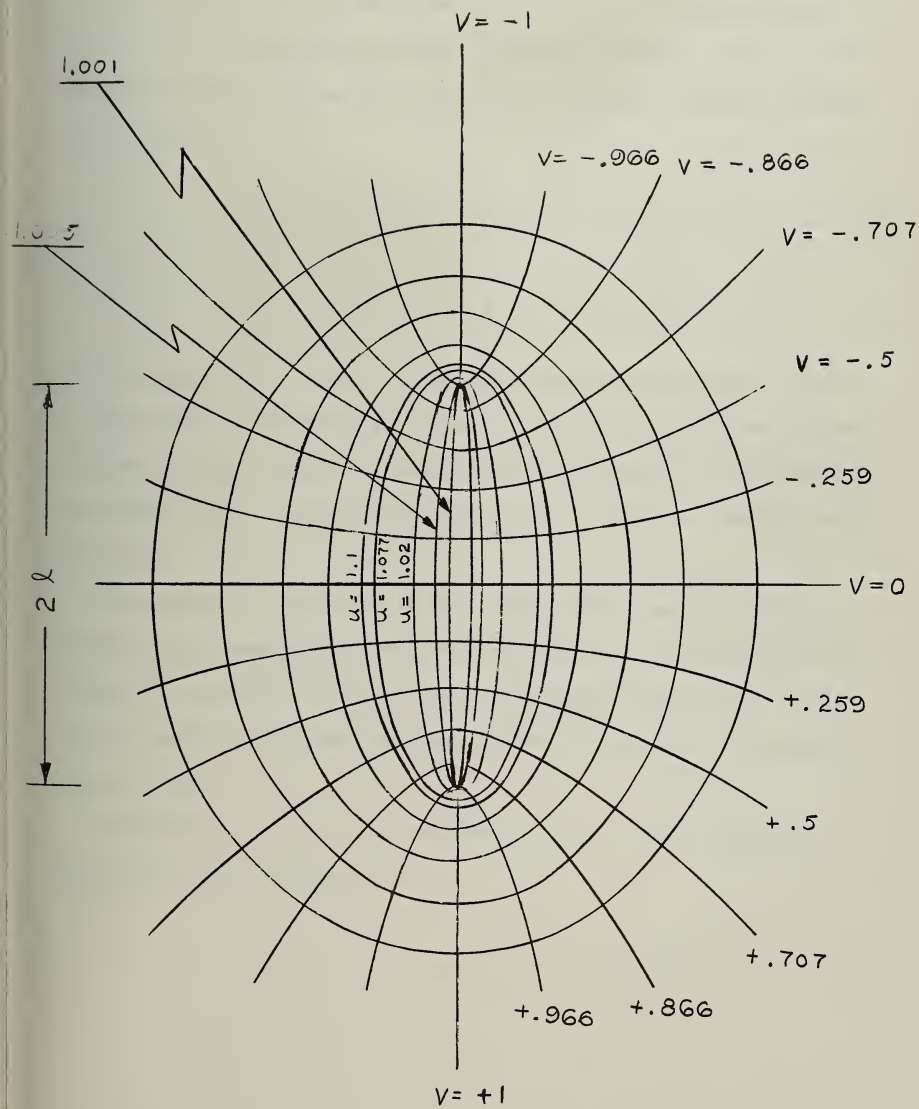


FIGURE 7 PROLATE SPHEROIDAL COORDINATE SYSTEM



With this identification of coordinate variables, the results of the analysis presented at the beginning of Section 2 are immediately applicable. It is clear from the results in Table I, and Eqs. 6 and 7, that the differential equations which apply to the prolate spheroidal system are as follows:

$$(u^2 - 1) \mathcal{U}'' + ((\beta l u)^2 - k_k) \mathcal{U} = 0 \quad (36)$$

$$(1 - v^2) \mathcal{V}'' + (k_k - (\beta l v)^2) \mathcal{V} = 0 \quad (37)$$

The functions  $\mathcal{U}$  and  $\mathcal{V}$  are only incompletely tabulated. Hence, the first task in the spheroid problem is to devise a system for the calculation of these functions, including the determination of the family of eigenvalues,  $k_k$ , so that the functions  $\mathcal{V}_k$  comprise a complete orthogonal set.

The system of calculation finally adopted was selected with an eye toward the most advantageous use of the ILLIAC and its library of service routines. An outline of the system is presented in Section 2.3.3. The details, together with some numerical values, will appear in a separate technical report.

Essentially, the  $\mathcal{V}$ -functions are calculated from a series of associated Legendre polynomials:

$$\mathcal{V}_k = (1 - v^2)^{\frac{1}{2}} \sum_n d_{kn} P_n^1 , \quad (38)$$



where the  $d_{kn}$  satisfy the recursion relationship:

$$-(\beta l)^2 \left[ \frac{(n-2)(n-1)}{(2n-3)(2n-1)} \right] d_{k,n-2} + \left[ k_k - n(n+1) - (\beta l)^2 \left\{ \frac{2n(n+1)-3}{(2n-1)(2n+3)} \right\} \right] d_{k,n} \\ - (\beta l)^2 \left[ \frac{(n+3)(n+2)}{(2n+3)(2n+5)} \right] d_{k,n+2} = 0$$

(We note here that the eigenvalues  $k_k$  depend on  $\beta l$  so that the matching of the field components at a boundary between dielectrics is complicated.) The "radial" functions,  $\underline{\mathcal{V}}$ , are calculated from a series of spherical Bessel functions, the coefficients in which satisfy a recursion relation very similar to that given above.

### 2.2.1 Conducting Prolate Spheroid without Dielectric Coating

Referring back to Eqs. 8 and 10, after inserting the scale factors for the prolate spheroidal coordinate system, it can be seen that the field expressions are as follows ( $U_{k_3}$  is the solution of Eq. 36 which satisfies the radiation condition):

$$H_\phi = \frac{1}{l((u^2-1)(1-v^2))^{\frac{1}{2}}} \sum_k \sigma_k U_{k_3} V_k \quad (40)$$

$$E_v = -\frac{1}{j\omega\epsilon l^2((u^2-v^2)(1-v^2))^{\frac{1}{2}}} \sum_k \sigma_k \frac{dU_{k_3}}{du} V_k \quad . \quad (41)$$

As was done in the case of the spherical radiator, the tangential component of the electric field,  $E_\alpha$ , is specified to be zero over the (conducting) surface  $u=u_i$ , except over the azimuthal slots. The field on that surface is then expanded in the orthogonal set of  $\underline{\mathcal{V}}$ -functions as follows:

$$E_v \Big|_{u=u_i} = E_u \Big|_{u=u_i} = - \sum_k \frac{\sigma_k U'_{k_3}(u_i) V_k}{j\omega\epsilon_0 l^2((u_i^2-v^2)(1-v^2))^{\frac{1}{2}}} \quad .$$



It follows from the boundary conditions and Eq. 37 that the statement of orthogonality among the  $\nabla$ -functions is as follows:

$$\int_{-1}^1 \frac{V_k V_n dv}{(1-v^2)} = 0 \quad \text{if } k \neq n$$

so that

$$\tau_k = - \frac{\int w \epsilon l^2 \int_{s_{tot}} E_a (u_i^2 - v^2)^{\frac{1}{2}} V_k dv}{U'_{k_3(u_i)} \int_{-1}^1 \frac{V_k^2 dv}{(1-v^2)}}. \quad (42)$$

The actual evaluation of the coefficients is done in terms of the series (38) and (40) so that

$$\tau_k = - \frac{\int w \epsilon l^2 \sum_n d_{kn} \int_{s_{tot}} E_a (u_i^2 - v^2)^{\frac{1}{2}} P_n^1 dv}{U'_{k_3(u_i)} \sum_n d_{kn}^2 \int_{-1}^1 (P_n^1)^2 dv}.$$

In the numerical calculation of the  $\nabla$ -functions, there is an arbitrary constant to be chosen. It appears from the latter equation that a very convenient choice would be one which leads to the following equation:

$$\sum_n d_{kn}^2 \int_{-1}^1 (P_n^1)^2 dv = \sum_n d_{kn}^2 \frac{2n(n+1)}{2n+1} = 1$$

The arbitrary constant is so chosen in the calculation described in Section 2.2.3.

Also, in the calculation of the distant field, it is convenient to have a familiar asymptotic form for the  $U$ -functions as  $\beta u \rightarrow \beta + \infty$ . The arbitrary constant in the Bessel function series for these functions



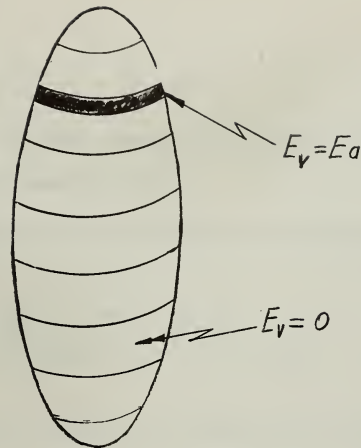


FIGURE 8 SPHEROIDAL RADIATOR

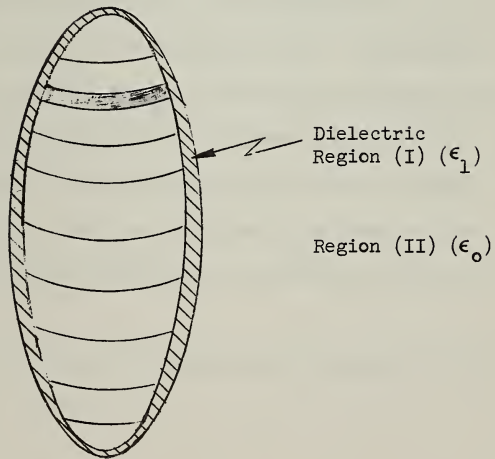


FIGURE 9 SPHEROIDAL RADIATOR WITH DIELECTRIC COATING



is chosen so that

$$\mathcal{U}_k(\beta lu) \xrightarrow{u \rightarrow \infty} \hat{\mathcal{Z}}_k(\beta lu) ,$$

that is, the  $\mathcal{U}$ -function is made asymptotically equal to the corresponding order of spherical Bessel function.

With these normalizations, the equation for calculating the distant field becomes

$$H_\phi = \frac{e^{-j\beta lu}}{\ell u(1-u^2)^{\frac{1}{2}}} \sum j^{k+1} \sigma_k V_k \quad (43)$$

### 2.2.2 Conducting Prolate Spheroid with Dielectric Coating

Let the conducting spheroid coincide with the surface  $u = u_1$ , and let the dielectric coating extend from the surface  $u = u_1$  to the surface  $u = u_2$ . The dielectric region will be designated (I) and the remainder of exterior space will be designated (II). Differential equations of the type (36) and (37) apply to both regions; however, the propagation constants and the eigenvalues are different for the two regions. This complicates the boundary value problem since the eigenfunctions on one side of the boundary are different from those on the other side of the boundary, which means that the coefficients cannot be equated term by term.

In region (I), the equations for the tangential components are the same as (8) and (10), with  $\epsilon = \epsilon_1$ ,



$$H_{\phi r} = \left[ l^2(u^2 - 1)(1 - v^2) \right]^{-\frac{1}{2}} \sum_k (a_k U_{k1} + b_k U_{k2}) V_k \quad (8p)$$

$$E_{vr} = - \left[ \frac{(u^2 - v^2)(1 - v^2)}{\jmath \omega \epsilon_0 l^2} \right]^{\frac{1}{2}} \sum_k (a_k \frac{dU_{k1}}{du} + b_k \frac{dU_{k2}}{du}) V_k \quad . \quad (10p)$$

In region (II), the equations are of the type of (40) and (41); however, in writing the expressions, the eigenvalue symbol,  $\lambda$ , will be replaced by the letter  $j$ , to underscore the fact that the functions are different in the two regions:

$$H_{\phi II} = \left[ l^2(u^2 - 1)(1 - v^2) \right]^{-\frac{1}{2}} \sum_j c_j U_{j3} V_j \quad (40a)$$

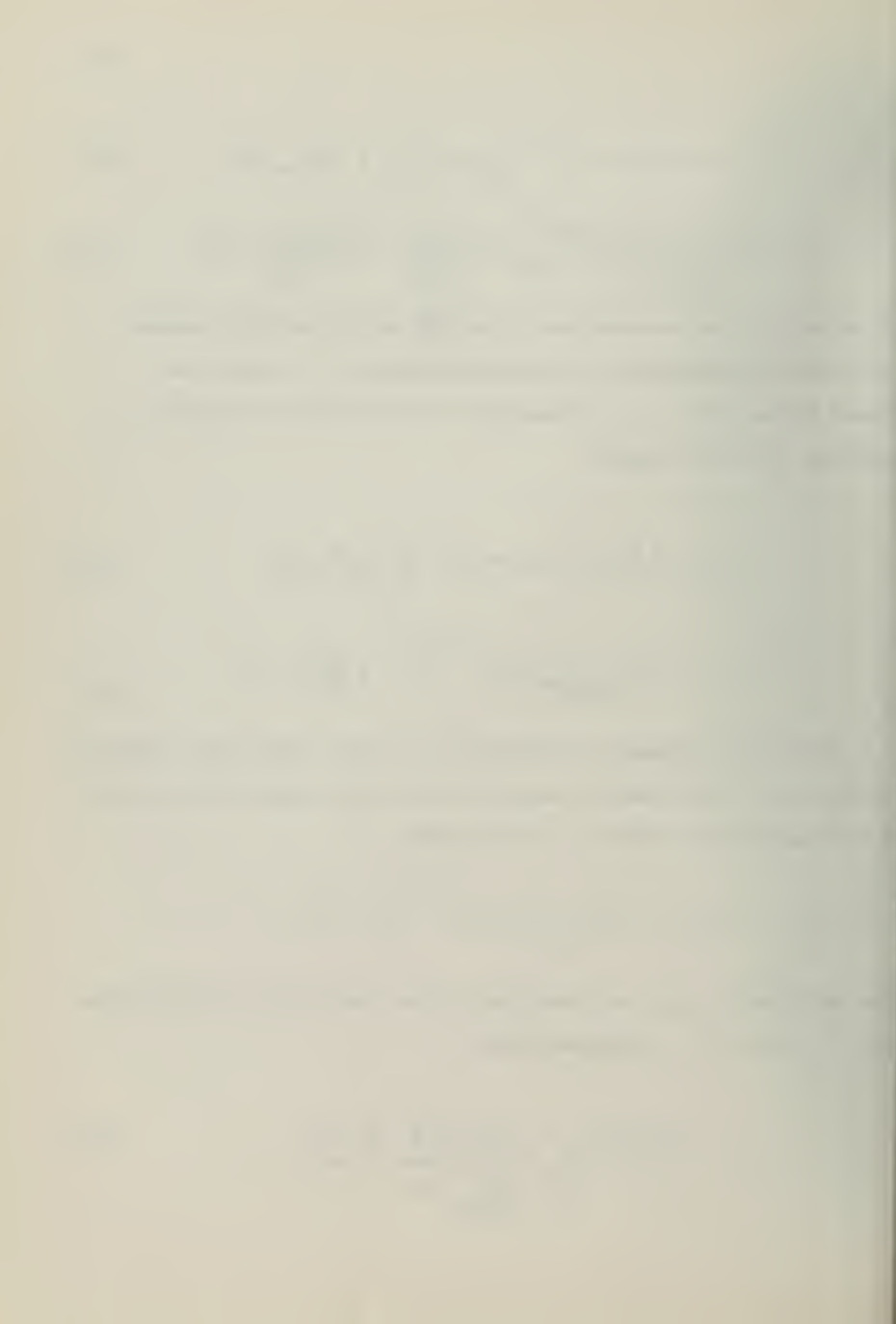
$$E_{vr} = - \left[ \frac{(u^2 - v^2)(1 - v^2)}{\jmath \omega \epsilon_0 l^2} \right]^{\frac{1}{2}} \sum_j c_j \frac{dU_{j3}}{du} V_j \quad . \quad (41a)$$

The field is presumed to be known over the inner (conducting) spheroidal surface,  $u_1$ , (the tangential electric field is zero except over the slots) and is expanded in a series of  $V$ -functions:

$$E_{vr} \Big|_{u=u_1} = E_a = - \left[ \frac{(u_1^2 - v^2)(1 - v^2)}{\jmath \omega \epsilon_0 l^2} \right]^{\frac{1}{2}} \sum_k \alpha_k V_k \quad .$$

The coefficients,  $\alpha_k$ , are determined in the usual way by a multiplication by  $\sqrt{n}(1 - v^2)^{\frac{1}{2}}$ , with the result:

$$\alpha_k = - \frac{\jmath \omega \epsilon_0 l^2 \int_{slot} E_a \left[ \frac{u_1^2 - v^2}{1 - v^2} \right]^{\frac{1}{2}} V_k dv}{\int_{-1}^1 \frac{V_k^2}{(1 - v^2)} dv} \quad . \quad (42a)$$



The actual computation of these coefficients can be done with Legendre polynomials and  $\ell$ -coefficients as indicated in Section 2.2.1, under Eq. 42. Thus, the application of the boundary condition at the surface  $u_1$  leads to a set of  $k$  equations in the unknown coefficients  $a_k$  and  $b_k$ , as follows:

$$a_k \frac{dU_{k_1}(\beta, l u_1)}{du} + b_k \frac{dU_{k_2}(\beta, l u_1)}{du} = \alpha_k . \quad (44)$$

Two more sets of equations are obtained from the boundary conditions at the surface  $u = u_2$ . The condition on the magnetic field gives the result

$$\sum_k (a_k U_{k_1}(\beta, l u_2) + b_k U_{k_2}(\beta, l u_2)) \frac{V_k}{(1-v^2)^{\frac{1}{2}}} = \sum_j c_j U_{j_3}(\beta, l u_2) \frac{V_j}{(1-v^2)^{\frac{1}{2}}} \quad (45).$$

while the condition on the electric field gives the equation

$$\sum_k (a_k \frac{dU_{k_1}(\beta, l u_2)}{du} + b_k \frac{dU_{k_2}(\beta, l u_2)}{du}) \frac{V_k}{(1-v^2)^{\frac{1}{2}}} = \frac{\epsilon_1}{\epsilon_0} \sum_j c_j \frac{dU_{j_3}}{du} \frac{V_j}{(1-v^2)^{\frac{1}{2}}} \quad (46).$$

Equation 44 can be employed to remove the variable,  $b_k$ , from Eqs. 45 and 46 as follows:

$$b_k = \frac{\alpha_k - a_k \frac{U'_{k_1}(\beta, l u_1)}{U'_{k_2}(\beta, l u_1)}}{U'_{k_2}(\beta, l u_1)}$$

so

$$\sum_k \left[ a_k (U_{k_1}(\beta, l u_2) - \frac{U'_{k_1}(\beta, l u_1)}{U'_{k_2}(\beta, l u_1)} U_{k_2}(\beta, l u_2)) \right] \frac{V_k}{(1-v^2)^{\frac{1}{2}}}$$

$$+ \sum_k \alpha_k \frac{U_{k_2}(\beta, l u_2)}{U'_{k_2}(\beta, l u_1)} \frac{V_k}{(1-v^2)^{\frac{1}{2}}} = \sum_j c_j U_{j_3}(\beta, l u_2) \frac{V_j}{(1-v^2)^{\frac{1}{2}}},$$



$$\sum_k \left[ \alpha_k \left( U'_{k_1}(\beta, l u_1) - \frac{U'_{k_2}(\beta, l u_1)}{U'_{k_2}(\beta, l u_1)} U'_{k_2}(\beta, l u_2) \right) \right] \frac{V_k}{(1-v^2)^{\frac{1}{2}}}$$

$$+ \sum_k \alpha_k \frac{U'_{k_2}(\beta, l u_2)}{U'_{k_2}(\beta, l u_1)} \frac{V_k}{(1-v^2)^{\frac{1}{2}}} = \frac{\varepsilon_1}{\varepsilon_0} \sum_j c_j U'_{j_3}(\beta, l u_2) \frac{V_j}{(1-v^2)^{\frac{1}{2}}}.$$

The quantities  $V_k$  and  $V_j$  can be replaced as follows:

$$\frac{V_k}{(1-v^2)^{\frac{1}{2}}} = \sum_n d_{kn}(\beta, l) P_n^1, \quad \frac{V_j}{(1-v^2)^{\frac{1}{2}}} = \sum_n d_{jn}(\beta, l) P_n^1.$$

The reason for the latter step is that now the corresponding orders of the Legendre polynomials can be equated term by term, whereas this is not possible for the  $\checkmark$ -functions. When this is done, and the substitutions

$$B_k \equiv U_{k_1}(\beta, l u_1) - U'_{k_1}(\beta, l u_1) \frac{U'_{k_2}(\beta, l u_2)}{U'_{k_2}(\beta, l u_1)}$$

$$B'_k \equiv U'_{k_1}(\beta, l u_1) - U'_{k_1}(\beta, l u_1) \frac{U'_{k_2}(\beta, l u_2)}{U'_{k_2}(\beta, l u_1)}$$

are introduced to save writing, the result is

$$\sum_k \alpha_k B_k d_{kn}(\beta, l) + \alpha_k \frac{U_{k_2}(\beta, l u_2)}{U'_{k_2}(\beta, l u_1)} d_{kn}(\beta, l) = \sum_j c_j U'_{j_3}(\beta, l u_2) d_{jn}(\beta, l) \quad (47)$$

$$\sum_k \alpha_k B'_k d_{kn}(\beta, l) + \alpha_k \frac{U'_{k_2}(\beta, l u_2)}{U'_{k_2}(\beta, l u_1)} d_{kn}(\beta, l) = \frac{\varepsilon_1}{\varepsilon_0} \sum_j c_j U'_{j_3}(\beta, l u_2) d_{jn}(\beta, l) \quad (48)$$



These latter equations, (47) and (48), must be solved for the unknown coefficients  $C_j$  (and  $a_k$ ). The equations are valid for each value of  $n$ , so that each of the equations can be written down the number of times which is required to solve for the  $k+j$  unknown coefficients. Of course, the solutions to the equations are strictly correct only for an infinite set. However, the series expansion of the fields, and those for the  $\sqrt{-}$ -functions, are presumed to be convergent representations. Hence, it will be permissible in an actual computation to replace the infinite sums by sums having a finite number of terms. Then, the number of equations which must be handled is, of course, at least twice the number of terms,  $N$ , which are required for a sufficiently accurate distant field representation. The fact that the  $d_{kn}$ -coefficients peak rather sharply about the value,  $d_{kk}$ , (i.e. the  $\sqrt{-}$ -function of a given order closely resembles the Legendre polynomial of the corresponding order) means that a finite set of equations can be essentially decoupled from the infinite set, and this finite set may not be appreciably greater than the minimum number required ( $2N$ ). Hence, in practice, one can start with some small number of equations (say a number of equal to three times  $\beta_l$ ), obtain the solutions, then increase the number successively in steps of four and repeat until the following two conditions are satisfied: 1) The coefficients determined do not change appreciably as the number of equations is increased and 2) the magnitude of the highest order coefficients determined are some small percentage of the largest (the latter condition will guarantee the former, but the largest coefficient may sometimes be hard to find).



It is worthy of special mention that the odd orders and the even orders are completely decoupled, and this good fortune cuts the number of simultaneous equations in a set in half. However, the  $\alpha_k$ 's and  $C_j$ 's (and perhaps the  $\alpha_k$ 's) are complex numbers, and the necessity for equating the real parts and the imaginary parts separately doubles the number again.

Once the  $C_j$ 's have been determined, Eq. 41a can be used to determine the distant field, wherein the  $U_{j3}$ -function is replaced by its asymptotic form, as was done in Eq. 43.

### 2.2.3 Numerical Calculations Associated with Prolate Spheroidal Radiators

There are two very serious obstacles to the carrying out of the numerical calculations for spheroidal radiators. The first is the sparsity of tabulated values of the functions (especially for large values of  $\beta l$ ), as well as the lack of a thorough study of the properties of the functions), and the second is the difficulty of handling the large systems of equations which arise in the coated spheroid problem. Both of these obstacles can be surmounted with the aid of a large scale digital computer. The next few pages describe briefly the system by which the spheroidal functions,  $V_k$  and  $U_k$  were calculated in connection with the present work.

The similarity of the differential equation, (37), for the  $V$ -functions to the corresponding equation in spherical coordinates, (12), suggests that the  $V$ -functions can be determined from a series of the spherical functions. Thus, since the  $V_s$  functions which are the solutions to (12)



form a complete orthogonal set, it is possible to represent the spheroidal functions in a series as follows:

$$V_k = \sum_{n=1}^{\infty} d_{kn} V_{sn} .$$

If this series is substituted into Eq. 37, and the necessary conditions of convergence assumed, the result is

$$(1-v^2) \sum_n d_{kn} V_{sn}'' + (k_k - (\beta l v)^2) \sum_n d_{kn} V_{sn} = 0 .$$

Equation 12, with  $k_s = n(n+1)$ , can be multiplied by constants  $d_{kn}$  and the results added together to give the equation

$$(1-v^2) \sum_n d_{kn} V_{sn}'' + \sum_n n(n+1) d_{kn} V_{sn} = 0 .$$

From these latter two equations, the following result can be obtained:

$$\sum_{n=1}^{\infty} d_{kn} (k_k - n(n+1) - (\beta l v)^2) V_{sn} = 0 .$$

In view of the identity,

$$V_{sn} = (1-v^2)^{\frac{1}{2}} P_n^1 ,$$

the result in terms of the more familiar Legendre polynomials is equally valid:

$$\sum_{n=1}^{\infty} d_{kn} (k_k - n(n+1) - (\beta l v)^2) P_n^1 = 0 . \quad (49)$$

From this equation (for a particular  $k$ ), a whole set of equations can be generated by utilizing the orthogonality properties of the Legendre polynomials, and this is a particularly fruitful step since, as discussed in Appendix A, it results in stationary expressions for the determination of



the eigenvalues, as well as recurrence relationships for the coefficients. To generate the new set of equations, we can imagine multiplying Eq. 49 first by a Legendre polynomial of order one, then by one of order two, and so on. Each equation so obtained is then integrated over the complete range of orthogonality (-1 to +1). The process can be symbolized as follows:

$$\int_{-1}^1 \sum_n d_{kn} (k_k - n(n+1) - (\beta \ell v)^2) P_n^1 P_m^1 dv = 0$$

or

$$\sum_n d_{kn} \left[ k_k - n(n+1) \int_{-1}^1 P_n^1 P_m^1 dv - (\beta \ell)^2 \int_{-1}^1 v^2 P_n^1 P_m^1 dv \right] = 0. \quad (50)$$

With the recurrence relationship for Legendre polynomials to be found in Section 2.1.3, the last integral can be transformed and evaluated in general, and the value of the first integral is well known. The actual values for the integrals depend on whether the Legendre polynomials are normalized. The results for both situations are included here, since the coefficients  $d_{kn}$  are best obtained from the unnormalized results, while the eigenvalues are most easily obtained from the normalized result.

If the Legendre polynomials are not normalized, the integrals are evaluated as follows:

$$\begin{aligned} \int_{-1}^1 P_n^1 P_m^1 dv &= \frac{2n(n+1)}{2n+1}, \quad n=m \\ &= 0, \quad n \neq m \end{aligned};$$

$$\begin{aligned} \int_{-1}^1 v^2 P_n^1 P_m^1 dv &= [(2n+1)(2m+1)]^{-1} \left[ \int_{-1}^1 n_m P_{n+1}^1 P_{m+1}^1 dv + \right. \\ &\quad \left. (n+1)(m) \int_{-1}^1 P_{m+1}^1 P_{n-1}^1 dv + n(m+1) \int_{-1}^1 P_{n+1}^1 P_{m-1}^1 dv + (n+1)(m+1) \int_{-1}^1 P_{n-1}^1 P_{m-1}^1 dv \right]. \end{aligned}$$



It is clear from this form that the latter integral in Eq. 50 is zero unless a)  $m = n$  b)  $m = n-2$  or c)  $m = n+2$ . Thus, the typical member of the set of equations has the form

$$d_{k,n-2} \left[ \frac{-(\beta l)^2(n-2)(n-1)}{(2n-1)(2n-3)} \right] + d_{k,n} \left[ k_k - n(n+1) - (\beta l)^2 \left( \frac{2n(n+1)-3}{(2n-1)(2n+3)} \right) \right] \\ + d_{k,n+2} \left[ \frac{-(\beta l)^2(n+2)(n+3)}{(2n+3)(2n+5)} \right] = 0 .$$

This is the result which was stated earlier in Eq. 39. These relationships can be employed to determine the coefficients, once the eigenvalues,  $k_k$ , have been determined.

In the eigenvalue calculation, for practical reasons which will become clear below, it is helpful to employ normalized Legendre polynomials. The integrals are evaluated in the same way as that indicated above for the unnormalized functions. The equations which are so obtained can be symbolized as follows:

$$\sum_n d_{kn} L_{nm} = 0 \quad (51)$$

or by the matrix equation

$$\mathcal{D} \mathcal{L} = 0$$

in which

$$L_{nm} = k_k - n(n+1) - (\beta l)^2 \left[ \frac{2n(n+1)-3}{(2n-1)(2n+3)} \right], \quad m = n$$

$$L_{n,n+2} = L_{n-2,m} = \frac{-(\beta l)^2}{2n+3} \left[ \frac{(n+3)(n+2)(n+1)n}{(2n+5)(2n+1)} \right]^{\frac{1}{2}}, \quad \begin{matrix} m' = n'-2 \\ m = n+2 \end{matrix}$$

$$L_{nm} = 0, \text{ otherwise}$$



The conditions for the consistency of the set of Eqs. 51 is the vanishing of the determinant of the coefficients as follows:

$$\left| L_{nm} \right| = 0 . \quad (52)$$

The eigenvalues,  $k_k$ , are those numbers for which Eq. 52 is satisfied.

The problem of eigenvalue determination is thus in this case equivalent to the problem of finding the eigenvalues of a symmetric (infinite) matrix.

The main object in developing the spheroidal functions in the fashion described is to take advantage of the service routines in the ILLIAC library which are capable of finding the eigenvalues of symmetric matrices as large as  $128 \times 128$ , with accuracy of 10 or 11 decimal places. The fact (as is shown in Appendix A) that the foregoing relationships have stationary properties, together with the potential sizes of matrices which can be handled, makes it possible to determine the eigenvalues of nearly all interesting orders of the functions in a relatively short time.

In the actual program, the equations (and therefore the eigenvalues) were scaled by  $((\beta l)^2)$ , and a routine was written which generates the matrix elements in the form required by the matrix eigenvalue service routine. It is worthy of special mention that the equations (coefficients) having  $n$  odd can be handled independently from those having  $n$  even, which means, for example, that to obtain a set of  $l$  eigenvalues, one needs to handle only  $\frac{l}{2}$  order matrices. The eigenvalues for  $\beta l = 5, 8$ , and 12 are presented in Table 7. The effect of matrix size was also investigated, with the surprising result that for  $\beta l = 8$ , for example,



except for the last five or six values, a  $23 \times 23$  matrix gives results which agree with those given by a  $40 \times 40$  matrix.

With the eigenvalues so determined, Eq. 39 can be employed to find the coefficients. However, as with the Bessel functions of the first kind, (see Section 2.1.3), a straight upward use of the recursion form is not generally practicable. In the programs for this work, the coefficients for the lower order functions were evaluated by a downward continued fractions technique, the form of which can be obtained by rewriting Eq. 39 in a fashion similar to that described in Section 2.1.3 in connection with the  $\hat{J}_n$  functions. For the higher order functions, this scheme was employed for those coefficients  $d_{kn}$  in the range  $n \geq k$ . Then a switch was made and the remaining coefficients  $d_{kn}$ ,  $1 \leq n \leq k$ , were calculated from the recurrence formulas in a straight upward fashion (this double-barreled approach proved to be absolutely essential in the calculation of the higher order functions). The coefficients were all generated on the assumption that  $d_{kk} = 1$ , and then were normalized by dividing each by dividing each by the quantity,  $\sum_n d_{kn}^2 \frac{2n(n+1)}{2n+1}$ . This normalization is equivalent to an adjustment of the functions so as to give the following equation:

$$\int_{-1}^1 \frac{V_k^2}{(1-v^2)} dv = \sum_n d_{kn}^2 \int_{-1}^1 (P_n^1)^2 dv = 1.$$

This result is particularly convenient in the numerical work associated with Eqs. 42 and 42a.

The quantities which are needed in the radiation problem are those as follows (see Eq. 40 for example):



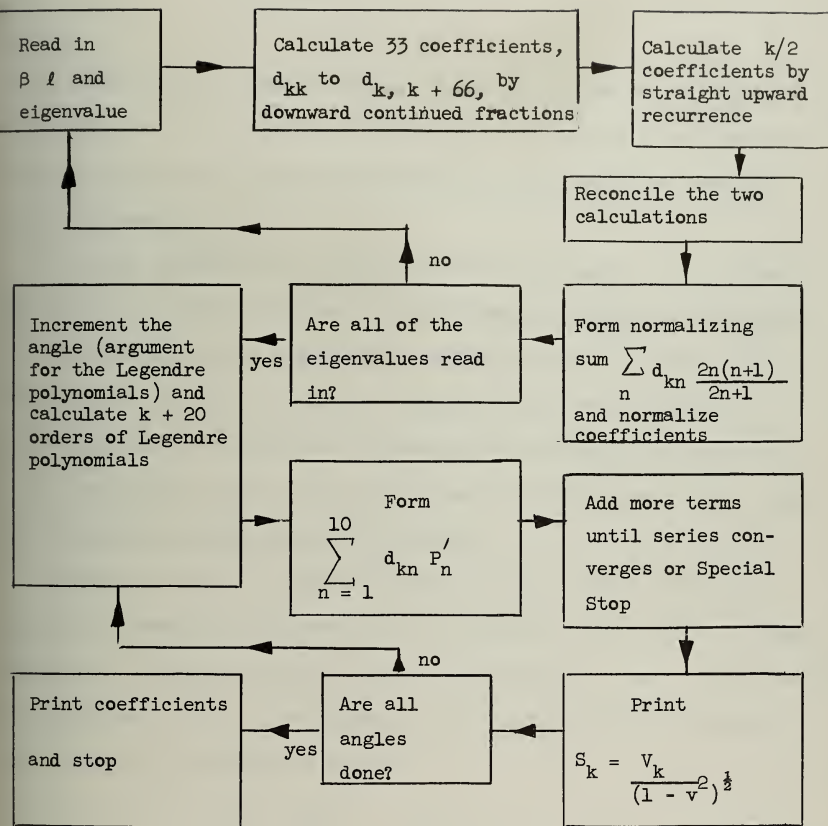


FIGURE 10 SIMPLIFIED FLOW CHART FOR MACHINE CALCULATION OF SPHEROIDAL  $V$ -FUNCTIONS



$$\frac{V_k}{(1-u^2)^{\frac{1}{2}}} = \sum_n d_{kn} P_n^1 .$$

These quantities are computed by the ILLIAC using a program, a simplified flow chart for which is given in Figure 10. The details of the calculation, and some of the values computed will be published in a separate technical report.

The next problem is the evaluation of the functions  $U$ , which satisfy Eq. 36. It is necessary to obtain two independent solutions for Eq. 36, those which are respectively analogous to the  $\hat{J}_n$  and  $\hat{N}_n$  functions in spherical coordinates, together with their derivatives. These independent solutions are identified by the symbols  $U_{k_1}$  and  $U_{k_2}$  in the preceding sections. The calculation of the function  $U_{k_2}$  and its derivative presents the most difficulty.

Equation 36 bears a strong resemblance to the radial differential equation in spherical coordinates (Eq. 11 with  $k_s = n(n+1)$ ). It seems appropriate therefore to try to express the functions,  $U_k$ , in terms of the functions,  $\hat{Z}_n$ . Consequently, it is assumed that the solutions to Eq. 36 can be expressed as follows:

$$U_k = \sum_{-\infty}^{\infty} a_{kn} \hat{J}_n(\beta \mu) . \quad (53)$$

(Publications by Schmid<sup>8</sup> imply that such a representation may be mathematically proper.) Assuming the necessary conditions of convergence, this series is substituted into Eq. 36. The properties of the function as dictated by Eq. 11 are employed to reduce the result to the statement



$$\sum_n a_{kn} \hat{J}_n'' + \sum_n (k - n(n+1)) a_{kn} \hat{J}_n = 0 . \quad (54)$$

With a repeated use of the expression for the derivative function,

$$\frac{d}{dx} \hat{J}_n = \frac{1}{2n+1} \left[ (n+1) \hat{J}_{n-1} - n \hat{J}_{n+1} \right] ,$$

the term involving the second derivative can be replaced, and Eq.

54 put into the form

$$\sum_{n=-\infty}^{\infty} \frac{a_{kn} (\beta l)^2}{(2n+1)} \left[ \frac{n(n+1)}{2n-1} \hat{J}_{n-2} - \hat{J}_n \left[ \frac{(n+1)(n-1)}{2n-1} + \frac{n(n+2)}{2n+3} \right] + \hat{J}_{n+2} \frac{n(n+1)}{2n+3} \right]$$

$$+ \sum_{n=-\infty}^{\infty} a_{kn} (k - n(n+1)) \hat{J}_n = 0 .$$

If now the coefficients of the terms,  $\hat{J}_n$ , are individually put equal to zero, the resulting expressions can be put into a form as follows:

$$\begin{aligned} a_{k,n-2} & \left[ \frac{(n-2)(n-1)}{(2n-3)(2n-1)} \right] + a_{k,n} \left[ \frac{k - n(n+1)}{(\beta l)^2} - \frac{2n(n+1) - 3}{(2n-1)(2n+3)} \right] \\ & + a_{k,n+2} \left[ \frac{(n+2)(n+3)}{(2n+3)(2n+5)} \right] = 0 . \end{aligned} \quad (55)$$

Note the similarity of this relationship to that of Eq. 39. The similarity is such that if the condition  $a_{kk} = d_{kk}$  were imposed, the magnitudes of the remaining coefficients would be equal. (The signs would be such that  $a_{k,k+2} = -d_{k,k+2}$ ,  $a_{k,k+4} = d_{k,k+4}$ , and so on, alternating.) As with the coefficients, if  $k$  is odd (even), only the odd (even) coefficients are non-zero.



A glance at the first term in (55) shows that the positive side of the recurrence chain breaks off at  $n=1$  and  $n=2$ , while from the last term it is clear that the negative side of the recurrence chain breaks off at  $n=-2$  and  $n=-3$ . As a result, the value of  $a_{kn}$  corresponding to one of these particular four values can be assigned, and on the basis of this assignment, a positive (negative) side, odd (even) set of coefficients can be determined. Furthermore, if it happens that  $a_{k,1} = a_{k,-2}$ ,  $a_{k,2} = a_{k,-3}$ , then the coefficients generated on the positive side from  $a_{k,1}$  ( $a_{k,2}$ ) are the same as those generated on the negative side by  $a_{k,-2}$  ( $a_{k,-3}$ ), since in Eq. 55,  $n$  can be changed to  $-(n+1)$  without a change in the equation. Thus, suppose for example one of the coefficients, say  $a_{k,1}$ , is assigned a value. Then, since Eq. 36 is a differential equation of second order, there is still one constant to be assigned. If this second constant is set by putting  $a_{k,-3}=0$  ( $a_{k,1}$  assigned), the coefficients are all determined, and the series gives the spheroidal functions of the first kind, as follows:

$$U_{k_1} = \sum_{n=-1,0}^{\infty} a_{kn} \hat{J}_n(\beta \ell u) \quad (56)$$

where the prime indicates that the sum is on odd (even) values of  $n$  only. (The even set results from the assignment of  $a_{k,+2}$ , with  $a_{k,-2}=0$ .) On the other hand, if  $a_{k,-2}$  ( $a_{k,-3}$ ) is assigned to fix one of the constants, while  $a_{k,2}$  ( $a_{k,1}$ ) is put equal to zero to fix the other, the series is

$$U_{k_2} = \sum_{n=-\infty}^{0,1} a_{kn} \hat{J}_n(\beta \ell u) . \quad (57)$$



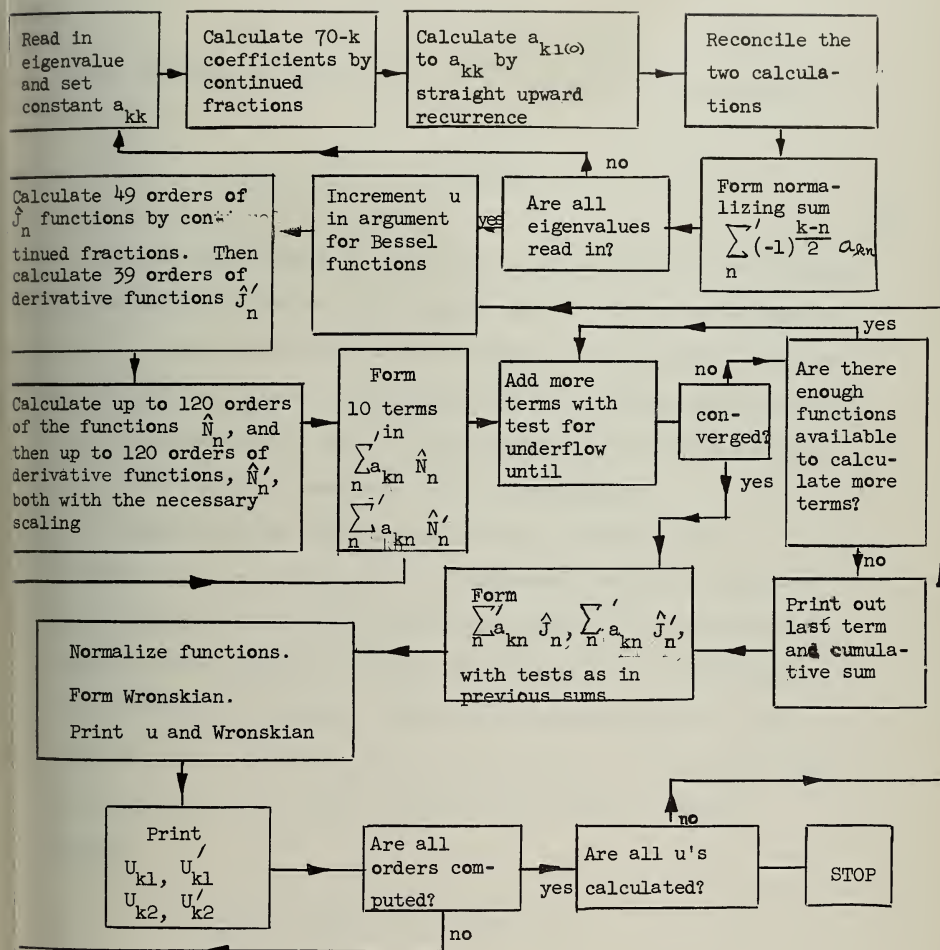


FIGURE 11 SIMPLIFIED FLOW CHART FOR CALCULATION OF THE SPHEROIDAL  $U$ -FUNCTIONS



In practice it is convenient to take advantage of the relationship

$$\hat{J}_n = (-1)^{n-1} \hat{N}_{n-1}$$

and so transform the series, (57), into a sum over positive values of

$n$ ,

$$U_{k_2} = \sum_{n=1,0}^{\infty} a_{kn} \hat{N}_n(\beta lu) \quad (58)$$

in which the coefficients are identical to those in Eq. 56. Unfortunately, the series (58) converges rather slowly when  $u$  is in the neighborhood of unity. Some difficulties were encountered in the programs which were written for the ILLIAC in the calculations of the higher order functions, since the magnitudes of the  $\hat{N}_n$ -functions approach machine capacity before the functions converge to a desirable accuracy.

A simplified flow chart of the program to calculate the  $\hat{N}$ -functions is given in Fig. 11. An interesting feature of this program is the print out which indicates that there is an insufficient number of terms available and also provides a measure of the over-all accuracy of the calculation. This latter is an internal check which is based upon the value of the Wronskian determinant of  $U_{k_1}$  and  $U_{k_2}$ . This quantity,  $\nabla W$ , has a constant value as can be shown as follows:

$$\frac{d \nabla W}{du} = U''_{k_1} U_{k_2} - U''_{k_2} U_{k_1} ,$$

$$(u^2 - 1) U''_{k_1} + ((\beta lu)^2 - k_2) U_{k_1} = 0 ,$$

$$(u^2 - 1) U''_{k_2} + ((\beta lu)^2 - k_1) U_{k_2} = 0 .$$



Multiply the first of these latter two equations by  $U_{k_2}$ , the second by  $U_{k_1}$ , and subtract, to obtain the result

$$U''_{k_1} U_{k_2} - U''_{k_2} U_{k_1} = 0$$

or

$$\nabla W = \text{constant} .$$

The value of the constant can be found by obtaining the solutions to (36) in the limit as  $u$  approaches infinity. In that case

$$U = A \cos \beta u + B \sin \beta u$$

so that

$$\nabla W = -\beta l .$$

In the program, after the independent calculation of each of the functions  $U_{k_1}$ ,  $U'_{k_1}$ ,  $U_{k_2}$ , and  $U'_{k_2}$ , the quantity

$$\frac{\nabla W}{\beta l} = \frac{1}{\beta l} [U'_{k_1} U_{k_2} - U'_{k_2} U_{k_1}]$$

is formed in the machine and the result printed out along with the functions.

The closeness of the number printed to the exact value, -1, is a good measure of the over-all accuracy of the calculation. A facsimile of a typical print out is given in Table 2.



TABLE 2. FACSIMILE OF A TYPICAL ILLIAC PRINT OUT  
OF THE SPHEROIDAL FUNCTIONS,  $U$ .

The first two lines of print indicate that there were not enough of the functions  $\hat{N}_n$ , and  $\hat{N}'_n$  to calculate  $U_{32}$  and  $U'_{32}$  to the specified accuracy. In these first two lines, the first number is the value of the last term computed, while the second number is the cumulative sum (both scaled). These numbers indicate that in this case the functions  $U_{32}$  and  $U'_{32}$  are good to about seven figures, and this is born out by the amount by which the scaled Wronskian differs from -1.

Number	exp.	Number	exp.
+21992	-69	+20614	-62
-281529	-68	+127821	-61
$u$		$W/\beta l$	
+11000	+01	-10000071	+01
$U_{31}$		$U'_{31}$	
+749599554	+00	-162453319	+01
			+206136057
			+00
			+102257024
			+02



For convenience in the calculation of the radiation pattern, the arbitrary constant ( $a_{k,1}$  and so on) can be fixed in such a way that as  $\beta \omega \rightarrow \infty$ ,

$$U_{k_1} \rightarrow \hat{J}_k(\beta \omega), U_{k_2} \rightarrow \hat{N}_k(\beta \omega) \text{ and } U_{k_3} \rightarrow \hat{H}_k(\beta \omega).$$

To accomplish this normalization, it is only necessary to enforce the following condition:

$$U_{k_3} = \sum_n a_{kn} \hat{H}_n(\beta \omega) \xrightarrow{\beta \omega \rightarrow \infty} \sum_n a_{kn} j^{n+1} e^{-j\beta \omega} = j^{k+1} e^{-j\beta \omega}$$

or

$$\sum_{n=-1,0}^{\infty} a_{kn} j^{(n-k)} = 1.$$

Since the sum is over only odd (even)  $n$ , this is accomplished in the machine by making  $a_{kk}$  positive, and changing the signs of alternate coefficients in the summation process.

The radiation patterns of the uncoated spheroid are then easily calculated, with the spheroidal functions determined in the way described above. The pattern calculation is based on Eqs. 42 and 43 and is done almost exactly as described in Section 2.1.3, with the spheroidal functions replacing the spherical functions as follows:  $U'_{k_1} \leftrightarrow \hat{J}'_n$ ,  $U'_{k_2} \leftrightarrow \hat{N}'_n$ , and  $V_k(1-v^2)^{-\frac{1}{2}} \leftrightarrow P_n^1$ . Some of the results are presented in Figs. 21 to 27, with some corresponding coated patterns alongside for comparison. The patterns in Fig. 21, for the smaller values of  $\beta L$ , were calculated on a desk calculator using functions modified from those computed by Myers and Wells<sup>9</sup>, and coefficients tabulated by Stratton, et al.<sup>10</sup>. These latter calculations were done early in the investigation to study the feasibility of the method and are subject to greater error than the others;



in these calculations, the digital computer was employed only to solve the systems of equations which arise in the coated spheroid problem (12 equations in 12 unknowns was the maximum size in this case).

The biggest job in the computation program is in connection with the coated spheroidal radiator. The calculation is based on Eqs. 47 and 48 and the operations indicated therein are carried out in exactly the manner indicated. Fortunately, the odd and even orders can be handled separately. The pair of equations, (47) and (48), are replaced by the four equations obtained by equating separately the real and imaginary parts of (47) and (48). A guess is made as to the number of equations required for convergence, and the augmented matrix for this number of equations is generated by the machine in the form required by the ILLIAC library service routine which obtains the solutions of a set of linear equations (a maximum of 143).

The variation of the coefficients,  $C_j$ , as a function of the number of equations was investigated. The results of one such investigation are presented in Table 3. It is clear from these data that the process, as discussed near the end of section 2.2.2, is actually a convergent one, and in principle could be carried out to any desired accuracy. The coefficients,  $\text{Re } C_j$ , and  $\text{Im } C_j$ , so calculated are fed back into the machine and used in the basic routine for radiation pattern calculation.

We now leave the study of prolate spheroidal radiators, and take up once more the study of the sphere, in order to remove the restriction of axial symmetry on the sources .



TABLE 3. COMPARISON OF THE COEFFICIENTS CALCULATED FROM DIFFERENT NUMBERS OF EQUATIONS IN THE COATED PROLATE SPHEROID PROBLEM.

The similarity in the numbers shows that the infinite system can be replaced by a finite system of equations. The example is for the parameters as follows:  $\beta_0 l = 5$ ,  $\beta_1 l = 8$ ,  $u_1 = 1.077$ ,  $u_2 = 1.1$ , slot at  $v = 0$ .

	20 equations	24 equations	28 equations	32 equations
$Re c_j$				
1	.035669646	.035669590	.035669589	.035669589
3	-.061748146	-.061748740	-.061748754	-.061748750
5	.009879699	.009881601	.009881658	.009881652
7	-.000092924	-.000092948	-.000092949	-.000092947
9	.000000405	.000000406	.000000406	.000000405
11		-.000000001	-.000000001	-.000000001
13			.000000000	.000000000
15				.000000000
$Im c_j$				
1	.048023926	.048023784	.048023780	.048023780
3	-.009061661	-.009061355	-.009061345	-.009061346
5	.033134300	.033143465	.033143727	.033143723
7	-.002083803	-.002083607	-.002083989	-.002083994
9	.000076310	.000083883	.000084252	.000084262
11		-.000002187	-.000002383	-.000002392
13			.000000045	.000000048
15				-.000000001



### 3. SPHERE WITH ARBITRARY SOURCE CONFIGURATIONS

The analysis for the fields which result from the excitation of a spheroidal conductor by an arbitrary slot is very complicated. In fact, it appears that only the sphere can be treated numerically with existing techniques. However, in spherical coordinates, it is possible to represent the fields in terms of a pair of scalars, as indicated in the following developments. In this process, one or the other of the field variables is eliminated from Maxwell's equations to obtain the vector Helmholtz equation

$$\nabla \times \nabla \times \mathbf{B} - \omega^2 \mu \epsilon \mathbf{B} = 0 \quad (59)$$

where  $\mathbf{B}$  is either  $\bar{\mathbf{E}}$  or  $\bar{\mathbf{H}}$ . The problem is then simplified by the division of all possible fields into parts in which either  $\bar{\mathbf{E}}$  or  $\bar{\mathbf{H}}$  is transverse to the radial direction, with consequent representation in terms of a vector (or Hertz) potential which has only an  $\hat{r}$ -component. Thus, for TM fields

$$\bar{\mathbf{H}} = \nabla \times f \hat{r} \quad (60)$$

and for TE fields

$$\bar{\mathbf{E}} = \nabla \times g \hat{r} \quad (61)$$

The substitution of (60) into (59) gives for example

$$\nabla \times \nabla \times f \hat{r} - \beta^2 f \hat{r} = \nabla \Psi \quad (62)$$

where  $\Psi$  is arbitrary. If  $\Psi$  is chosen so that  $\Psi = \frac{\partial f}{\partial r}$  the following equation is obtained for  $f$  :



$$\nabla^2 \left( \frac{f}{r} \right) + \beta^2 \left( \frac{f}{r} \right) = 0 \quad (63)$$

and a similar result can be obtained for  $g$ . The scalar Helmholtz equation, (62), is separable in spherical coordinates, and the solutions have the form

$$\frac{f}{r} = [a_{vm} j_v(\beta r) + b_{vm} n_v(\beta r)] \times [c_{vm} P_v^m(\cos\theta) + d_{vm} Q_v^m(\cos\theta)] \times [e_{vm} \cos m\phi + f_{vm} \sin m\phi], \quad (64)$$

with the constants selected so that the boundary conditions are satisfied. For the moment, for brevity, let the solutions for be represented as

$$f = R'(r) T'(\theta, \phi) \quad (65)$$

where  $R'(r)$  and  $T'(\theta, \phi)$  are defined appropriately. With this notation, expressions for the fields can be written as follows:

a) TM fields

$$\bar{H}_r = \nabla \times R' T' \hat{r} = -\hat{r} \times R' \nabla T' \quad (66)$$

$$j\omega \epsilon \bar{E} = -\hat{r} \cdot \nabla R' \nabla T' + \frac{\partial R'}{\partial r} \nabla T' \quad (67)$$

b) TE fields ( $g = R''(r) T''(\theta, \phi)$ )

$$\bar{E}_r = \nabla \times R'' T'' \hat{r} = -\hat{r} \times R'' \nabla T'' \quad (68)$$

$$-j\omega \mu \bar{H} = -\hat{r} \cdot \nabla \cdot R'' \nabla T'' + \frac{\partial R''}{\partial r} \nabla T'' . \quad (69)$$



Thus for example, the transverse component of any electric field can be written

$$\bar{E}_T = \sum_i R''_i \nabla T''_i \times \hat{r} + \frac{\partial R'_i}{\partial r} \nabla T'_i \quad (70)$$

where the constants in  $R'$ ,  $T'$ ,  $R''$ , and  $T''$ , are determined by application of the boundary conditions, and the summation over the index  $i$  is to be interpreted as a summation over terms involving all permissible combinations of  $\nu$  and  $m$  in Eq. 64.

In any complete region (including both  $\theta = 0$  and  $\theta = \pi$ ), the constant  $d'_{\nu m}$  in Eq. 64 must be zero, in order to avoid infinities on the z-axis, and the index  $\nu$  must be an integer. To simplify the analysis, it is convenient to treat separately the parts of the solution involving  $\sin m\phi$  (odd solutions) from those involving

$\cos m\phi$  (even solutions). It can also be seen that the quantity  $R$ , as defined from Eq. 64 will contain  $r$  as a multiplier. It is convenient therefore to represent the radial variations in terms of the functions  $\hat{J}_n(x) = x J_n(x)$  and  $\hat{N}_n(x) = x N_n(x)$ , which were employed in the analysis in the previous sections (let the constants absorb the quantity  $\beta$  which is also needed as a multiplier in order to change the functions). With these changes, and the definitions,

$T_{re} = P_n^m \cos m\phi$  and  $T_{ro} = P_n^m \sin m\phi$ , Eqs. 70 take the following form:

$$\begin{aligned} \bar{E}_T = & \sum_n (a''_{nme} \hat{J}_n(\beta r) + b''_{nme} \hat{N}_n(\beta r)) \nabla T_{re} \times \hat{r} \\ & + (a''_{nmo} \hat{J}_n + b''_{nmo} \hat{N}_n) \nabla T_{ro} \times \hat{r} \\ & + \frac{1}{j\omega\epsilon} (c'_{nme} \frac{d\hat{J}_n}{dr} + d_{nme} \frac{d\hat{N}_n}{dr}) \nabla T_{re} \\ & + \frac{1}{j\omega\epsilon} (c'_{nmo} \frac{d\hat{J}_n}{dr} + d'_{nmo} \frac{d\hat{N}_n}{dr}) \nabla T_{ro} \end{aligned} \quad (71)$$



It is convenient in the theoretical discussions to define vector functions as follows:

$$\bar{e}_{\text{eg}}'' = \nabla T_{\text{eg}} \times \hat{r} , \quad \bar{e}_{\text{eg}}' = \nabla T_{\text{eg}}$$

along with appropriate scalar functions of  $\hat{r}$  so that Eq. 71 can be written in the simpler form

$$\bar{E}_T = \sum \mathcal{V}_{ie}''(\beta r) \bar{e}_{ie}'' + \mathcal{V}_{io}''(\beta r) \bar{e}_{io}'' + \mathcal{V}_{ie}'(\beta r) \bar{e}_{ie}' + \mathcal{V}_{io}'(\beta r) \bar{e}_{io}' . \quad (72)$$

It is shown in Appendix B that the vector functions  $\bar{e}_{\text{eg}}''$  and  $\bar{e}_{\text{eg}}'$  have orthogonality properties which permit field expansions of the vector  $E_T$  rather than one component of it as was done in the case of axially symmetric excitation. In the next section, the use of these expansions in the solutions for a conducting sphere in free space is illustrated. The development serves the dual purpose of providing a review for the reader and standardizing the notation so that comparisons to the dielectric coated sphere problem can be more readily made.

### 3.1 The Slot Excited Conducting Sphere in Free Space

Let a conducting sphere of radius  $r_i$  be excited by applying a (known) electric field in an opening which is cut somewhere on its surface. Then, the electric field is known everywhere on the surface,  $\hat{r} = \hat{r}_i$ , viz., it is zero over most of the surface and  $\bar{E}_{Ta}$  in the slot opening. Thus, from (72), the following equation can be written:

$$\bar{E}_T \Big|_{\hat{r}=\hat{r}_i} = \bar{E}_{Ta} = \sum_i \mathcal{V}_{ie}''(\beta_0 r_i) \bar{e}_{ie}'' + \mathcal{V}_{io}''(\beta_0 r_i) \bar{e}_{io}'' + \mathcal{V}_{ie}'(\beta_0 r_i) \bar{e}_{ie}' + \mathcal{V}_{io}'(\beta_0 r_i) \bar{e}_{io}' . \quad (73)$$



Since  $\bar{E}_{T_0}$  is known, the orthogonality relations listed (and demonstrated) in Appendix B can be employed to determine the following equation for the excitation expansion coefficients:

$$U_{ie}''(\beta_0 r_i) = \frac{\int_{S_{tot}} \bar{E}_{T_0} \cdot \bar{e}_{ie}'' dS}{\int_{r=r_i} e_{ie}''^2 dS} \quad (74)$$

$$U_{eo}''(\beta_0 r_i) = \frac{\int_{S_{tot}} \bar{E}_{T_0} \cdot \bar{e}_{eo}'' dS}{\int_{r=r_i} e_{eo}''^2 dS} \quad (75)$$

$$U_{ie}'(\beta_0 r_i) = \frac{\int_{S_{tot}} \bar{E}_{T_0} \cdot \bar{e}_{ie}' dS}{\int_{r=r_i} e_{ie}'^2 dS} \quad (76)$$

$$U_{eo}'(\beta_0 r_i) = \frac{\int_{S_{tot}} \bar{E}_{T_0} \cdot \bar{e}_{eo}' dS}{\int_{r=r_i} e_{eo}'^2 dS} \quad (77)$$

Of course, Eq. 73 with the coefficients calculated from (74)-(77) must be exactly equal to Eq. 71 with  $r$  set equal to  $r_i$ . For the problem of the conducting sphere in free space, however, Eq. 71 is simplified because of the requirement that the solution must represent outgoing waves as  $r \rightarrow \infty$ . This implies that the constants in (71) must be related as follows:

$$a_{nm} = -j b_{nm}, \quad c_{nm} = -j d_{nm} \quad . \quad (78)$$

Thus, the expression for the transverse electric field can be written



$$\bar{E}_r = \sum_n a''_{nm\theta} \hat{H}_n(\beta_0 r) \bar{e}_{r\theta}'' + \frac{c'_{nm\theta}}{jw\epsilon_0} \frac{d\hat{H}_n(\beta_0 r)}{dr} \bar{e}_{r\theta}' . \quad (79)$$

An evaluation of this expression at  $r = r_i$ , and subsequent comparison of it to Eq. 73 indicates the manner in which the constants can be evaluated numerically, and the result is

$$a''_{nm\theta} = \frac{\mathcal{V}_{r\theta}''(r_i)}{\hat{H}_n(\beta_0 r_i)} = \frac{\int_{S_{TOT}} \bar{E}_{Ta} \cdot \bar{e}_{r\theta}'' dS}{\hat{H}_n(\beta_0 r_i) \int_{r=r_i} e_{r\theta}''^2 dS} \quad (80)$$

$$c'_{nm\theta} = \frac{jw\epsilon_0 \mathcal{V}_{r\theta}'(r_i)}{\frac{d\hat{H}_n(\beta_0 r_i)}{dr}} = \frac{jw\epsilon_0 \int_{S_{TOT}} \bar{E}_{Ta} \cdot \bar{e}_{r\theta}' dS}{\frac{d\hat{H}_n(\beta_0 r_i)}{dr} \int_{r=r_i} e_{r\theta}'^2 dS} . \quad (81)$$

The best form for the computation of the fields is probably

$$\begin{aligned} \bar{E}_r &= \sum_n a''_{nm\theta} \hat{H}_n(\beta_0 r) \left[ \frac{\hat{\theta} m}{r \sin \theta} P_n^m \left\{ \begin{matrix} -\sin m\phi \\ \cos m\phi \end{matrix} \right\} - \frac{\hat{\phi}}{r} \frac{dP_n^m}{d\theta} \left\{ \begin{matrix} \cos m\phi \\ \sin m\phi \end{matrix} \right\} \right] \\ &\quad + \sum_n c'_{nm\theta} \frac{d\hat{H}_n(\beta_0 r)}{dr} \left[ \frac{\hat{\theta}}{r} \frac{dP_n^m}{d\theta} \left\{ \begin{matrix} \cos m\phi \\ \sin m\phi \end{matrix} \right\} + \frac{\hat{\phi} m}{r \sin \theta} P_n^m \left\{ \begin{matrix} -\sin m\phi \\ \cos m\phi \end{matrix} \right\} \right] \end{aligned}$$

since

$$\bar{e}_{r\theta}' = \nabla T_{r\theta} = \frac{\hat{\theta}}{r} \frac{dP_n^m}{d\theta} \left\{ \begin{matrix} \cos m\phi \\ \sin m\phi \end{matrix} \right\} + \frac{\hat{\phi} m}{r \sin \theta} P_n^m \left\{ \begin{matrix} -\sin m\phi \\ \cos m\phi \end{matrix} \right\}$$

and

$$\bar{e}_{r\theta}'' = \nabla T_{r\theta} \times \hat{r} = \frac{\hat{\theta} m}{r \sin \theta} P_n^m \left\{ \begin{matrix} -\sin m\phi \\ \cos m\phi \end{matrix} \right\} - \frac{\hat{\phi}}{r} \frac{dP_n^m}{d\theta} \left\{ \begin{matrix} \cos m\phi \\ \sin m\phi \end{matrix} \right\} .$$



Also, in view of these latter two relations, the following forms for the evaluation of the integrals in (74) - (77) can be written down:

$$\begin{aligned} \int_{\text{slot}} \bar{E}_{\tau_a} \cdot \bar{e}_{\tau_a}'' dS &= \int_{\text{slot}} \left[ \frac{E_{\theta a} m}{\sin \theta} P_n^m \times \left\{ \begin{array}{c} -\sin m\phi \\ \cos m\phi \end{array} \right\} \right. \\ &\quad \left. - E_{\phi a} \frac{dP_n^m}{d\theta} \times \left\{ \begin{array}{c} \cos m\phi \\ \sin m\phi \end{array} \right\} \right] + \sin \theta d\theta d\phi \\ \int_{\text{slot}} \bar{E}_{\tau_a} \cdot \bar{e}_{\tau_a}' dS &= \int_{\text{slot}} \left[ E_{\theta a} \frac{dP_n^m}{d\theta} \times \left\{ \begin{array}{c} \cos m\phi \\ \sin m\phi \end{array} \right\} \right. \\ &\quad \left. - E_{\phi a} \frac{m}{\sin \theta} P_n^m \times \left\{ \begin{array}{c} -\sin m\phi \\ \cos m\phi \end{array} \right\} \right] + \sin \theta d\theta d\phi \\ \int_{\tau=\tau_i} e_{\tau_a}'^2 dS &= \int e_{\tau_a}''^2 dS = \int_0^{2\pi} \int_0^\pi \left[ \left( \frac{dP_n^m}{d\theta} \right)^2 \left\{ \begin{array}{c} \cos^2 m\phi \\ \sin^2 m\phi \end{array} \right\} \right. \\ &\quad \left. + \frac{m^2}{\sin^2 \theta} (P_n^m)^2 \left\{ \begin{array}{c} \sin^2 m\phi \\ \cos^2 m\phi \end{array} \right\} \right] \sin \theta d\theta d\phi \\ &= \pi \int_0^\pi \left[ \left( \frac{dP_n^m}{d\theta} \right)^2 + \frac{m^2 P_n^m}{\sin^2 \theta} \right] \sin \theta d\theta d\phi \\ &= \pi \left[ \frac{2}{2n+1} \frac{(n+m)!}{(n-m)!} n(n+1) \right] (\text{Stratton, p. 417}). \end{aligned}$$



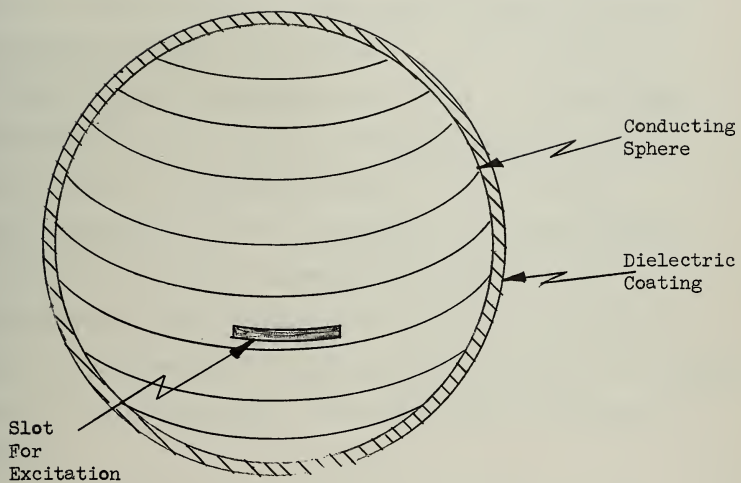


FIGURE 12 SLOT EXCITED SPHERICAL RADIATOR WITH DIELECTRIC COATING



### 3.2 The Slot Excited Conducting Sphere Coated with Dielectric

When the conducting spherical antenna is coated with dielectric material, the exterior space is split into two homogeneous regions, the region (I) of the spherical shell of dielectric ( $r_1 \leq r \leq r_2$ ) and the region (II) exterior to the shell ( $r > r_2$ ). As in the problem of the conducting sphere in free space, the tangential electric field is presumed to be zero on the surface  $r = r_1$ , except over the slot, where it has the prescribed value  $\bar{E}_{\tau_0}$ . In the region (I), the transverse electric field has the form precisely as given in (71). The field over the conducting surface,  $r = r_1$ , can be represented in the form of Eq. 73, in which the  $\mathcal{V}$ 's are regarded as the excitation coefficients, determined from relations (74) - (77). The expression given in (71), evaluated at  $r = r_1$ , must be equal term by term to an expression of the form of (73), to satisfy the boundary condition at the conducting sphere. This implies the following set of four equations:

$$\alpha_{nm\sigma}'' \hat{J}_n(\beta, r_1) + b_{nm\sigma}'' \hat{N}_n(\beta, r_1) = \mathcal{V}_{nm\sigma}'' \quad (82)$$

$$c_{nm\sigma}' \frac{\hat{d}_+ \hat{J}_n(\beta, r_1)}{dr_1} + d_{nm\sigma}' \frac{\hat{d}_+ \hat{N}_n(\beta, r_1)}{dr_1} = j\omega \epsilon_1 \mathcal{V}_{nm\sigma}' . \quad (83)$$

Next, the boundary conditions at the outer surface of the dielectric shell,  $r = r_2$  are applied. In region (II),  $r > r_2$ , the transverse electric field has the same form as that given in (79), since it must consist of outgoing spherical waves as  $r \rightarrow \infty$ . When the condition



$\bar{E}_{\tau_1} \Big|_{r=r_2} = \bar{E}_{\tau_2} \Big|_{r=r_2}$  is enforced (where again the form of Eq. 71 for the field in region (I) is employed), the result is the equation

$$\begin{aligned} & \sum_i \left[ a''_{nm\sigma} \hat{J}_n(\beta, r_2) + b''_{nm\sigma} \hat{N}_n(\beta, r_2) \right] \bar{e}_{i\sigma}'' \\ & + \left( c'_{nm\sigma} \frac{d \hat{J}_n(\beta, r_2)}{dr} + d'_{nm\sigma} \frac{d \hat{N}_n(\beta, r_2)}{dr} \right) \bar{e}_{i\sigma}' \\ & = \sum_i f''_{nm\sigma} \hat{H}_n(\beta, r_2) \bar{e}_{i\sigma}'' + g'_{nm\sigma} \frac{d \hat{H}_n(\beta, r_2)}{dr} \bar{e}_{i\sigma}' . \quad (85) \end{aligned}$$

This equation is satisfied if the following set of four equations is satisfied:

$$a''_{nm\sigma} \hat{J}_n(\beta, r_2) + b''_{nm\sigma} \hat{N}_n(\beta, r_2) = f''_{nm\sigma} \hat{H}_n(\beta, r_2) \quad (86)$$

$$c'_{nm\sigma} \frac{d \hat{J}_n(\beta, r_2)}{dr} + d'_{nm\sigma} \frac{d \hat{N}_n(\beta, r_2)}{dr} = \frac{\epsilon_1}{\epsilon_0} g'_{nm\sigma} \frac{d \hat{H}_n(\beta, r_2)}{dr} . \quad (87)$$

The boundary condition on the magnetic field  $\bar{H}_{\tau_1} \Big|_{r=r_2} = \bar{H}_{\tau_2} \Big|_{r=r_2}$  must now be enforced. A careful examination of the equations (66) - (69) shows that an equation for  $\bar{H}_{\tau_1}$  can be written as follows:

$$\begin{aligned} \bar{H}_{\tau_1} = & \sum_i - \frac{1}{j\omega\mu} \left( a''_{nm\sigma} \frac{d \hat{J}_n(\beta r)}{dr} + b''_{nm\sigma} \frac{d \hat{N}_n(\beta r)}{dr} \right) \nabla T_{i\sigma} \\ & + (c'_{nm\sigma} \hat{J}_n(\beta r) + d'_{nm\sigma} \hat{N}_n(\beta r)) \nabla T_{i\sigma} \times \hat{r} . \quad (88) \end{aligned}$$



In region (II), the functions must represent outgoing traveling waves.

Thus, the boundary condition on the magnetic field gives the following equation:

$$\begin{aligned} & \sum_i -\frac{1}{j\omega\mu_1} (a''_{nms} \frac{d\hat{J}_n(\beta_1 t_2)}{dt} + b''_{nms} \frac{d\hat{N}_n(\beta_1 t_2)}{dt}) \nabla T_{Lg} \\ & + (c'_{nms} \hat{J}_n(\beta_1 t_2) + d_{nms} \hat{N}_n(\beta_1 t_2)) \nabla T_{Lg} \times \hat{r} \\ & = \sum_i -\frac{1}{j\omega\mu_0} f''_{nms} \frac{d\hat{H}_n(\beta_0 t_2)}{dt} \nabla T_{Lg} + g'_{nms} \hat{H}_n(\beta_0 t_2) \nabla T_{Lg} \times \hat{r}. \end{aligned} \quad (89)$$

(The terms have orthogonality as mentioned under Eq. 72, where the notation was used for the vector functions.) This equation is satisfied if the following set of four equations is satisfied:

$$a''_{nms} \frac{d\hat{J}_n(\beta_1 t_2)}{dt} + b''_{nms} \frac{d\hat{N}_n(\beta_1 t_2)}{dt} = \frac{\mu_1}{\mu_0} f''_{nms} \frac{d\hat{H}_n(\beta_0 t_2)}{dt} \quad (90)$$

$$c'_{nms} \hat{J}_n(\beta_1 t_2) + d'_{nms} \hat{N}_n(\beta_1 t_2) = g'_{nms} \hat{H}_n(\beta_0 t_2). \quad (91)$$

The foregoing equations imply that the TM and TE field coefficients can be handled separately. The TM coefficients can be found from the sets of Eqs. 83, 87, and 91. These sets of equations are regarded as independent sets of equations for the field coefficients, and their solution is indicated by the display of the following matrix (the augmented matrix of any particular set):



$$\left[ \begin{array}{ccc|c} \frac{d\hat{J}_n(\beta, r_i)}{dr} & \frac{d\hat{N}_n(\beta, r_i)}{dr} & 0 & \text{WE}_n U'_{nm_0} \\ \hat{J}_n(\beta, r_i) & \hat{N}_n(\beta, r_i) & -\hat{H}_n(\beta_0 r_i) & 0 \\ \frac{d\hat{J}_n(\beta, r_2)}{dr} & \frac{d\hat{N}_n(\beta, r_2)}{dr} & -\frac{\epsilon_1}{\epsilon_0} \frac{d\hat{H}_n(\beta_0 r_2)}{dr} & 0 \end{array} \right] \text{TM}_0 .$$

The TE coefficients can be found from the sets of Eqs. 82, 86, and 90. The augmented matrix of any one set of these coefficients is as follows:

$$\left[ \begin{array}{ccc|c} \hat{J}_n(\beta, r_i) & \hat{N}_n(\beta, r_i) & 0 & U''_{nm_0} \\ \hat{J}_n(\beta, r_2) & \hat{N}_n(\beta, r_2) & -\hat{H}_n(\beta_0 r_2) & 0 \\ \frac{d\hat{J}_n(\beta, r_2)}{dr} & \frac{d\hat{N}_n(\beta, r_2)}{dr} & -\frac{\mu_1}{\mu_0} \frac{d\hat{H}_n(\beta_0 r_2)}{dr} & 0 \end{array} \right] \text{TE}_0 .$$

For the radiation pattern calculation, the coefficients  $f''_{nm_0}$  and  $g'_{nm_0}$  are needed explicitly. The results, obtained from the foregoing equations, can be written compactly as follows:



$$g'_{nm\delta} = j \frac{\omega \epsilon_r \mathcal{V}'_{nm\delta} \mathcal{W}(\hat{J}_n, \hat{N}_n)}{\Delta_{TM_n}} \quad (92)$$

$$f''_{nm\delta} = \frac{\mathcal{V}''_{nm\delta} \mathcal{W}(\hat{J}_n, N_n)}{\Delta_{TE_n}} \quad (93)$$

where  $\Delta_{TM_n}$  and  $\Delta_{TE_n}$  are respectively the determinants of the first three columns of the TM and TE matrices which are written down above. Note that the determinant for the TM coefficients is identical to the corresponding determinant (Eq. 29) in the case of the symmetrically excited sphere. Hence, the numerical results presented earlier can be applied here.

As in the case of axially symmetric excitation, the effect of the dielectric coating can be assessed by examining the ratios of the corresponding expansion coefficients in the coated and uncoated problems:

$$\frac{g'_{nm\delta}}{g'_{unC_{nm\delta}}} = \frac{\epsilon_r \beta_1}{\Delta_{TM_n}} \frac{d \hat{H}_n(\beta_0 r)}{d r} \quad (94)$$

$$\frac{f''_{nm\delta}}{f''_{unA''_{nm\delta}}} = \frac{\mu_r \beta_1}{\Delta_{TE_n}} \hat{H}_n(\beta_0 r) \quad (95)$$

The ratio in Eq. 94 was studied in Section 2.1.2; numerical results are given in Figs. 40 to 63, and Table 6. The ratio in Eq. 95 has not been



studied numerically, but in view of the fact that the only difference from the former is in the replacement of some of the functions by their derivatives (and the relationship  $\frac{d \hat{Z}_n}{d \chi} = \frac{n+1}{\chi} \hat{Z}_n - \hat{Z}_{n+1}$ ), it is likely that the latter ratio exhibits a similar behavior. Unfortunately the numerical study of the multitude of problems which are represented formally by the analysis (given in the preceding pages) of the coated spherical radiator with arbitrary slot configurations must be postponed to later investigations.



#### 4. SUMMARY AND RECOMMENDATIONS FOR FURTHER WORK

Analytical methods have been presented for the determination of the changes in the radiation patterns brought about by dielectric coatings on spheroidal radiators. Numerical results are included for spheres and prolate spheroids which are excited by axially symmetric slots. A description is given of the machine computation system which makes the analytical results useful. This system includes a program for the semi-automatic calculation of the radiation patterns of spherical radiators, a practical method for the determination of the eigenvalues of all of the orders of the spheroidal functions which are needed in order to obtain convergent representations, and a new method for the calculation of the spheroidal "radial" functions.

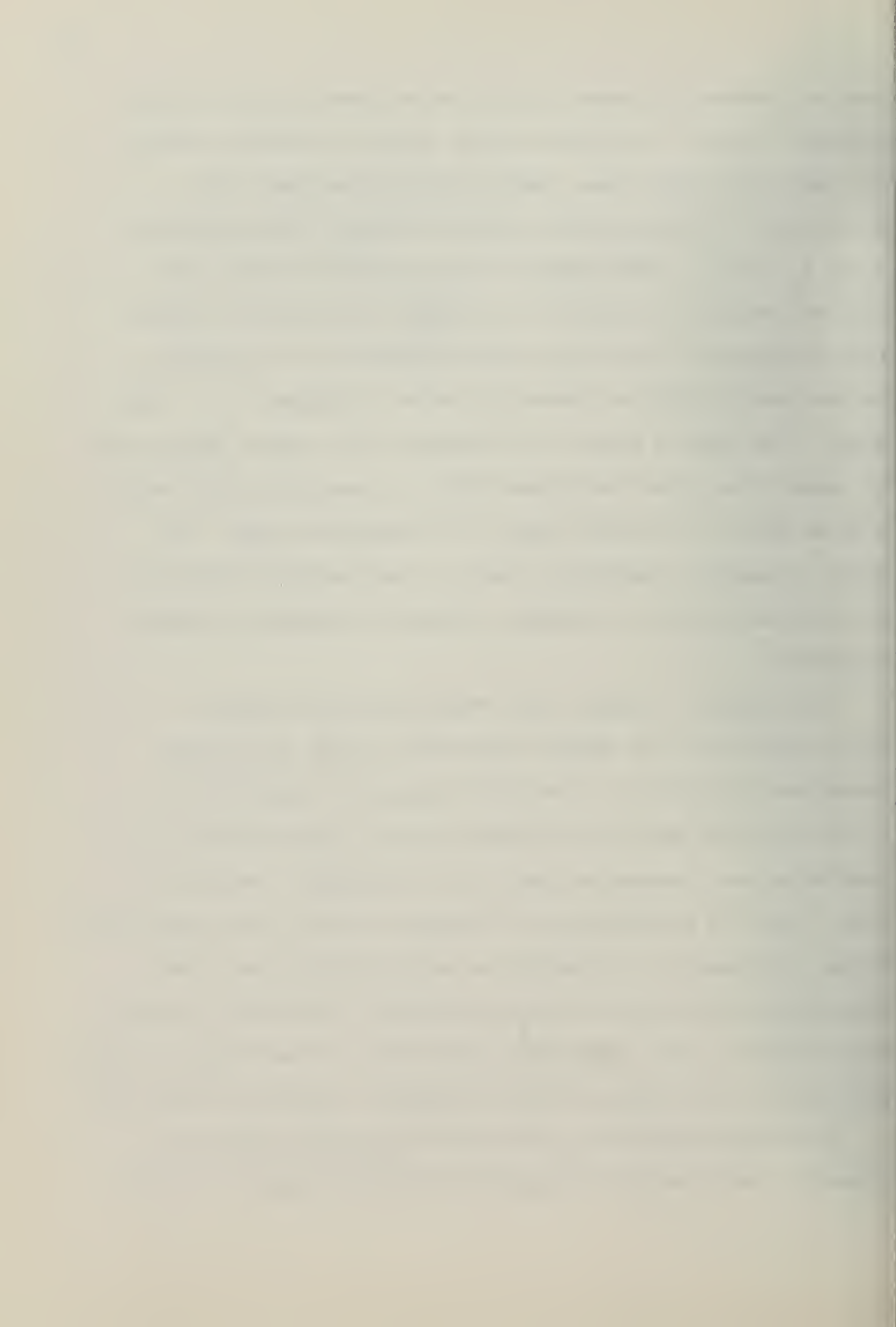
The comparison of the radiation patterns of an uncoated spherical radiator to those of a dielectric coated radiator having the same excitation shows that the effects of the coating may be very slight in some cases and very important in other cases. One effect of a coating of the order of several hundredth's of a wavelength on a moderate size radiator (a few wavelengths in diameter) is to introduce into the patterns some of the characteristics of a radiator which is somewhat larger, with an increase in the radiation in the general direction of the poles. In the patterns in which the excitation is by means of a nonequatorial slot (Figures 15 and 16, for example), the increase in radiation in the general direction of the opposite pole is similar to that which might be expected in the event of an increase in surface type waves traveling around the sphere, but the theoretical representations do not obviously permit such an interpretation. On the other



hand, as indicated in Figures 17 to 20, as the permittivity or coating thickness is varied, the patterns may go through the successive stages of slight deterioration from, complete deterioration from, and/or smoothing of the patterns of the uncoated radiator. If the quantities  $R_n$  and  $I_n$  ( pg. 26 ) which appear in the expressions for the coated spherical radiator are studied in the limit as the dielectric constant tends to infinity, it can be seen that the quantities in the symbolic brackets tend to sines and cosines, and become independent of  $n$ . Thus, except in the event of a zero in the argument of the cosines:  $(\beta_1(r_2-r_1))$ , the shape of the pattern tends toward that of a conducting sphere having a radius equal to the outside radius of the dielectric casing. This effect is apparently beginning to show up in the patterns of Figure 18 for the higher dielectric constants, although the smoothing is somewhat surprising.

In retrospect, it appears that some of the effects might be better understood if the analysis were recast in terms of spherical transmission line theory. In the latter theory, the contributions to the total field made by the different orders of the functions are regarded as modes propagating along a set of independent transmission lines. That such a representation is possible has been shown by Marcuvitz<sup>11</sup> Felsen, and others<sup>12</sup>. In principle one could calculate a set of mode transmission coefficients to relate the excitation coefficients (or mode input voltages) to the distant field coefficients, (or mode output voltages) which appear at the output of a kind of spherical transmission mode filter.

The radiation patterns of a few prolate spheroidal radiators are presented. Unfortunately, the system of calculation employed to obtain



these patterns is very much more clumsy and time consuming than the sphere calculations. However, the calculations which were carried out in connection with the coated spheroid problem are interesting for reasons which extend beyond the specific problem. For it has been demonstrated that the difficulties (of enforcing the boundary conditions) which arise in problems in which the (eigen-) functions are different on two sides of a boundary may not be insurmountable. The results in Table 3 indicate that satisfactorily accurate results can be obtained by including only a manageable number of equations out of the infinite set which is required for an exact representation.

Comparison of the patterns of the prolate spheroidal radiators to those of the spherical radiators lends support to the idea that the effects associated with spheroidal radiators resemble those associated with spherical radiators. This similarity, coupled with the difficulty in carrying out the prolate spheroidal solutions provides further motivation for studies of the spherical radiator, in order to be able to better judge which of the spheroid problems are likely to be the more interesting.

The following additional work is recommended:

- 1) The dielectric coated sphere problem should be studied analytically and numerically from the point of view of spherical transmission line theory and the feasibility of dielectric layers as spherical transmission line mode filters should be investigated. 2) The results of the present analysis for spherical radiators with arbitrary slot configurations should be applied to such problems as a traveling wave slot on a sphere. 3) The method of calculating the spheroidal functions should be extended and



improved since the method has promise in many other problems (for example, slot excited radiators whose cross section has an abrupt change in size and character).



TABLE 4. EXCITATION COEFFICIENTS FOR AN AXIALLY SYMMETRIC SLOT IN A SPHERICAL RADIATOR

The quantity tabulated is

$$\alpha_n = \frac{2n+1}{2n(n+1)} \int_{\nu_1}^{\nu_2} P_n^1(\nu) d\nu.$$

It is evaluated by a five point Simpson's rule integration over a slot which subtends two degrees. Values presented here are  $\alpha_n(10^\circ)$ ,  $n$  from one to eighty. Data and output tapes for slots at  $\theta = 10^\circ (10^\circ) 90^\circ$ ;  $n: 1(1)80$ , are on file at the U. of I. Antenna Laboratory.

$\alpha_n$

1(n)27	28(n)54	55(n)80
-79192 -03	-19009 -02	-60023 -03
+12995 -02	+19855 -02	+37965 -03
-17770 -02	-20092 -02	-15418 -03
+22137 -02	+19736 -02	-69286 -04
-25995 -02	-18817 -02	+28411 -03
+29261 -02	+17383 -02	-48410 -03
-31864 -02	-15491 -02	+66366 -03
+33751 -02	+13211 -02	-81800 -03
-34888 -02	-10623 -02	+94320 -03
+35260 -02	+78103 -03	-10363 -02
-34869 -02	-48628 -03	+10955 -02
+33739 -02	+18702 -03	-11199 -02
-31912 -02	+10789 -03	+11099 -02
+29446 -02	-38997 -03	-10667 -02
-26414 -02	+65138 -03	+99254 -03
+22903 -02	-88508 -03	-89065 -03
-19010 -02	+10851 -02	+76489 -03
+14841 -02	-12465 -02	-61976 -03
-10506 -02	+13658 -02	+46023 -03
+61184 -03	-14406 -02	-29156 -03
-17886 -03	+14702 -02	+11912 -03
-23754 -03	-14549 -02	+51733 -04
+62729 -03	+13967 -02	-21587 -03
-98125 -03	-12984 -02	+36850 -03
+12915 -02	+11641 -02	-50534 -03
-15513 -02	-99907 -03	+62269 -03
+17556 -02	+80896 -03	



TABLE 5. RESONANCE AND CONVERGENCE FACTORS FOR SPHERICAL RADIATORS.

The values tabulated are different orders of the combinations of the spherical Bessel functions which appear in the series expansions of the fields of a spherical radiator whose radius is 2.4 wavelengths. Data and output tapes for these quantities for different sphere sizes as follows:  $r/\lambda = .1(.05)1.05$ ,  $r/\lambda = 1.1(.1)2.4$ ,  $r/\lambda = 2.4(.8)4.8$ , are on file at the U. of I. Antenna Laboratory. The machine was instructed to calculate successively higher orders of the quantities until the exponent of the quantity  $\frac{\hat{N}'_n}{\hat{J}'^{1/2}_n + \hat{N}''^{1/2}_n}$  became less than  $10^{-5}$ . (Note +123 -02 means .00123)

	$\frac{1}{ H'_n ^2}$	$\frac{\hat{J}'_n}{\hat{J}'^{1/2}_n + \hat{N}''^{1/2}_n}$	$\frac{\hat{N}'_n}{\hat{J}'^{1/2}_n + \hat{N}''^{1/2}_n}$
1	+10044 +01	+52857 +00	+85147 +00
2	+10134 +01	+91823 +00	-41257 +00
3	+10273 +01	-22277 +00	-98875 +00
4	+10467 +01	-10219 +01	-48556 -01
5	+10725 +01	-39022 +00	+95930 +00
6	+11062 +01	+73515 +00	+75214 +00
7	+11496 +01	+10276 +01	-30595 +00
8	+12056 +01	+29563 +00	-10575 +01
9	+12790 +01	-68837 +00	-89730 +00
10	+13769 +01	-11699 +01	-90763 -01
11	+15114 +01	-96790 +00	+75798 +00
12	+17019 +01	-35622 +00	+12550 +01
13	+19758 +01	+29995 +00	+13732 +01
14	+23231 +01	+75329 +00	+13250 +01
15	+23902 +01	+79978 +00	+13231 +01
16	+13905 +01	+36431 +00	+11215 +01
17	+40526 +00	+69952 -01	+63274 +00
18	+88558 -01	+88559 -02	+29746 +00
19	+17242 -01	+90006 -03	+13131 +00
20	+30354 -02	+75697 -04	+55095 -01
21	+48040 -03	+52945 -05	+21918 -01
22	+68263 -04	+31008 -06	+82621 -02
23	+87336 -05	+15346 -07	+29553 -02
24	+10106 -05	+64788 -09	+10053 -02
25	+10627 -06	+23545 -10	+32599 -03
26	+10202 -07	+74262 -12	+10101 -03
27	+89809 -09	+20477 -13	+29968 -04
28	+72778 -10	+49690 -15	+85310 -05
29	+54488 -11	+10675 -16	+23343 -05
30	+37816 -12	+20412 -18	+61495 -06



TABLE 6. NUMBERS WHICH INDICATE THE RELATIVE IMPORTANCE OF DIELECTRIC COATINGS ON SPHERICAL RADIATORS.

The quantities tabulated are the ratios of the expansion coefficients for the field of a coated spherical radiator to the corresponding coefficients for the field of an uncoated spherical radiator which has the same excitation. The ratios of the real parts and of the imaginary parts are listed separately. The parameters are as follows: sphere radius 1.4 wavelengths, coating thickness .1 wavelength, dielectric constant 2.25. Data and output tapes are on file at the U. of I. Antenna Laboratory for other parameters as follows:

$$\begin{aligned}\epsilon_r &= 2.25, \quad t/\lambda = .1, \quad r/\lambda : .5(.1)1.6, \quad r/\lambda : 1.6(.8)4.8; \\ \epsilon_r &= 4.0, \quad t/\lambda = .1, \quad r/\lambda : .5(.1)1.6; \\ \epsilon_r &= 6.25, \quad r/\lambda = 1.6, \quad t/\lambda : .1(.05).3.\end{aligned}$$

order n	$\frac{R c_n}{R a_n}$	$\frac{I_m c_n}{I_m a_n}$
1	+15028 +01	+11541 +01
2	+11765 +01	+17843 +01
3	-14931 +01	+12138 +01
4	+13014 +01	+81140 +00
5	+10103 +01	+17359 +01
6	+17206 +00	+11925 +01
7	+27870 +01	+86526 +00
8	+18860 +01	+41378 +00
9	+30099 +01	+21814 -01
10	+17884 +02	+12306 +01
11	+18964 +02	+33046 +01
12	+11221 +02	+25209 +01
13	+91727 +01	+21946 +01
14	+85991 +01	+20354 +01
15	+85879 +01	+19403 +01



TABLE 7. EIGENVALUES OF THE SPHEROIDAL WAVE FUNCTION

(Differential equation $(1-v^2) \frac{dV^2}{dv^2} + ((\beta\ell v)^2 - k_j^2) V = 0 \quad V^{(+1)} = 0$ )			
	<u><math>\beta\ell = 5</math></u>	<u><math>\beta\ell = 8</math></u>	<u><math>\beta\ell = 12</math></u>
j	$k_j / (\beta\ell)^2$	$k_j / (\beta\ell)^2$	$k_j / (\beta\ell)^2$
	odd	odd	odd
1	.21401687	.12968845	.08528034
3	.93590450	.58438654	.39771381
5	1.70632729	.98196932	.67784891
7	2.74589040	1.39873600	.92487780
9	4.10404858	1.92299702	.1.16537067
11	5.78287310	2.57428143	1.44669764
13	7.78212780	3.35241653	1.78603032
15	10.10163380	4.25662492	2.18356789
17	12.74129183	5.28647244	2.63830632
19	15.70104605	6.44172000	3.14963127
21	18.98086382	7.72222957	3.71718528
23	22.58072513	9.12791755	4.34075224
25	26.50061724	10.65873113	5.02019593
27	30.74053164	12.31463555	5.75542732
29	35.30046262	14.09560733	6.54638607
31	40.18040621	16.00163007	7.39303017
33		18.03269202	8.29532979
35		20.18878471	9.25326322
37		22.46990174	10.26681421
39		24.87603848	11.33597068
41		27.40719101	12.46072310
43		30.06335668	13.64106440
45		32.84453316	14.87698883
47		35.75071871	16.16849184
49		38.78191194	17.51556974
51		41.93811159	18.91821961
53		45.21931685	20.37643922



TABLE 7. (CONTINUED)

<u><math>\beta\ell = 5</math></u>	<u><math>\beta\ell = 8</math></u>	<u><math>\beta\ell = 12</math></u>
$j$	$k_j / (\beta\ell)^2$	$k_j / (\beta\ell)^2$
odd	odd	odd
55	48.62552680	21.89022638
57	52.15674084	23.45957953
59	55.81295838	25.08449723
61		26.76497837
63		28.50102197
65		30.29262727
67		32.13979344
69		34.04251998
71		36.00080629
73		38.01465187
75		40.08405647
77		42.20901963
79		44.38954113
81		46.62562063
83		48.91725799
85		51.26445283
87		53.66720516
89		56.12551471
91		58.63938135
93		61.20880496
95		63.83378541
97		66.51432263
99		69.25041649
even	even	even
2 .58571819	.36532339	.24526082
4 1.29687773	.78777844	.54209080
6 2.18687186	1.18065149	.80489795
8 3.38487933	1.64517729	1.04264567
10 4.90339175	2.23271934	1.29907596



TABLE 7. (CONTINUED)

	<u><math>\beta\ell = 5</math></u>	<u><math>\beta\ell = 8</math></u>	<u><math>\beta\ell = 12</math></u>
j	$k_j / (\beta\ell)^2$	$k_j / (\beta\ell)^2$	$k_j / (\beta\ell)^2$
	even	even	even
12	6.74246023	2.94755097	1.60901445
14	8.90185691	3.78879486	1.97759588
16	11.38144804	4.75586192	2.40383322
18	14.18115935	5.84843150	2.88692212
20	17.30094848	7.06632312	3.42639552
22	20.74078997	8.40943005	4.02197700
24	24.50066795	9.87768612	4.67349590
26	28.58057205	11.47104867	5.38084249
28	32.98049534	13.18948916	6.14394374
30	37.70043302	15.03298816	6.96274954
32	42.74038172	17.00153171	7.83722457
34		19.09511000	8.76734344
36		21.31371552	9.75308732
38		23.65734288	10.79444239
40		26.12598793	11.89139790
42		28.71964731	13.04394555
44		31.43831867	14.25207898
46		34.28199994	15.51579320
48		37.25068942	16.83508408
50		40.34438605	18.20994839
52		43.56308857	19.64038338
54		46.90679620	21.12638702
56		50.37550829	22.66795726
58		53.96922417	24.26509285
60		57.68794341	25.91779241
62			27.62605496
64			29.38987949
66			31.20926533
68			33.08421174
70			35.01471814



TABLE 7. (CONTINUED)

<u><math>\beta\ell = 5</math></u>	<u><math>\beta\ell = 8</math></u>	<u><math>\beta\ell = 12</math></u>
$j$	$k_j / (\beta\ell)^2$	$k_j / (\beta\ell)^2$
even	even	even
72		37.00078420
74		39.04240935
76		41.13959327
78		43.29233563
80		45.50063613
82		47.76449461
84		50.08391077
86		52.45888438
88		54.88941528
90		57.37550344
92		59.91714850
94		62.51435054
96		65.16710946
98		67.87542497
100		70.63929714



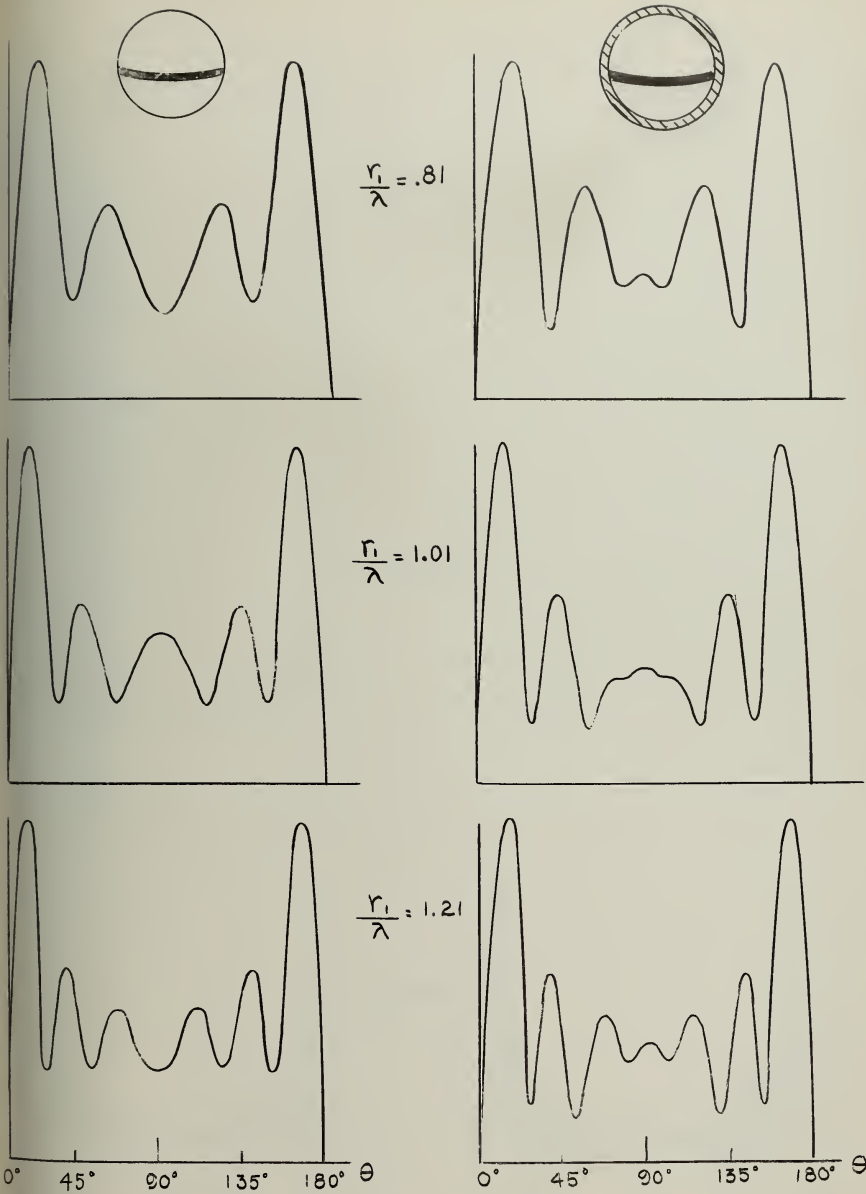


FIGURE 13 RADIATION PATTERNS,  $H_\phi$  VS.  $\theta$ , OF SPHERICAL ANTENNAS WITH DIFFERENT CONDUCTING SPHERE RADII  $r_1$  EXCITED BY EQUATORIAL SLOT. PATTERNS ON LEFT ARE WITH NO COATING. PATTERNS ON RIGHT ARE WITH COATING, THICKNESS  $0.05 \lambda$ ,  $\epsilon_r = 3$



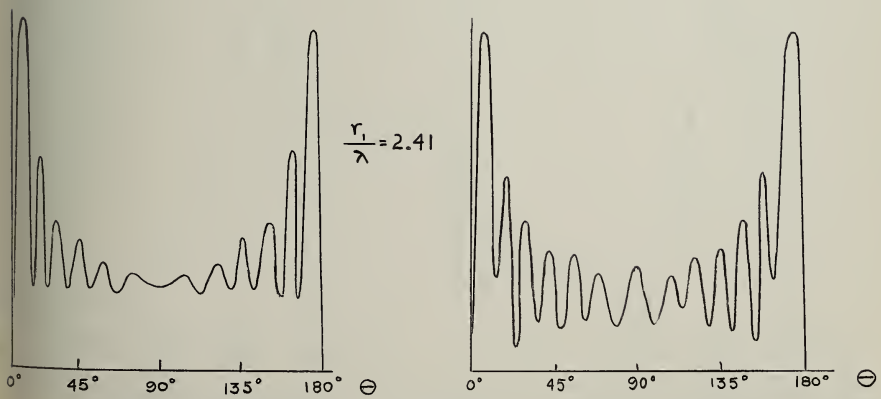
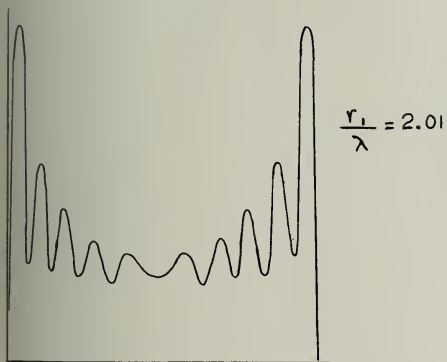
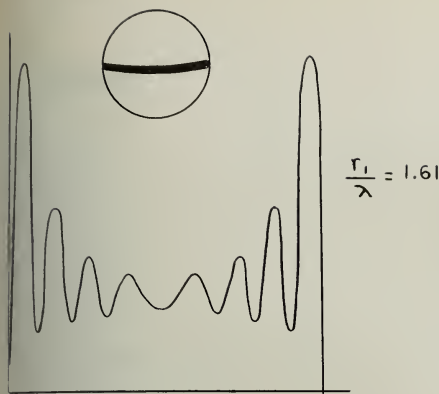
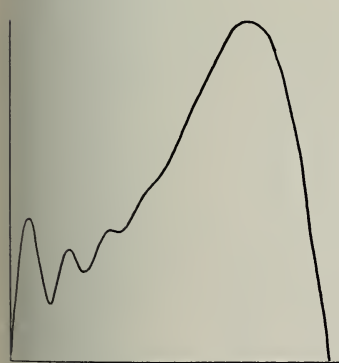
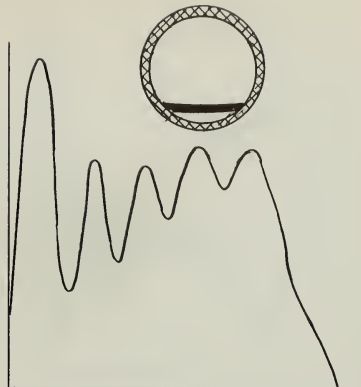


FIGURE 14 CONTINUATION OF FIGURE 13

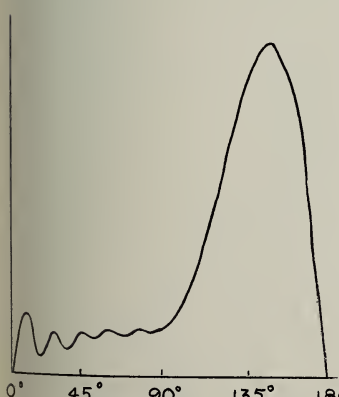
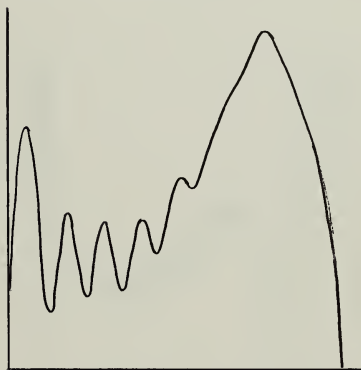




$$\frac{r_1}{\lambda} = .81$$



$$\frac{r_1}{\lambda} = 1.21$$



$$\frac{r_1}{\lambda} = 1.61$$

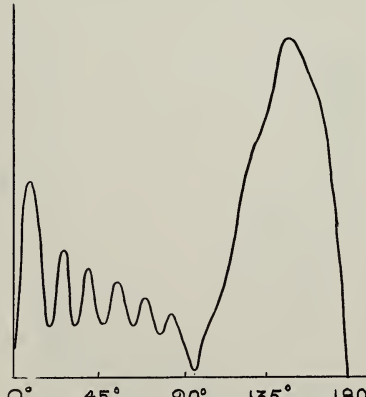


FIGURE 15 RADIATION PATTERNS,  $H_\phi$  VS.  $\theta$  OF SPHERICAL ANTENNAS WITH DIFFERENT CONDUCTING SPHERE RADII,  $r_1$ , EXCITED BY SLOT AT  $160^\circ$  LATITUDE. PATTERNS ON LEFT ARE WITH NO COATING, PATTERNS ON RIGHT ARE WITH COATING, THICKNESS  $.1\lambda$ ,  $\epsilon = 2.25$



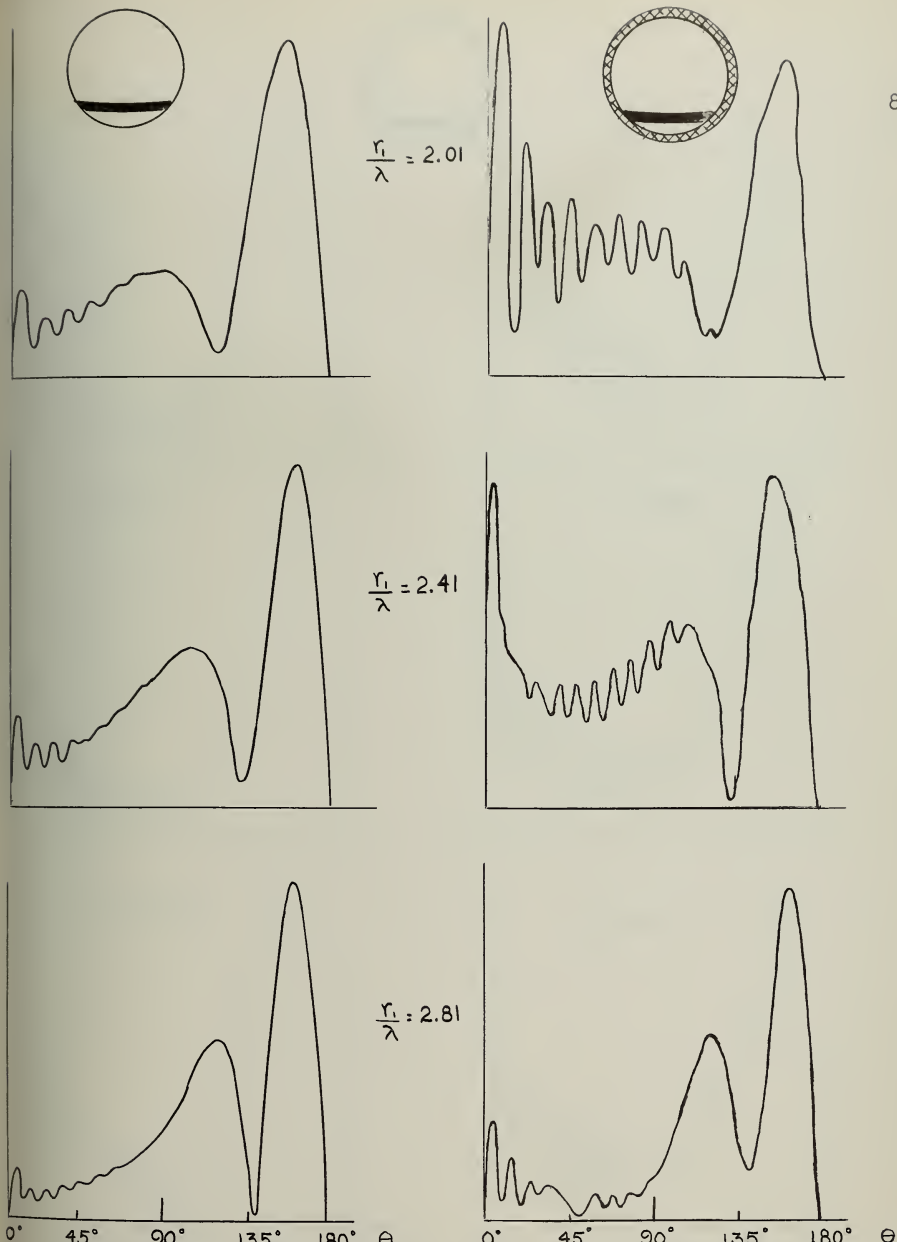


FIGURE 16 RADIATION PATTERNS,  $H_\phi$  VS  $\theta$ , OF SPHERICAL ANTENNAS WITH DIFFERENT CONDUCTING SPHERE RADII,  $r_1$ , EXCITED BY SLOT AT  $160^\circ$  LATITUDE. PATTERNS ON LEFT ARE WITH NO COATING, PATTERNS ON RIGHT ARE WITH COATING, THICKNESS  $.1\lambda$ ,  $\epsilon = 2.25$



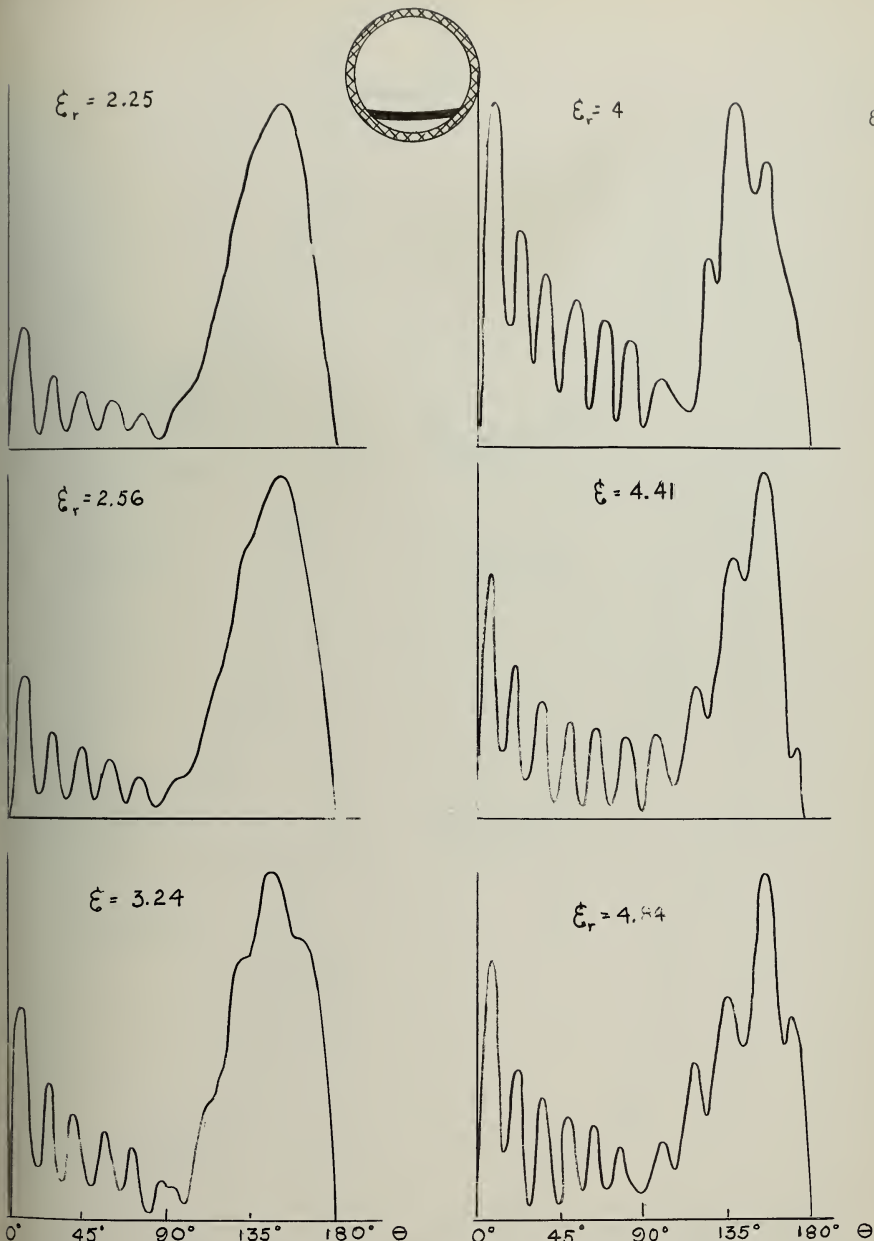


FIGURE 17 RADIATION PATTERNS,  $H_\phi$  VS  $\theta$ , OF COATED SPHERICAL ANTENNA,  $\frac{r}{\lambda} = 1.51$ , COATING THICKNESS  $.1\lambda$ , FOR DIFFERENT VALUES OF DIELECTRIC CONSTANT. SLOT AT  $160^\circ$ .



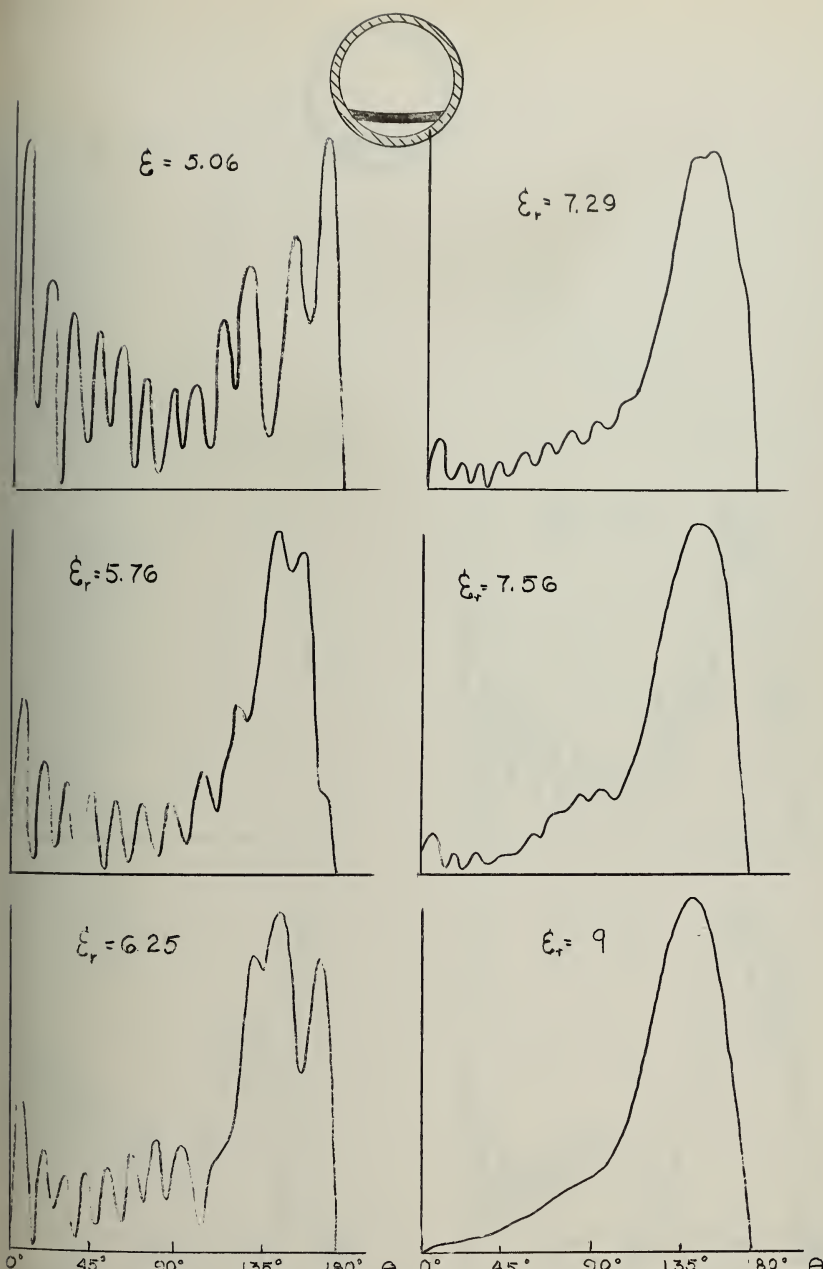


FIGURE 18 RADIATION PATTERNS,  $H_\phi$  VS  $\theta$ , OF COATED SPHERICAL ANTENNA,  $\frac{r}{\lambda} = 1.51$ , COATING THICKNESS  $.1\lambda$ , FOR DIFFERENT VALUES OF DIELECTRIC CONSTANT. SLOT AT  $160^\circ$ .



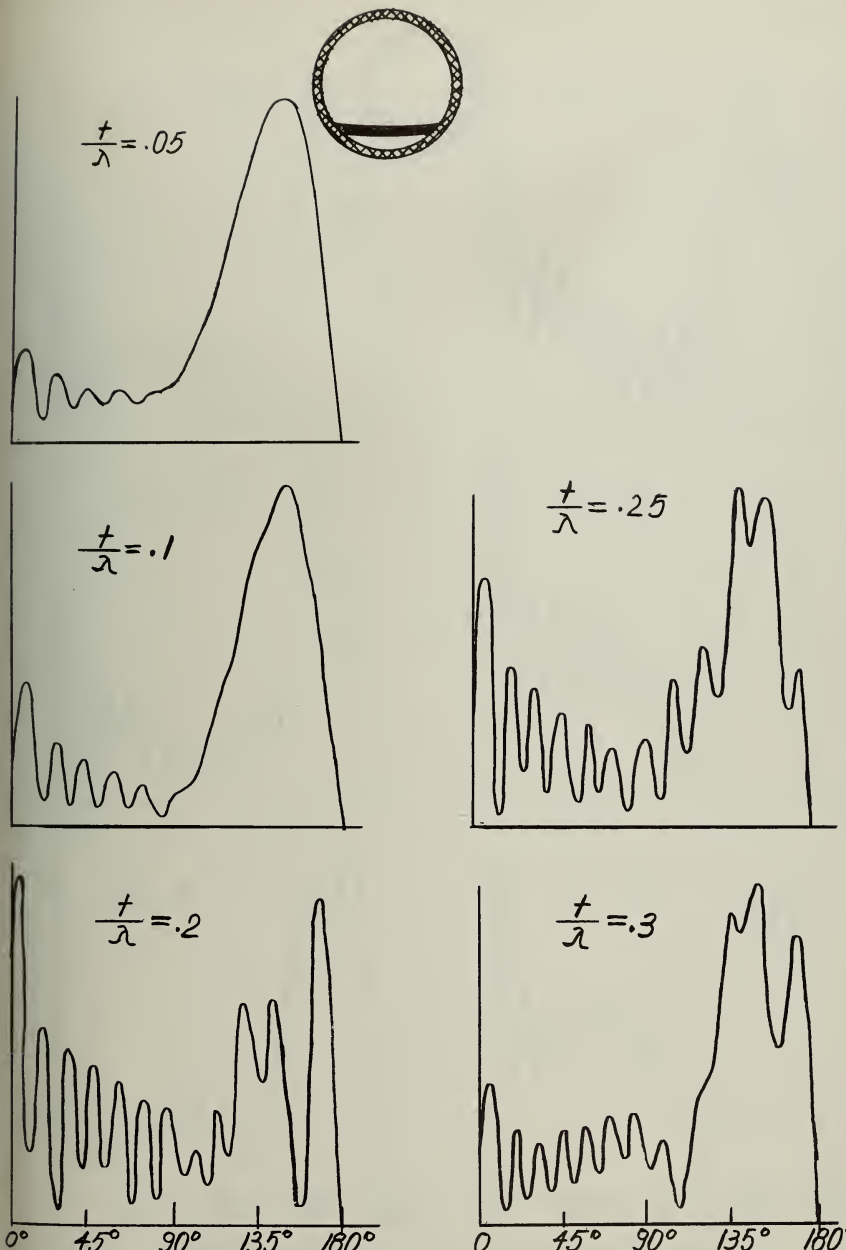


FIGURE 19 RADIATION PATTERNS,  $H_\phi$  VS.  $\theta$ , OF COATED SPHERICAL ANTENNAS,  $r/\lambda = 1.51$ , DIELECTRIC CONSTANT  $\epsilon = 2.56$ , FOR DIFFERENT COATING THICKNESSES. SLOT AT  $160^\circ$ .



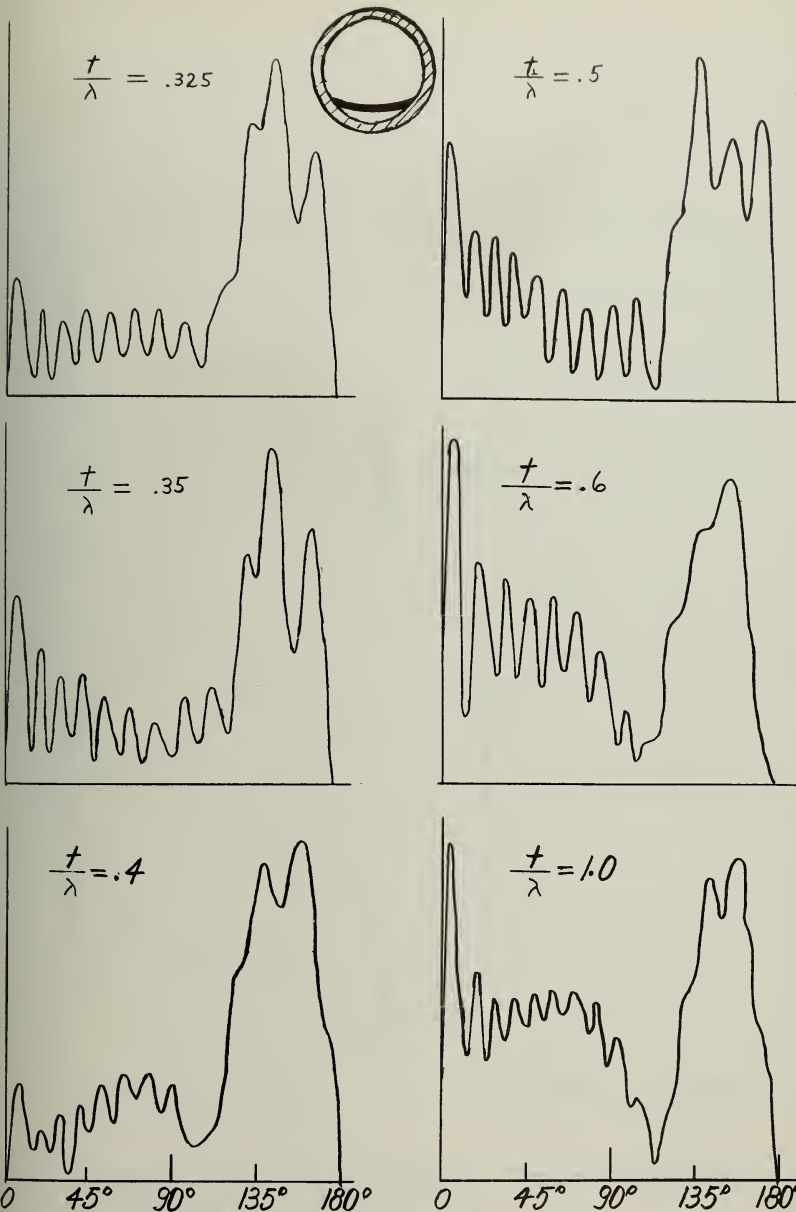


FIGURE 20 RADIATION PATTERNS,  $H_\phi$  VS.  $\theta$ , OF COATED SPHERICAL ANTENNAS,  
 $r/\lambda = 1.51$ , DIELECTRIC CONSTANT  $\epsilon_r = 2.56$ , FOR DIFFERENT  
COATING THICKNESSES. SLOT AT  $160^\circ$ .



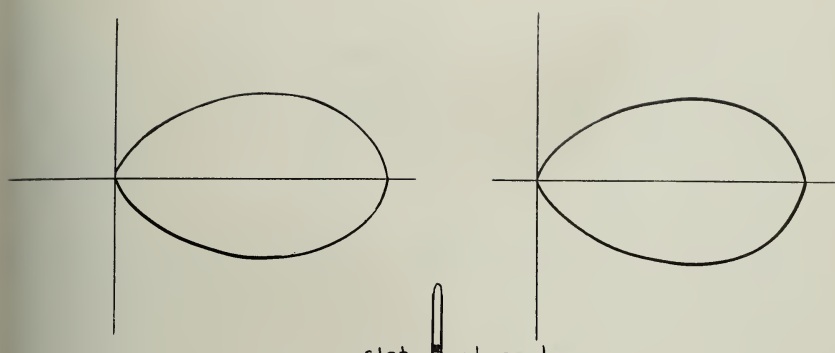
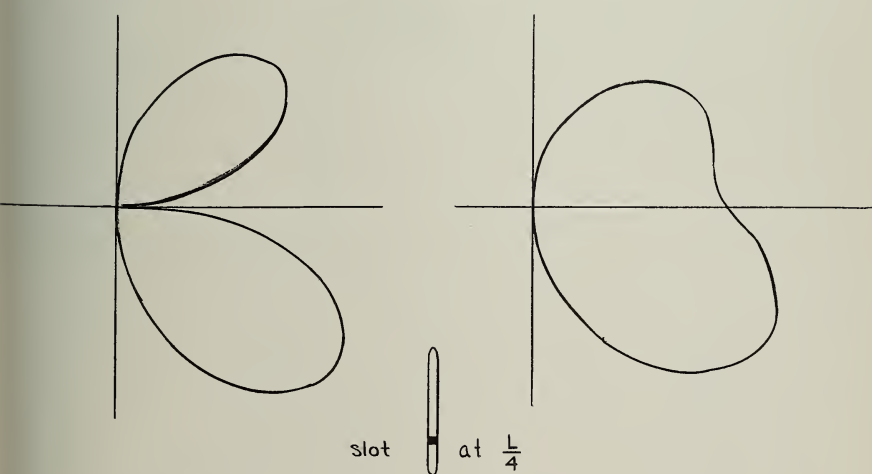
$\theta=0$  $\theta=0$ Uncoated  $u=1.00001$ Coated  $u_1=1.00001$   
 $u_2=1.001$ 

FIGURE 21 PROLATE SPHEROID RADIATION PATTERNS (ONE HALF OF SYMMETRIC PATTERN)  $\beta_0 \ell = 3$ ,  $\epsilon_r = \sqrt{\frac{4}{3}}$ ,  $H_\phi$  vs.  $\theta$



no coating

$$U_1 = 1.077$$

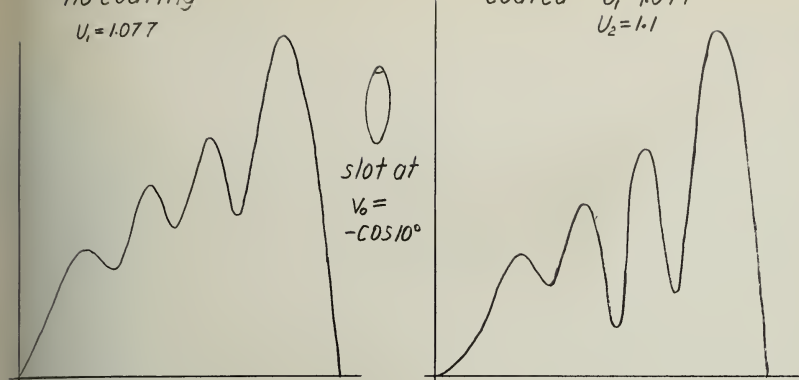
coated

$$U_1 = 1.077$$

$$U_2 = 1.1$$

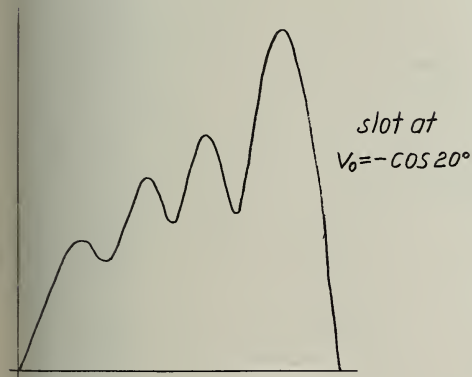
slot at

$$V_0 = -\cos 10^\circ$$



slot at

$$V_0 = -\cos 20^\circ$$



slot

$$at$$

$$V_0 = -\cos 30^\circ$$

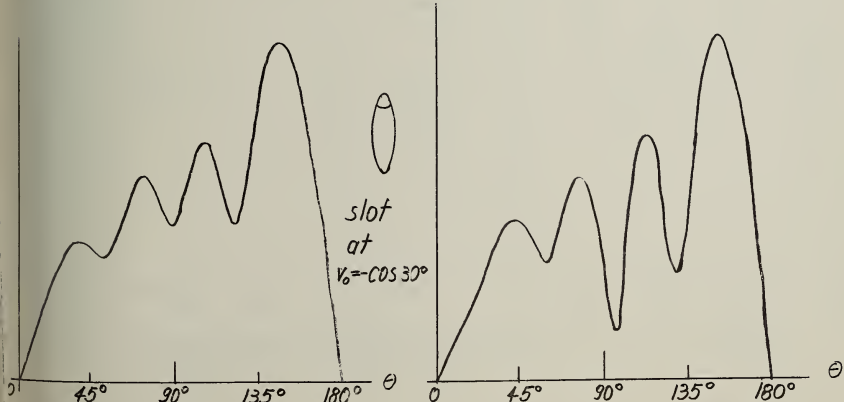
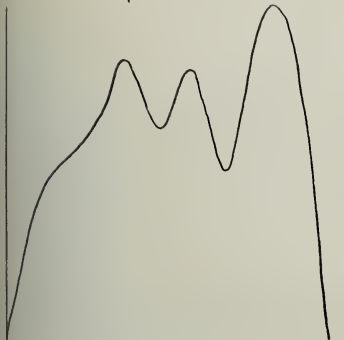


FIGURE 22 PROLATE SPHEROID RADIATION PATTERNS  $\beta_0 \ell = 5$ ,  $\epsilon_r = \sqrt{\frac{8}{3}}$ , FOR DIFFERENT SLOT PATTERNS,  $H_\phi$  VS.  $\theta$



no coating

$$U_1 = 1.077$$

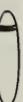


coated

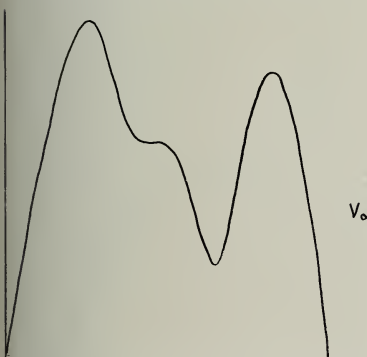
$$U_1 = 1.077$$

$$U_2 = 1.1$$

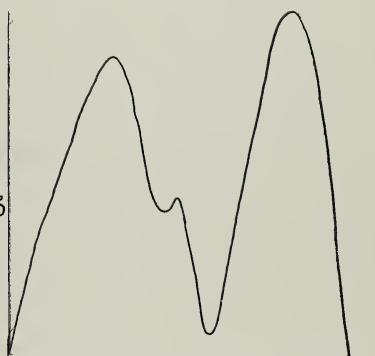
94



slot at  
 $V_o = -\cos 45^\circ$



slot at  
 $V_o = -\cos 60^\circ$



slot at  
 $V_o = 0$

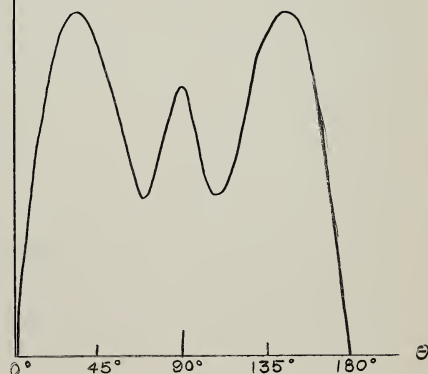
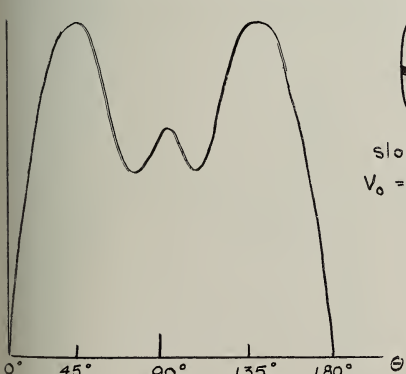


FIGURE 23 PROLATE SPHEROID RADIATION PATTERNS  $\beta_o$ ,  $l = 5$ ,  $\epsilon_r = \sqrt{\frac{8}{3}}$ , FOR DIFFERENT SLOT PATTERNS,  $H_\phi$  VS.  $\theta$



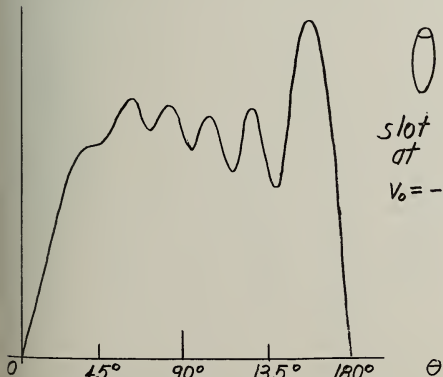
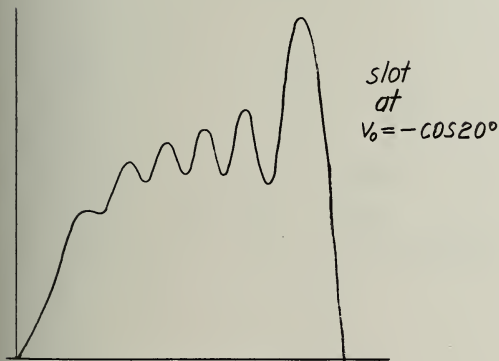
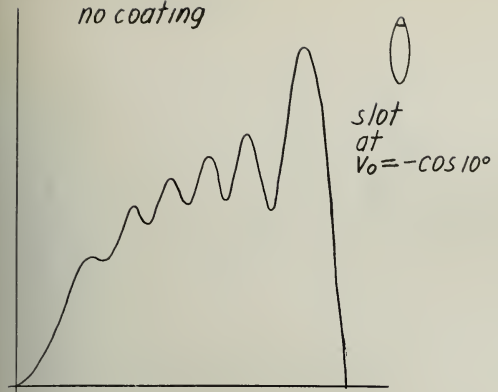


FIGURE 24 PROLATE SPHEROIDAL RADIATION PATTERNS,  $\beta_0 \ l = 8$ ,  $H_\phi$  VS  $\theta$ .



*no coating*

96

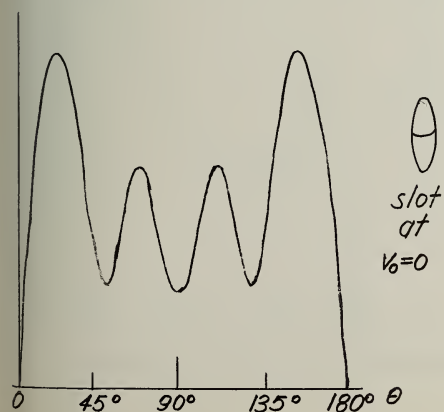
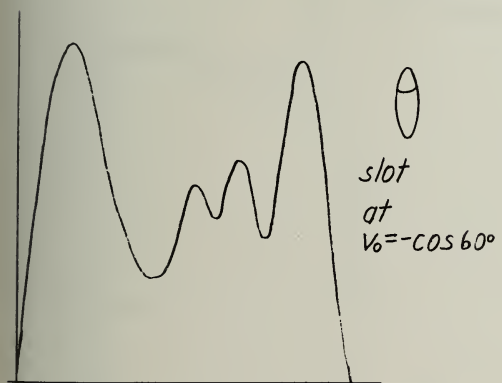
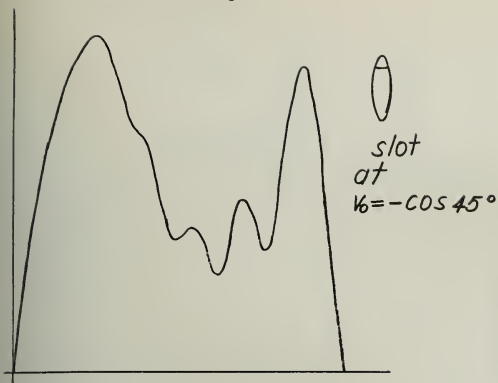


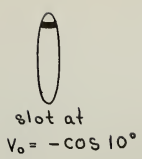
FIGURE 25 PROLATE SPHEROIDAL RADIATION PATTERNS,  $B_0 \ell = 8$ ,  $H_\phi$  VS.  $\theta$



no coating

$$\beta_0 l = 12$$

$$u_1 = 1.077$$



slot at

$$V_0 = -\cos 10^\circ$$

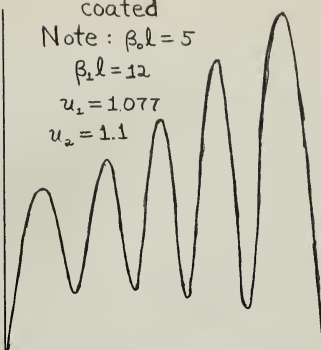
coated

$$\text{Note: } \beta_0 l = 5$$

$$\beta_1 l = 12$$

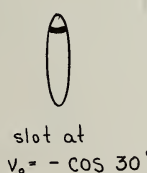
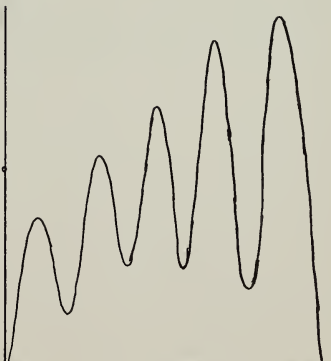
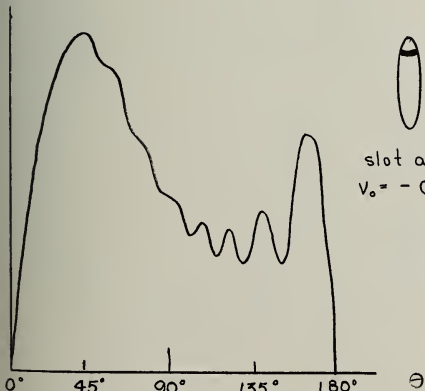
$$u_1 = 1.077$$

$$u_2 = 1.1$$

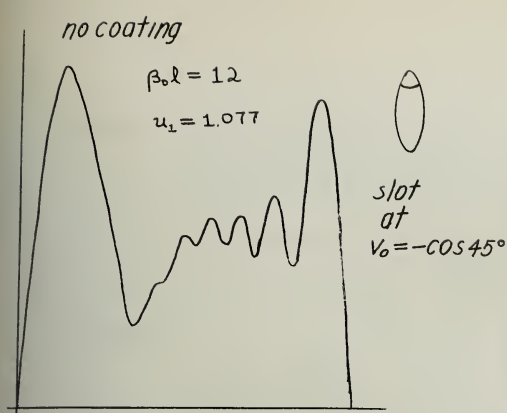


slot at  
 $V_0 = -\cos 20^\circ$

Note:  
conductor size that of Fig. 22

slot at  
 $V_0 = -\cos 30^\circ$ FIGURE 26 PROLATE SPHEROIDAL RADIATION PATTERNS  $\beta_0 l = 5, 12, H_\phi$  VS.  $\theta$





coated  
Note:

conductor size that of Fig 22

$$\beta_0 l = 5 \quad \beta_1 l = 12$$

$$u_1 = 1.077$$

$$u_2 = 1.1$$

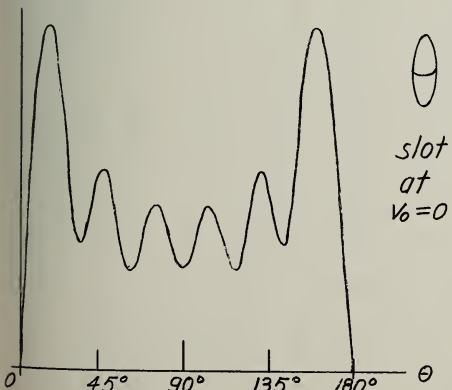
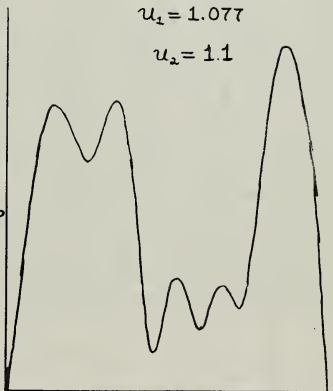
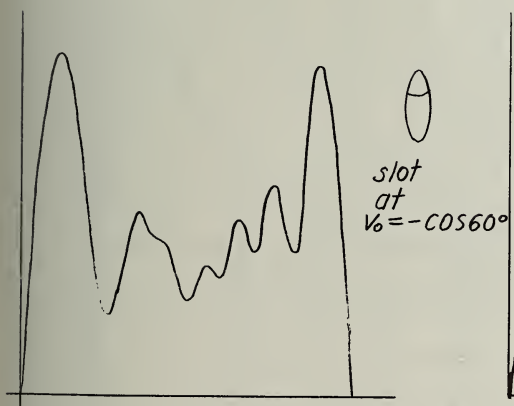
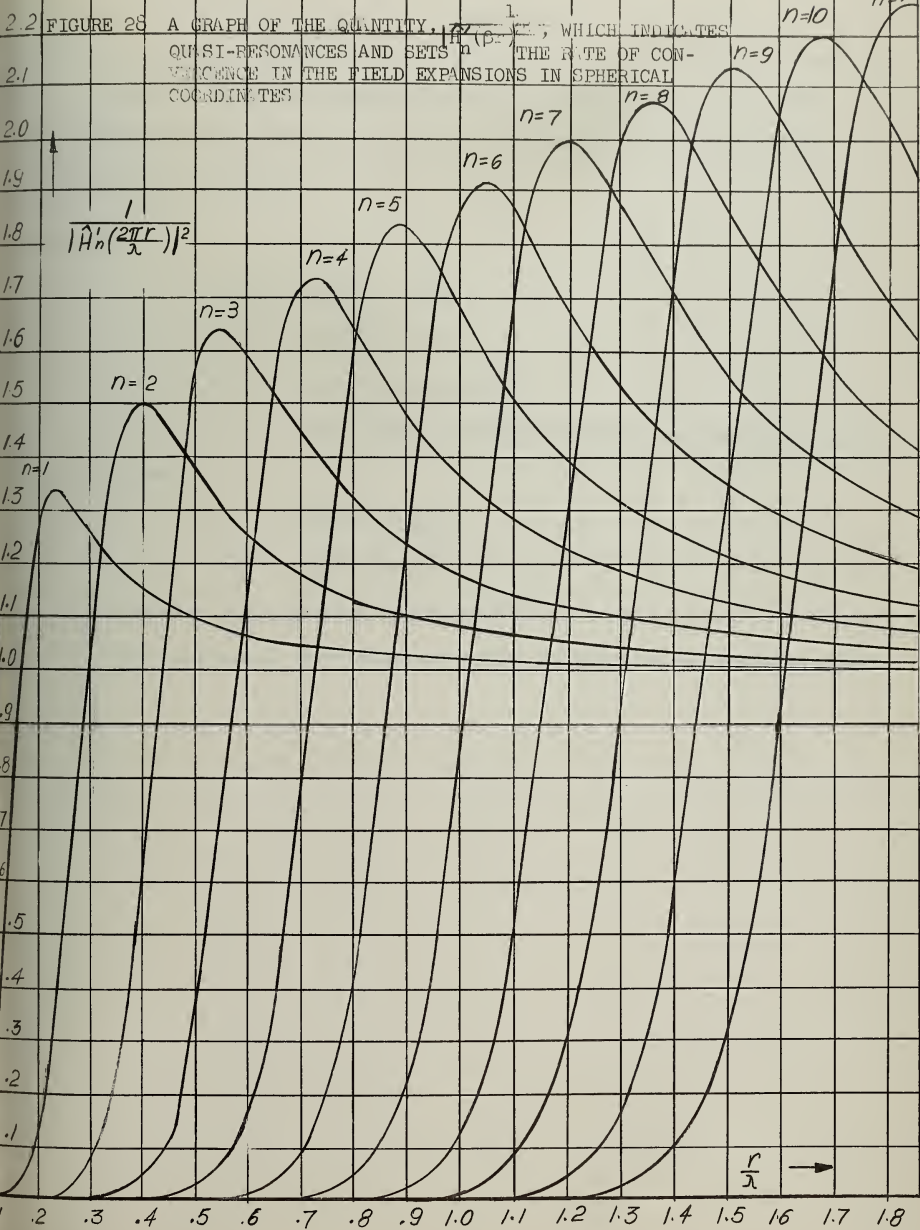


FIGURE 27 PROLATE SPHEROIDAL RADIATION PATTERNS  $\beta l = 5, 12$ ,  $H_\phi$  VS.  $\theta$







## NOTE:

In Figures 29 to 63, negative numbers are represented on the semi-log scales by the following conventions. (The lines joining points are merely aids for the eye)

## Real Part

○ positive value

X negative value

— — — — joins positive values

. — . — . joins negative values or positive and negative values

## Imaginary Part

• positive value

□ negative value

——— joins positive values

||||||| joins negative values or positive and negative values



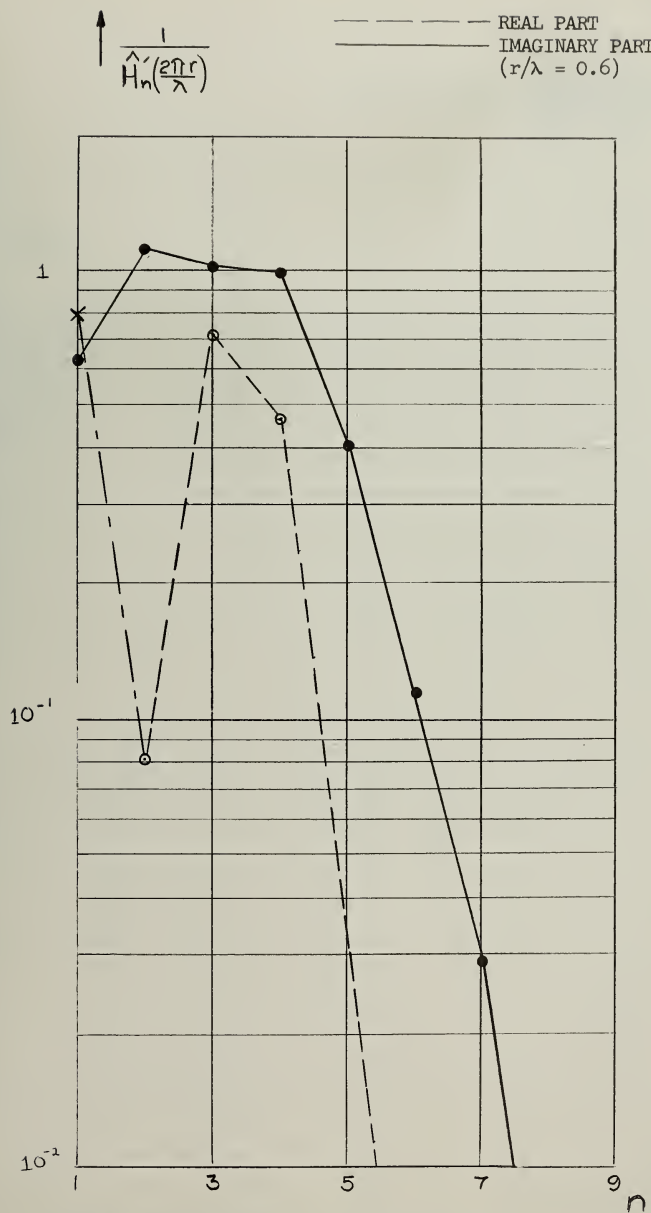
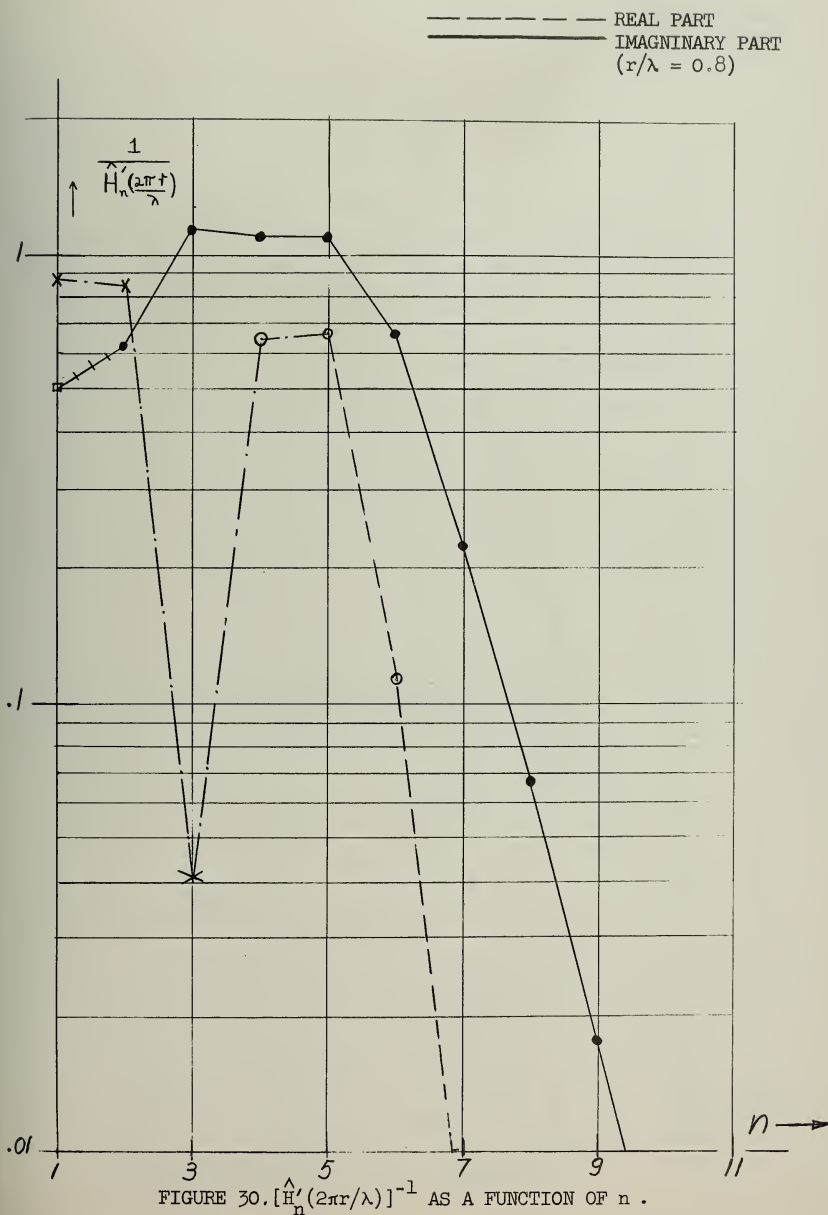


FIGURE 29.  $[\hat{H}'_n(2\pi r/\lambda)]^{-1}$  AS A FUNCTION OF  $n$ .







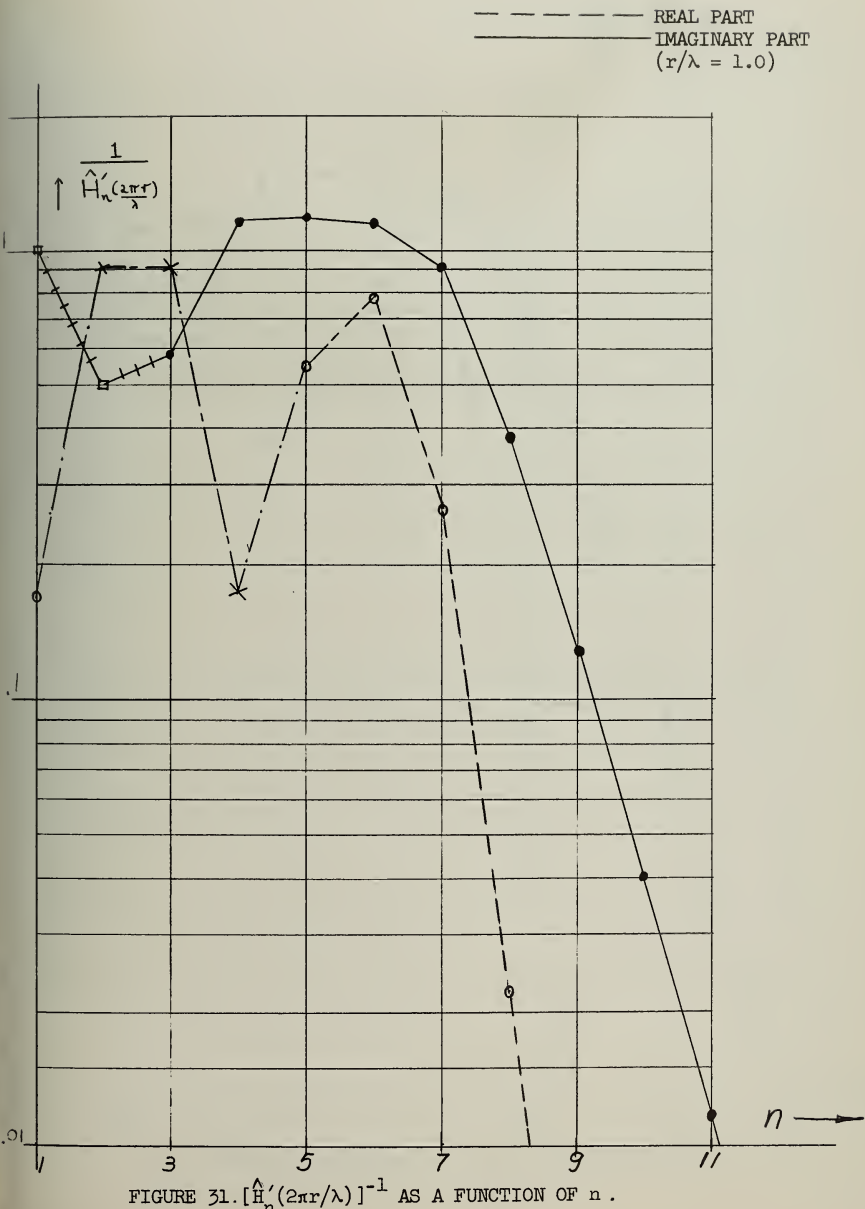


FIGURE 31.  $[\hat{H}'_n(2\pi r/\lambda)]^{-1}$  AS A FUNCTION OF  $n$ .



— — — REAL PART  
 — — IMAGINARY PART  
 $(r/\lambda = 1.2)$

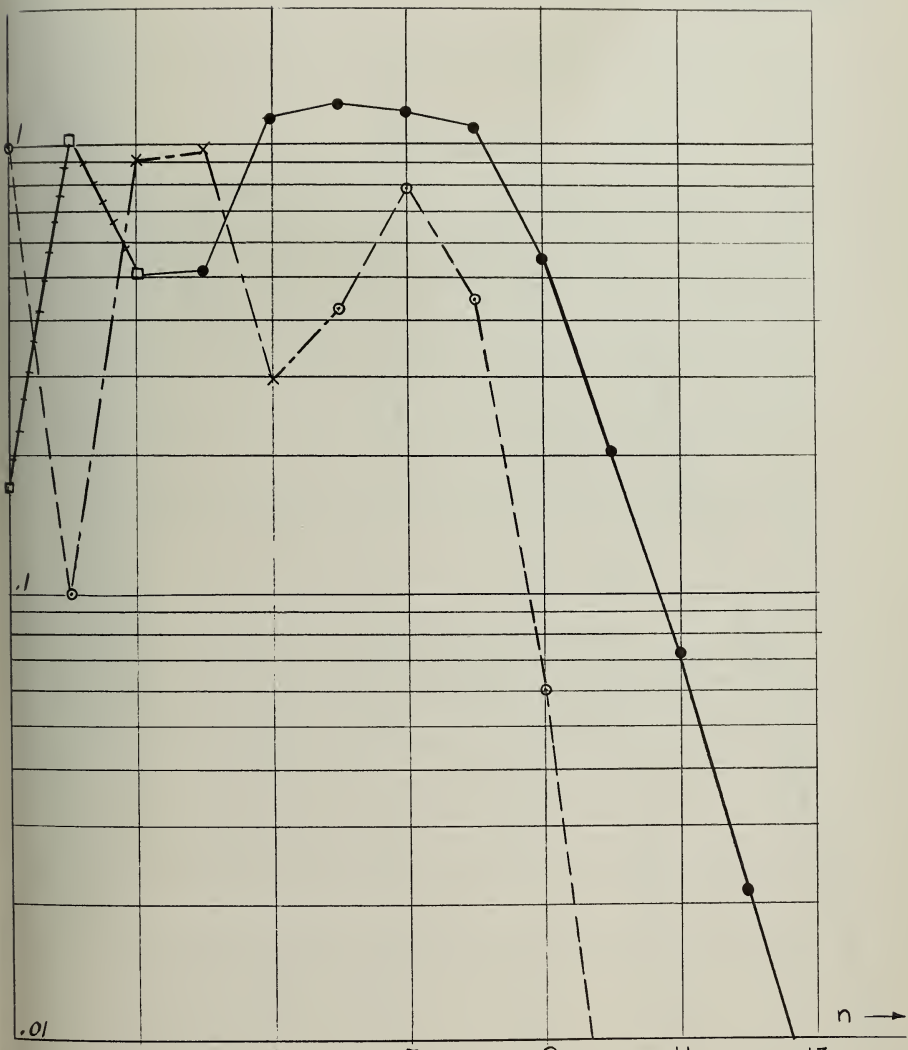


FIGURE 32.  $[H_n'(2\pi r/\lambda)]^{-1}$  AS A FUNCTION OF  $n$ .



— — — REAL PART  
 ————— IMAGINARY PART  
 $(r/\lambda = 1.4)$

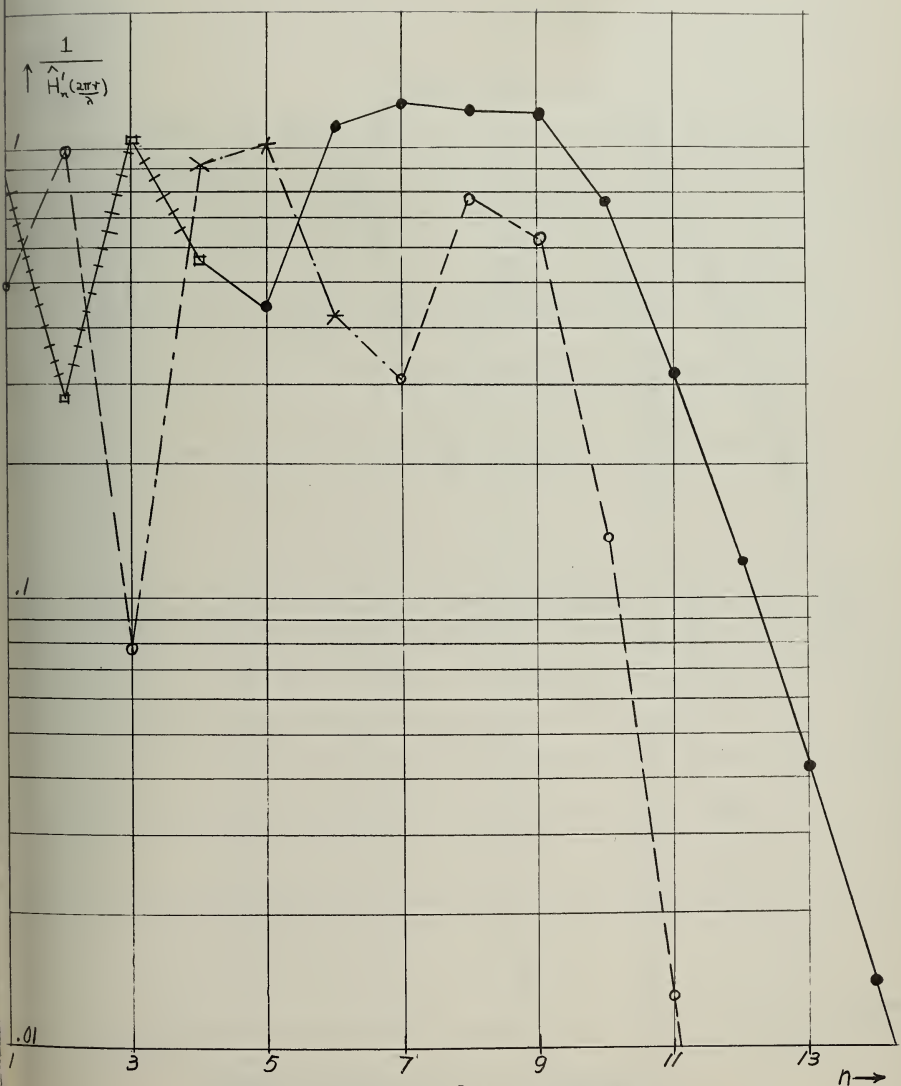


FIGURE 33.  $[\hat{H}'_n(2\pi r/\lambda)]^{-1}$  AS A FUNCTION OF  $n$ .



— — — REAL PART  
 — — IMAGINARY PART  
 $(r/\lambda = 1.6)$

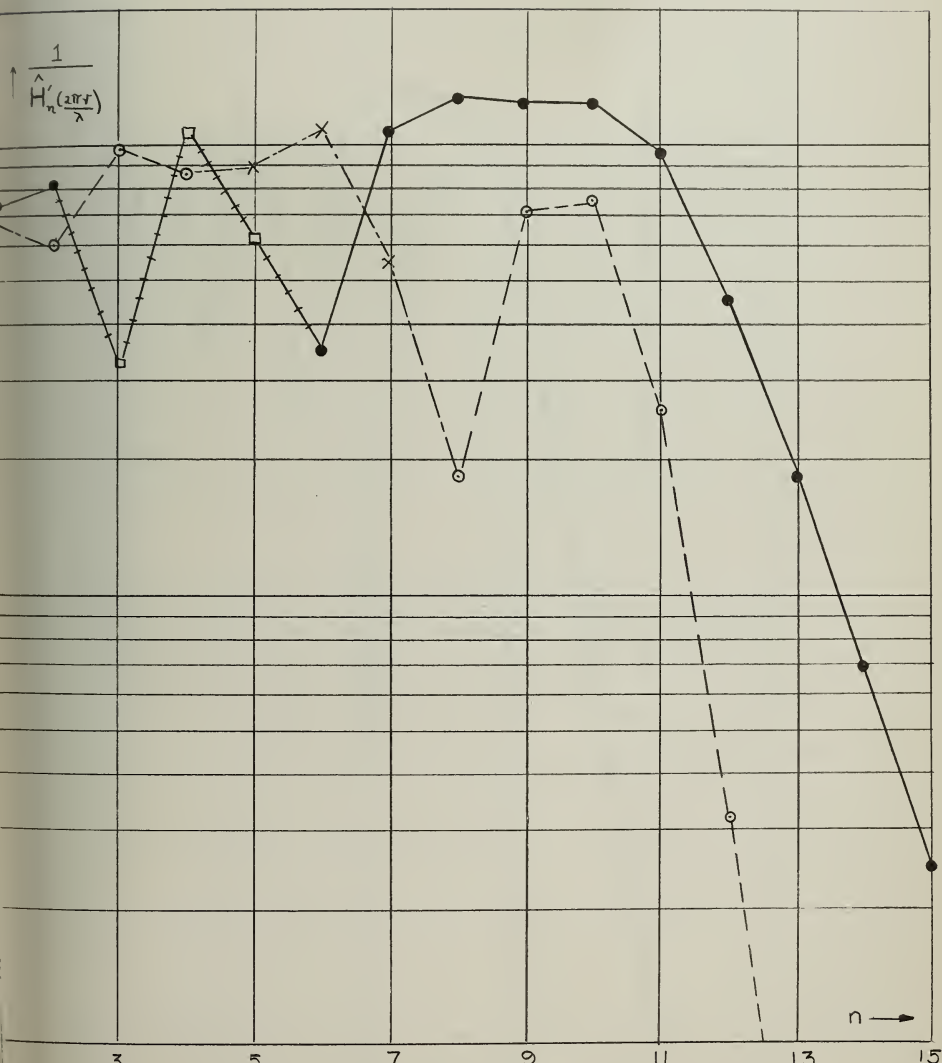


FIGURE 34.  $[\hat{H}'_n(2\pi r/\lambda)]^{-1}$  AS A FUNCTION OF n.



— — — REAL PART  
 ————— IMAGINARY PART  
 $(r/\lambda = 1,8)$

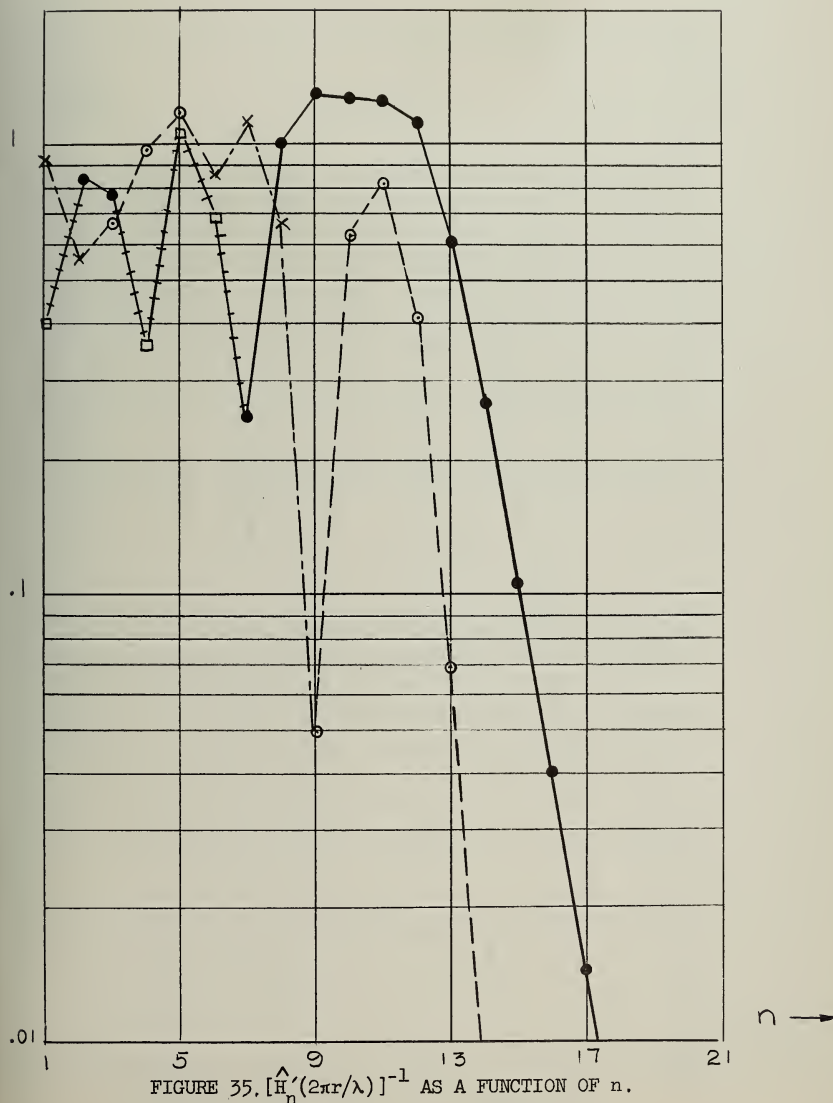
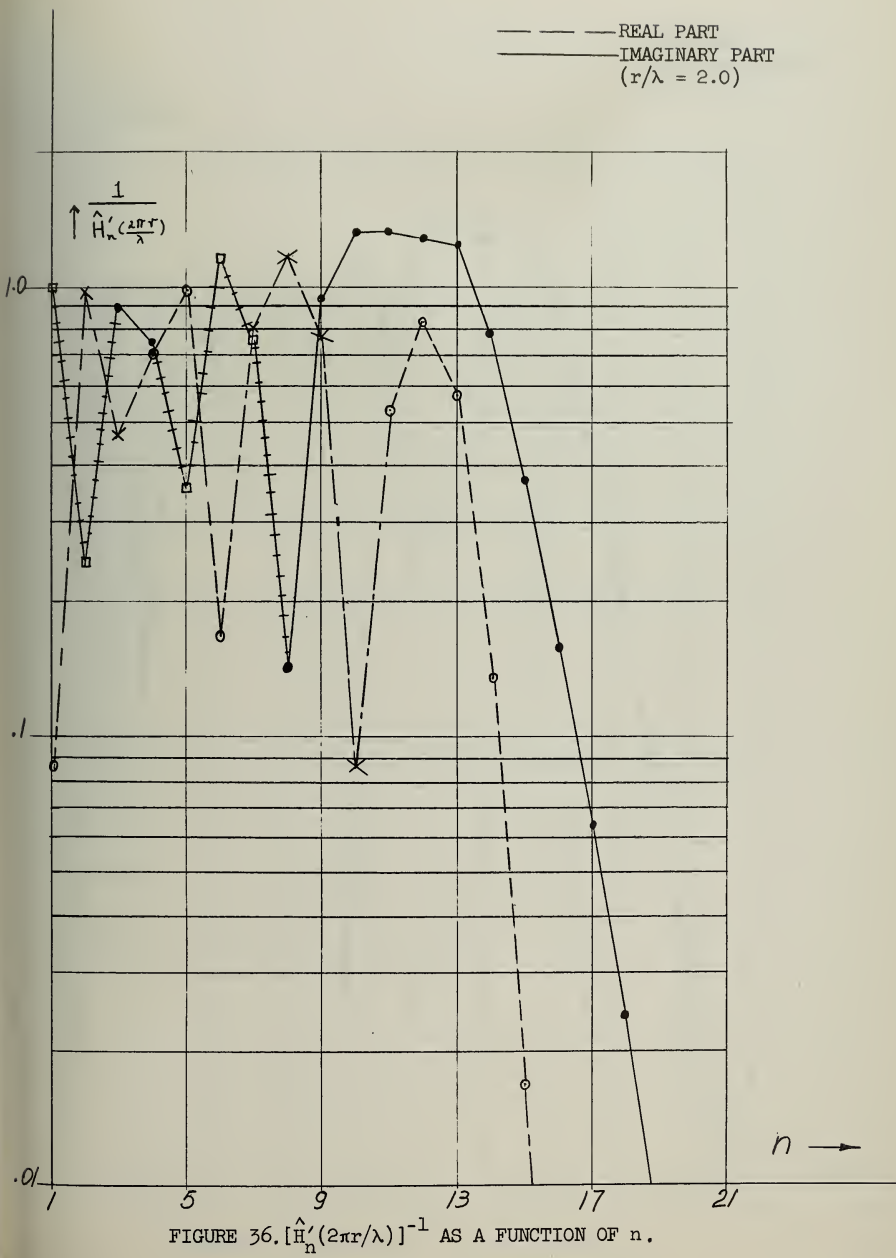
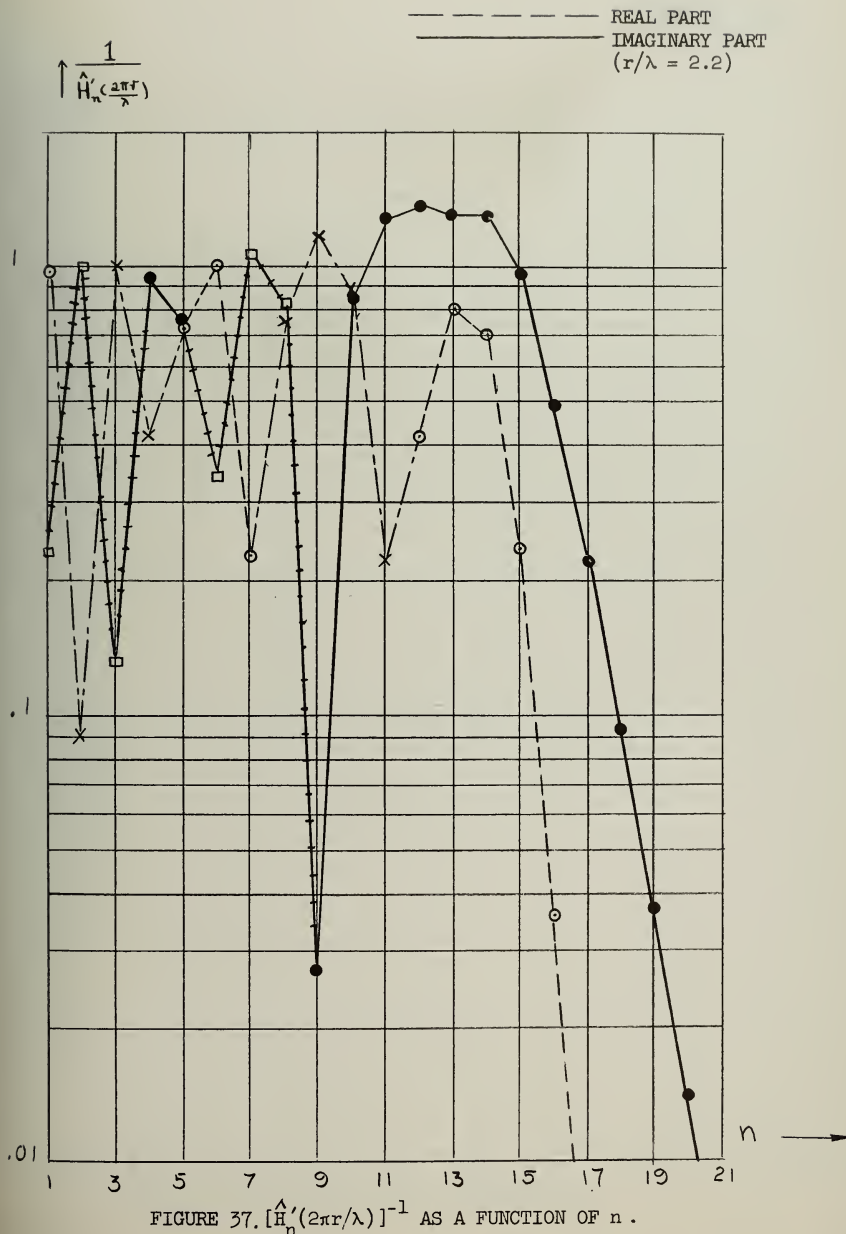


FIGURE 35.  $[\hat{H}_n'(2\pi r/\lambda)]^{-1}$  AS A FUNCTION OF n.











— — — — — REAL PART  
 —————— IMAGINARY PART  
 $(r/\lambda = 2.4)$

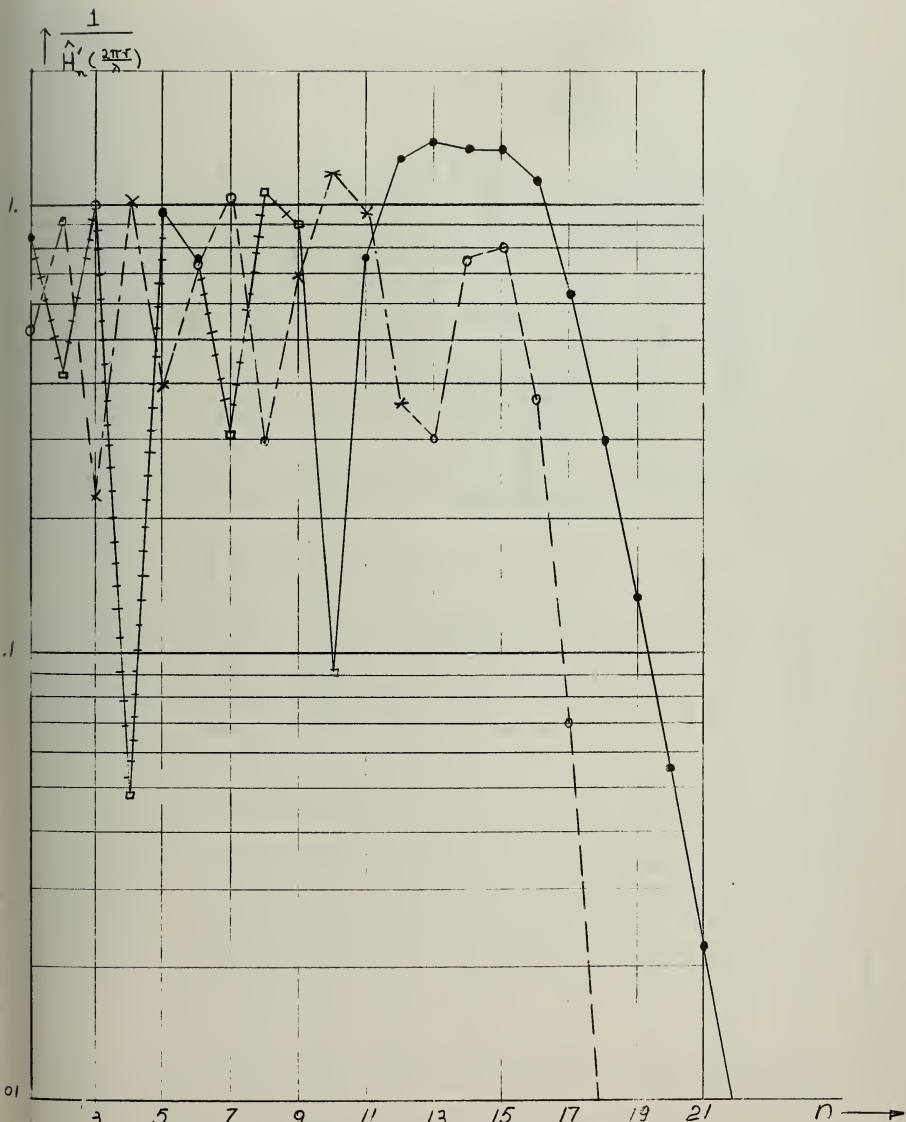


FIGURE 38.  $[H_n'(2\pi r/\lambda)]^{-1}$  AS A FUNCTION OF n.



— — — REAL PART  
 — — IMAGINARY PART  
 $(r/\lambda = 3.2)$

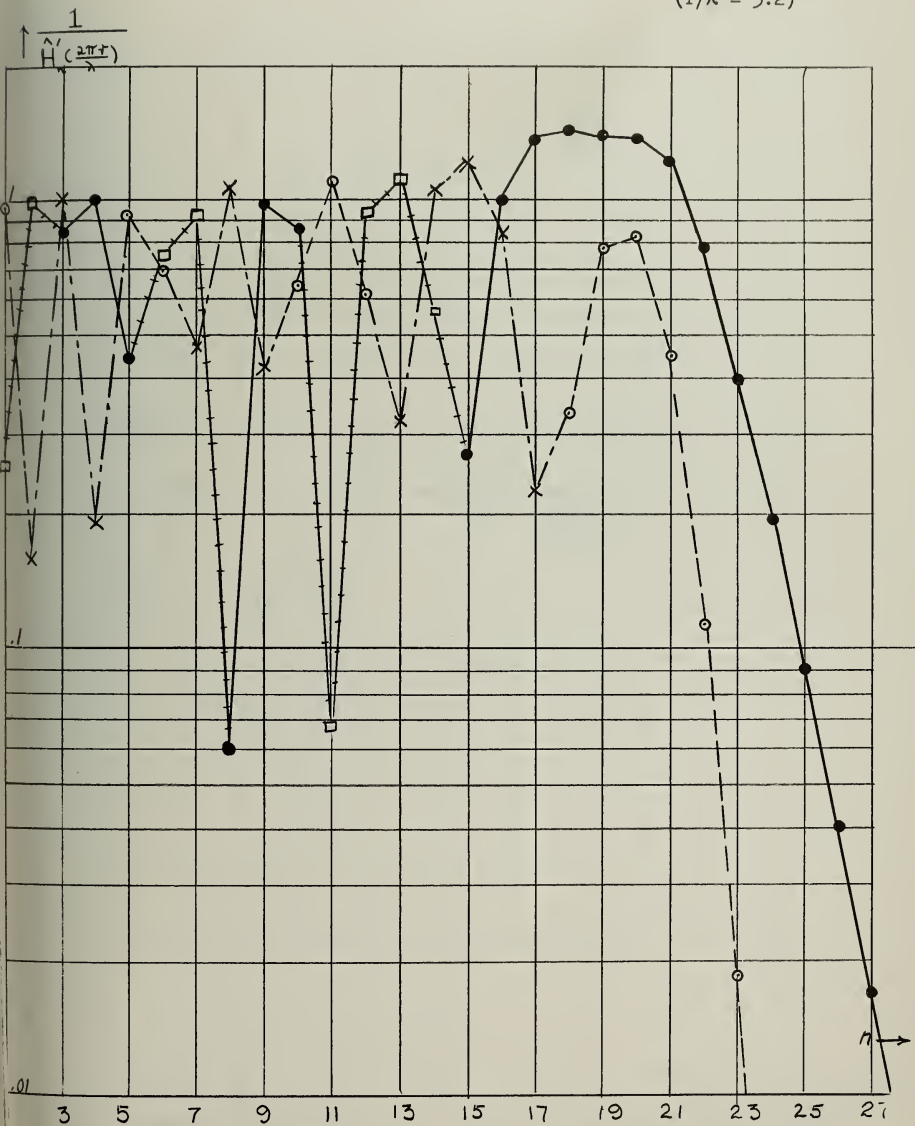


FIGURE 39.  $[H_n'(2\pi r/\lambda)]^{-1}$  AS A FUNCTION OF  $n$ .



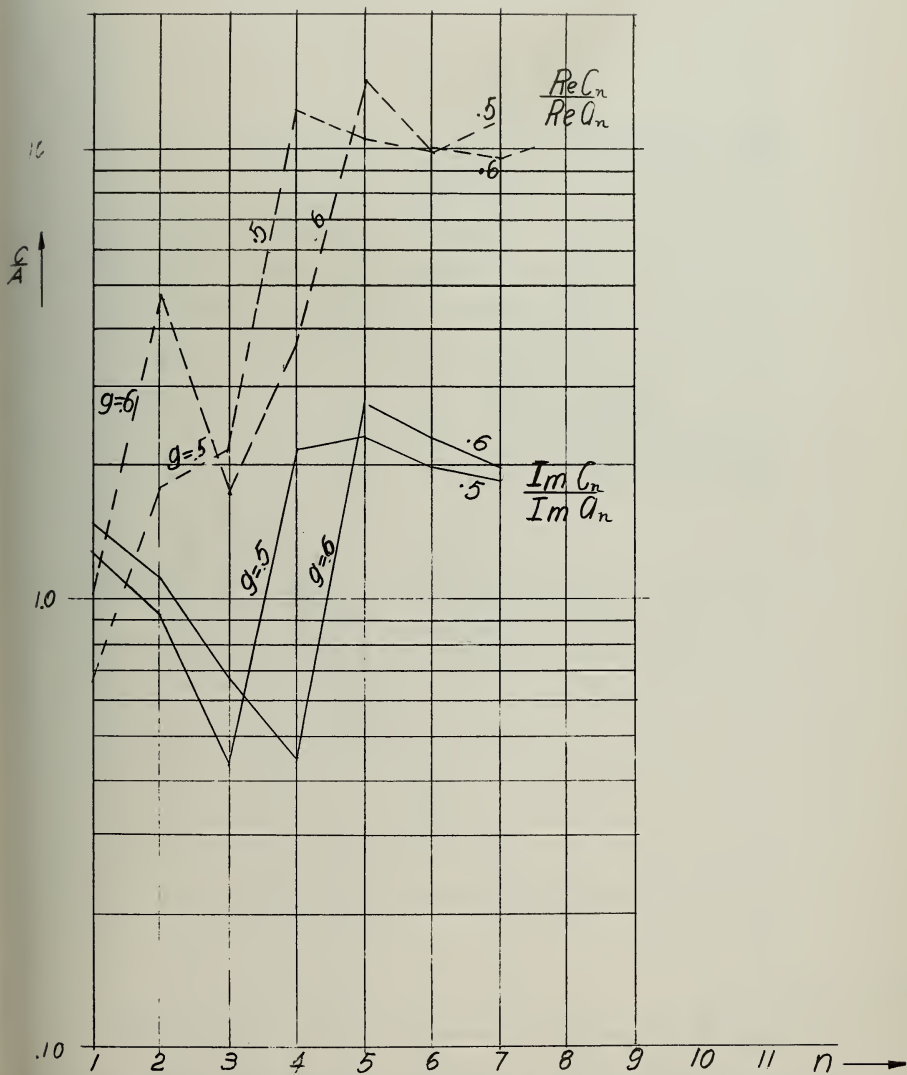


FIGURE 40 RATIO OF COEFFICIENTS,  $c_n$ , IN THE FIELD EXPANSION FOR THE COATED SPHERICAL RADIATOR TO THE COEFFICIENTS  $a_n$  IN THE EXPANSION FOR THE UNCOATED SPHERICAL RADIATOR WITH THE SAME EXCITATION  
 $(g = r/\lambda)$  COATING THICKNESS  $.1\lambda$ .  $\epsilon = 2.25$



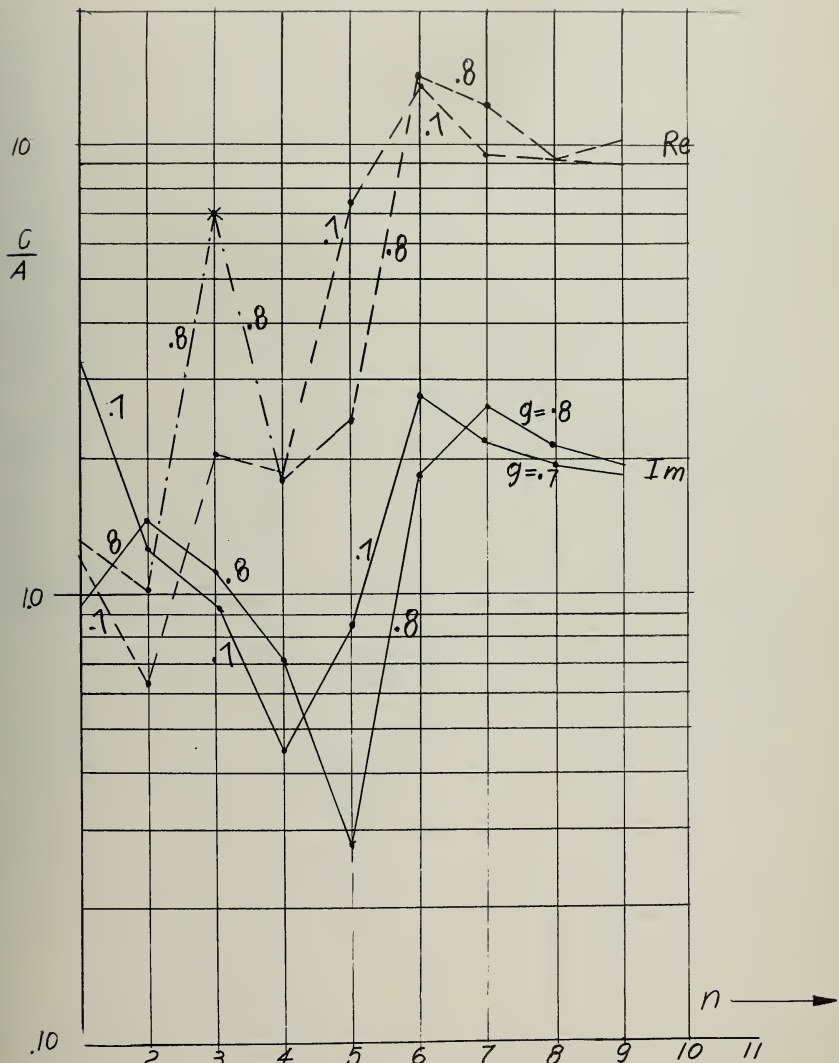


FIGURE 41 RATIO OF COEFFICIENTS,  $c_n$ , IN THE FIELD EXPANSION FOR THE COATED SPHERICAL RADIATOR TO THE COEFFICIENTS  $a_n$  IN THE EXPANSION FOR THE UNCOATED SPHERICAL RADIATOR WITH THE SAME EXCITATION.  
 $(g = r/\lambda)$ . COATING THICKNESS  $1\lambda$ .  $\epsilon = 2.25$



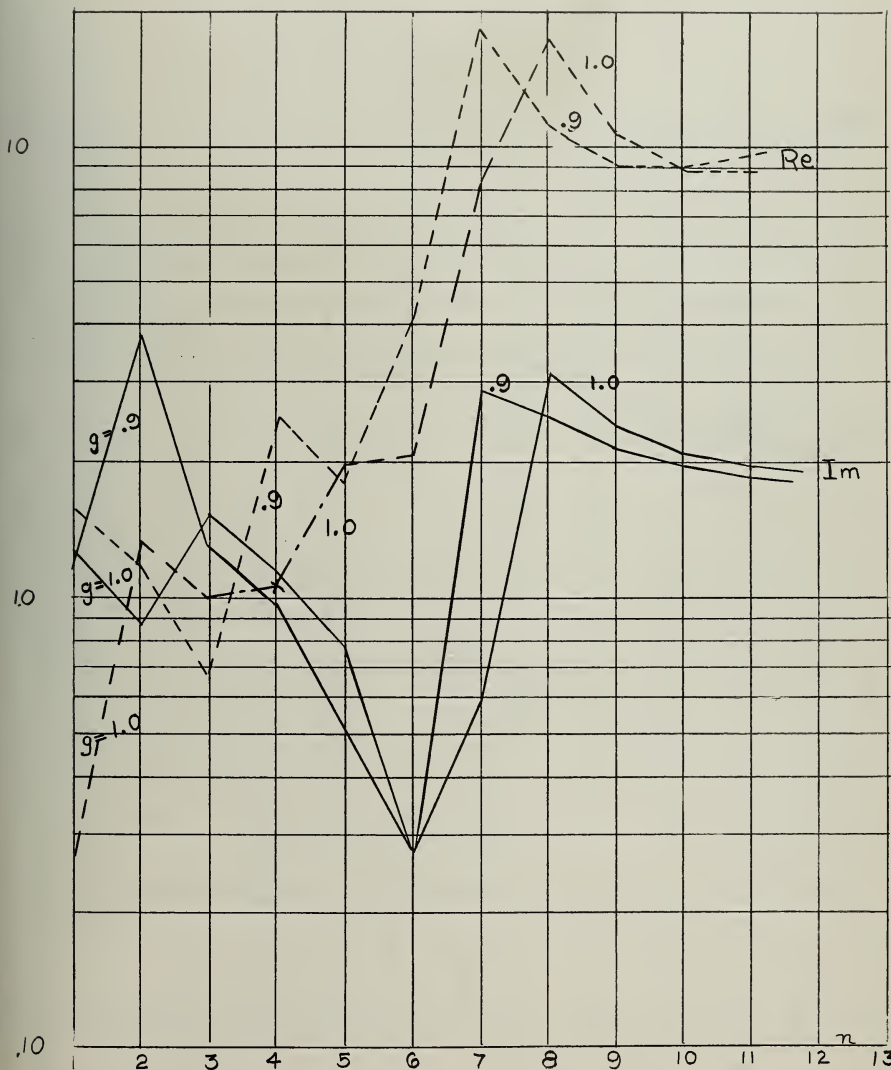
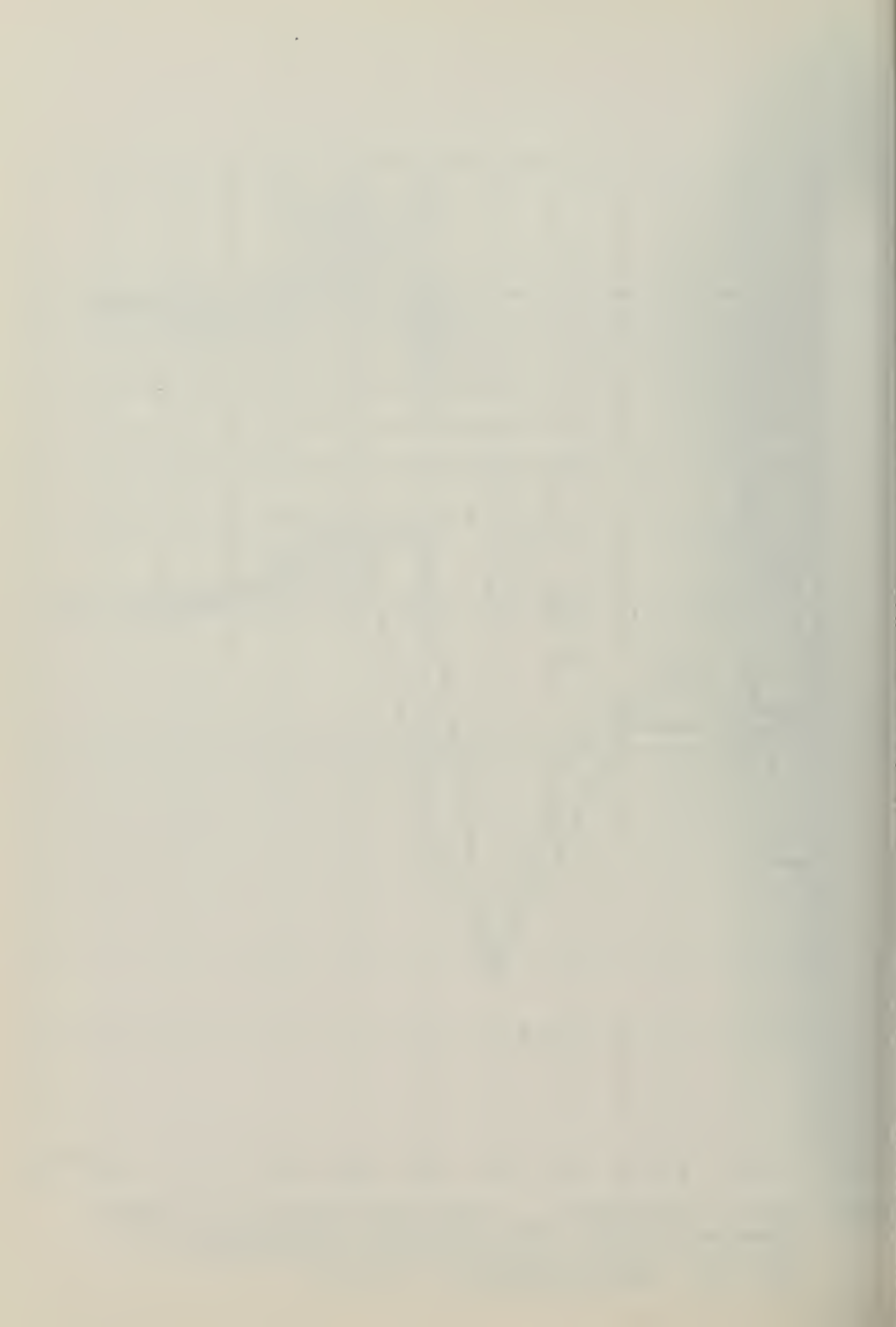


FIGURE 42 RATIO OF COEFFICIENTS,  $c_n$ , IN THE FIELD EXPANSION FOR THE COATED SPHERICAL RADIATOR TO THE COEFFICIENTS  $a_n$  IN THE EXPANSION FOR THE UNCOATED SPHERICAL RADIATOR WITH THE SAME EXCITATION.  
 $(g = r/\lambda)$ . COATING THICKNESS  $.1\lambda$ .  $\epsilon = 2.25$



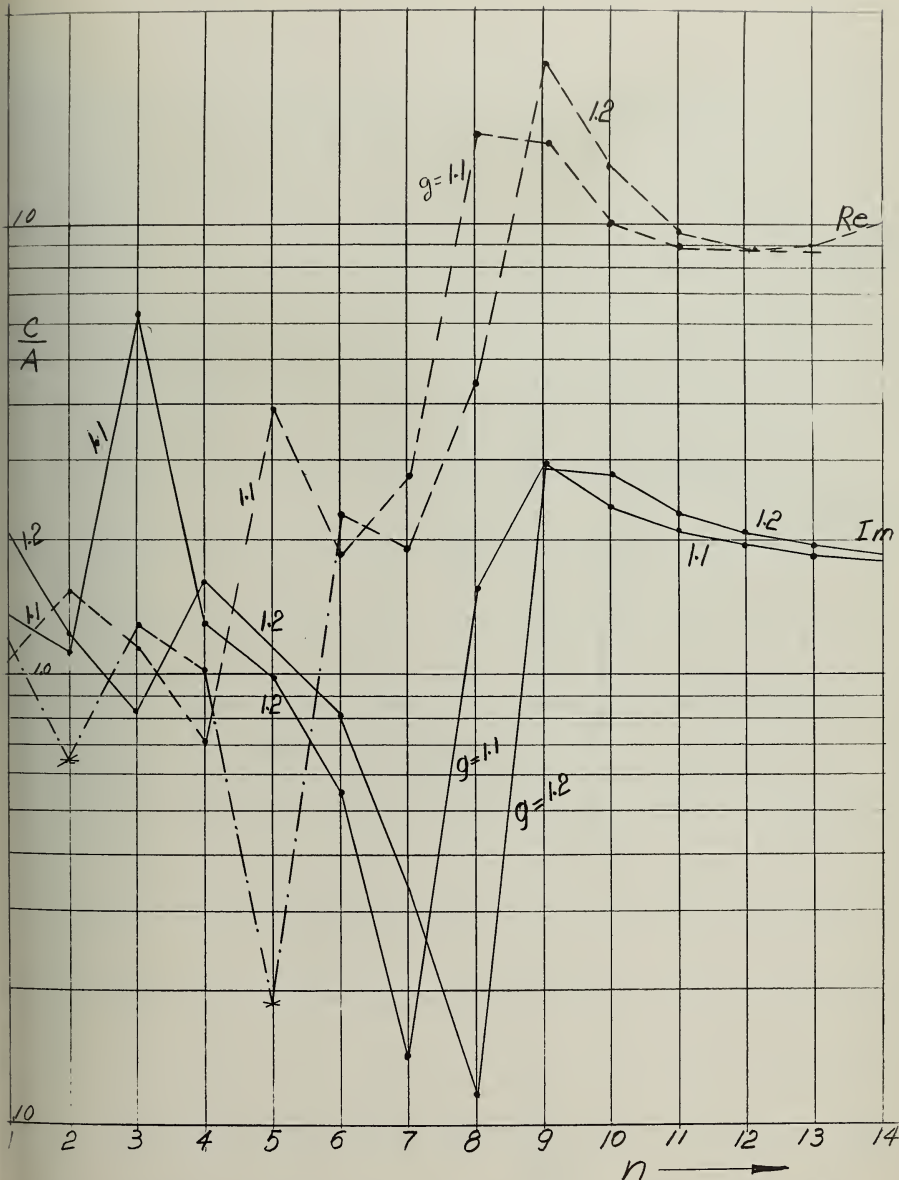


FIGURE 43 RATIO OF COEFFICIENTS,  $c_n$ , IN THE FIELD EXPANSION FOR THE COATED SPHERICAL RADIATOR TO THE COEFFICIENTS  $a_n$  IN THE EXPANSION FOR THE UNCOATED SPHERICAL RADIATOR WITH THE SAME EXCITATION.  
 $(g = r/\lambda)$ . COATING THICKNESS  $.1\lambda$ .  $\epsilon = 2.25$



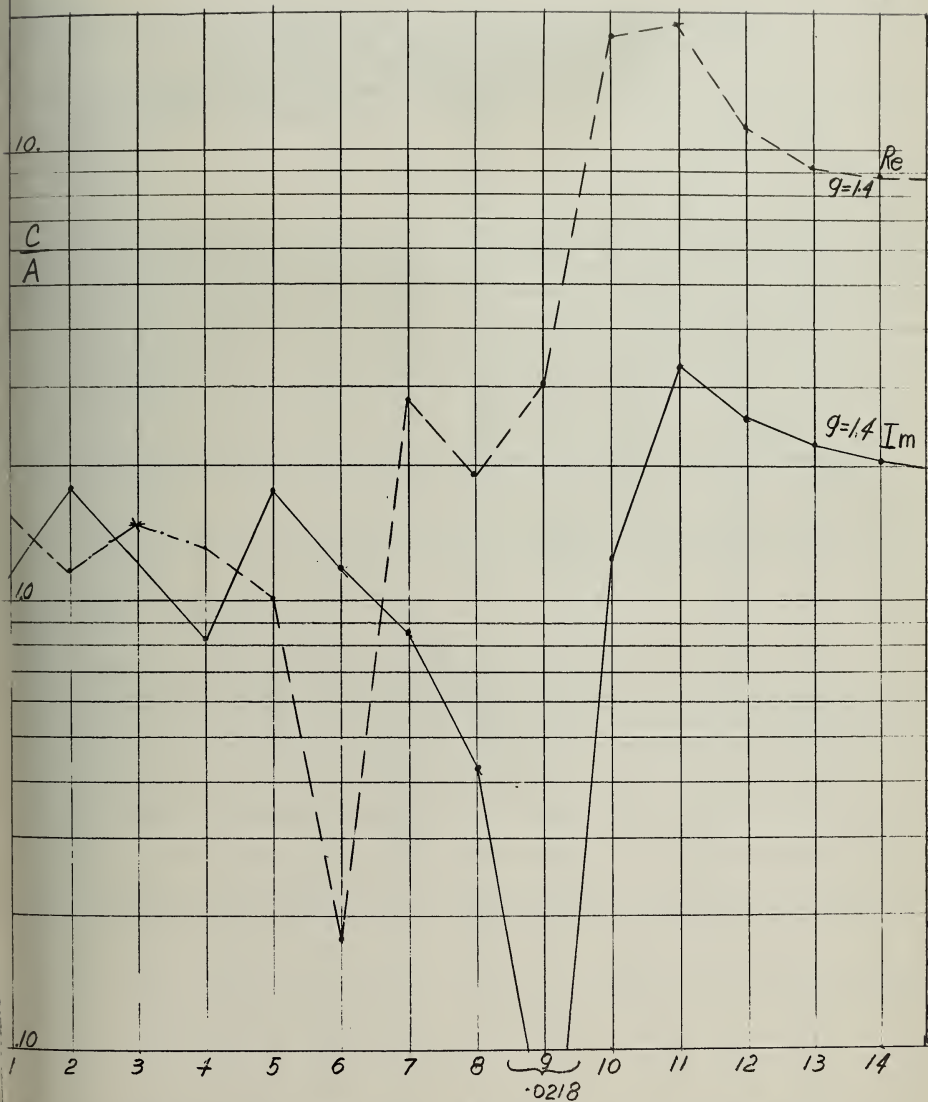


FIGURE 44 RATIO OF COEFFICIENTS,  $C_A$ , IN THE FIELD EXPANSION FOR THE COATED SPHERICAL RADIATOR TO THE COEFFICIENTS  $a_A$  IN THE EXPANSION FOR THE UNCOATED SPHERICAL RADIATOR WITH THE SAME EXCITATION.  
 $(g = r/\lambda)$ . COATING THICKNESS  $.1\lambda$ .  $\epsilon = 2.25$



FIGURE 45 RATIO OF COEFFICIENTS,  $c_n$ , IN THE FIELD EXPANSION FOR THE COATED SPHERICAL RADIATOR TO THE COEFFICIENTS,  $a_n$ , IN THE EXPANSION FOR THE UNCOATED SPHERICAL RADIATOR WITH THE SAME EXCITATION. ( $g = r/\lambda$ ). COATING THICKNESS  $.1\lambda$ .  $\epsilon = 2.25$

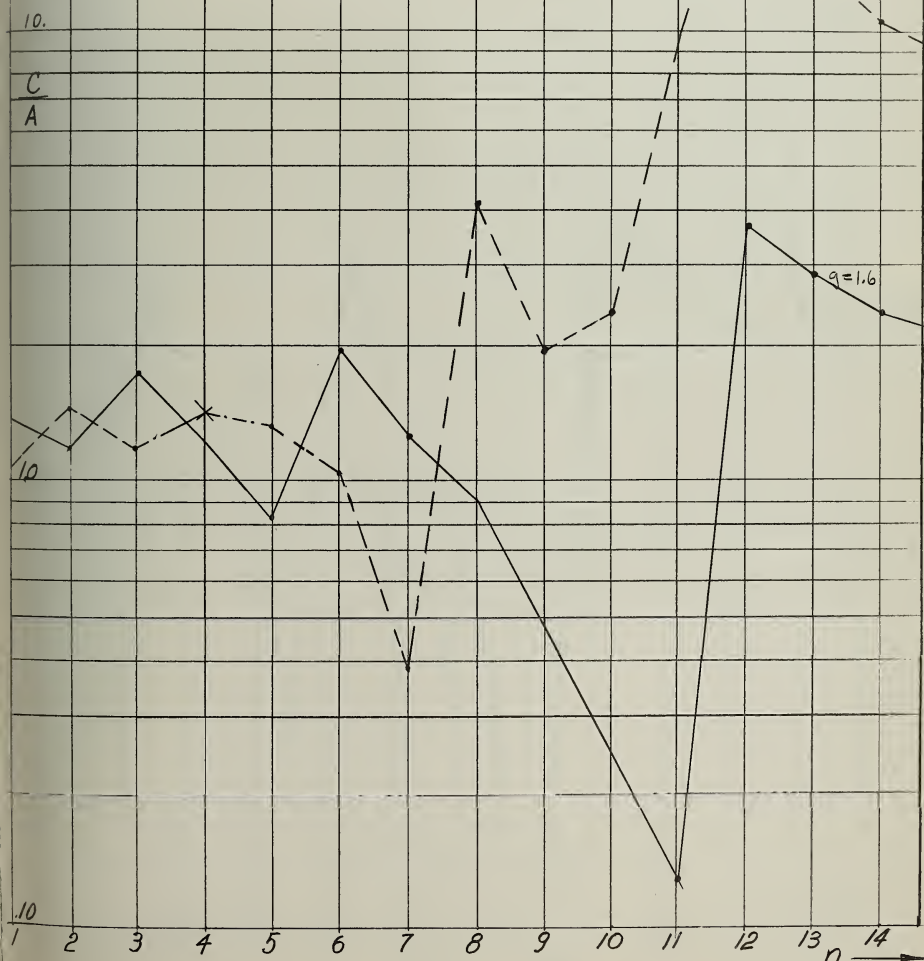




FIGURE 46 RATIO OF COEFFICIENTS,  $c_n/a_n$ , IN THE FIELD EXPANSION FOR THE COATED SPHERICAL RADIATOR TO THE COEFFICIENTS,  $a_n$ , IN THE EXPANSION FOR THE UNCOATED SPHERICAL RADIATOR WITH THE SAME EXCITATION. ( $g = r/\lambda$ ). COATING THICKNESS  $.1\lambda$ .  $\epsilon = 2.25$

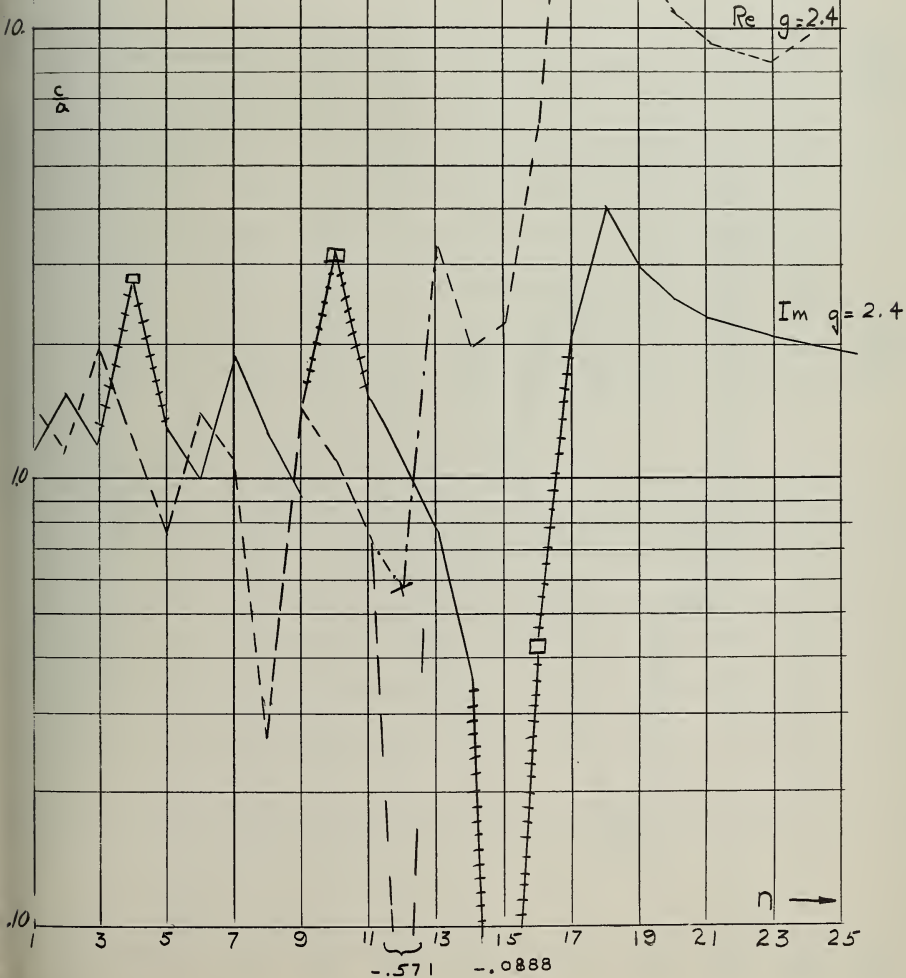




FIGURE 47 RATIO OF COEFFICIENTS,  $c_n$ , IN THE FIELD EXPANSION FOR THE COATED SPHERICAL RADIATOR TO THE COEFFICIENTS  $a_n$  IN THE EXPANSION FOR THE UNCOATED SPHERICAL RADIATOR WITH THE SAME EXCITATION.  
 $(g = r/\lambda)$ . COATING THICKNESS  $1\lambda$ .  $\epsilon = 2.25$

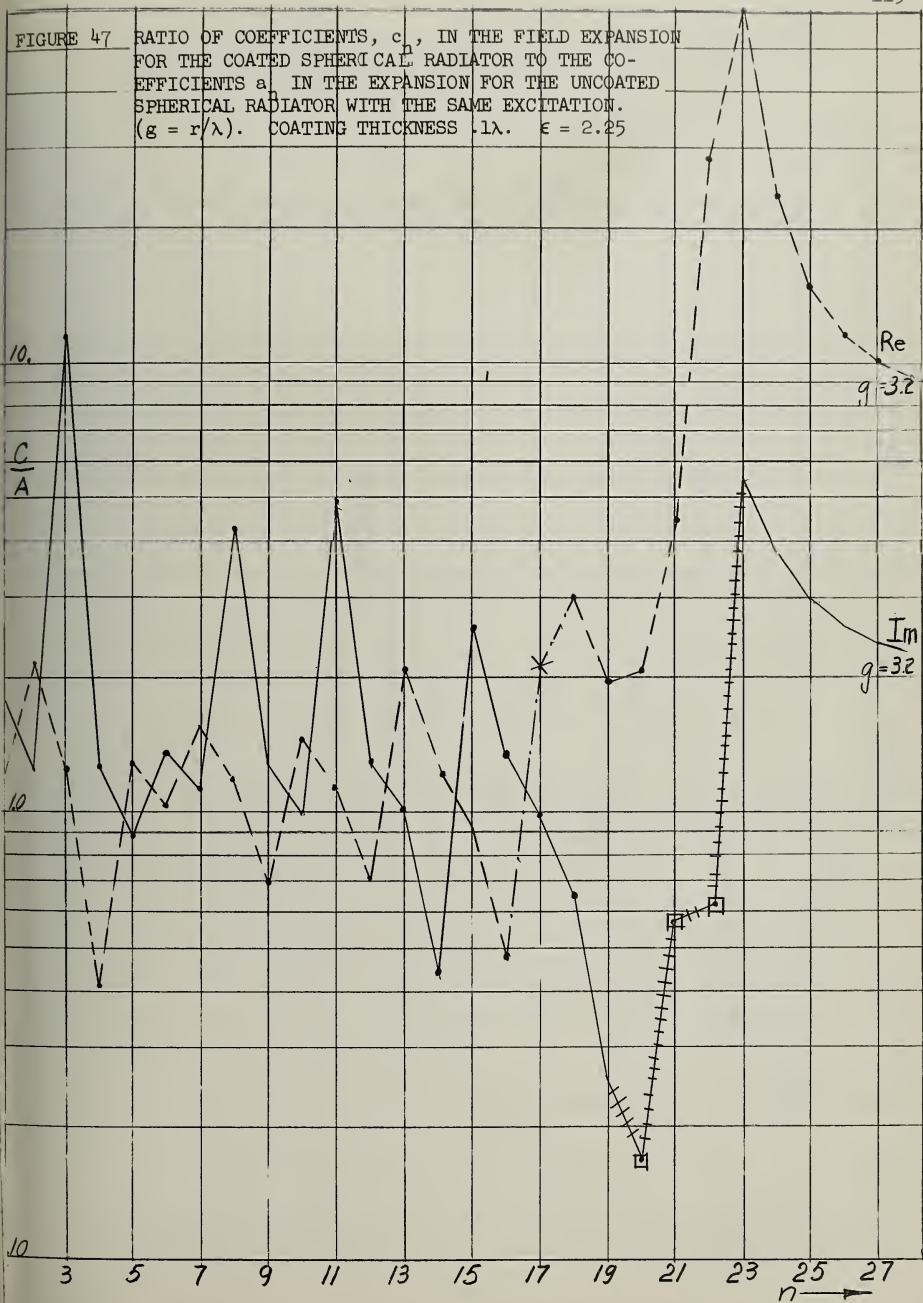




FIGURE 48 RATIO OF COEFFICIENTS,  $c_n$ , IN THE FIELD EXPANSION FOR THE COATED SPHERICAL RADIATOR TO THE COEFFICIENTS,  $a_n$ , IN THE EXPANSION FOR THE UNCOATED SPHERICAL RADIATOR WITH THE SAME EXCITATION.  
 $(g = r/\lambda)$ . COATING THICKNESS  $.1\lambda$ .  $\epsilon = 2.25$

10.

 $\frac{c}{a}$ 

10

10

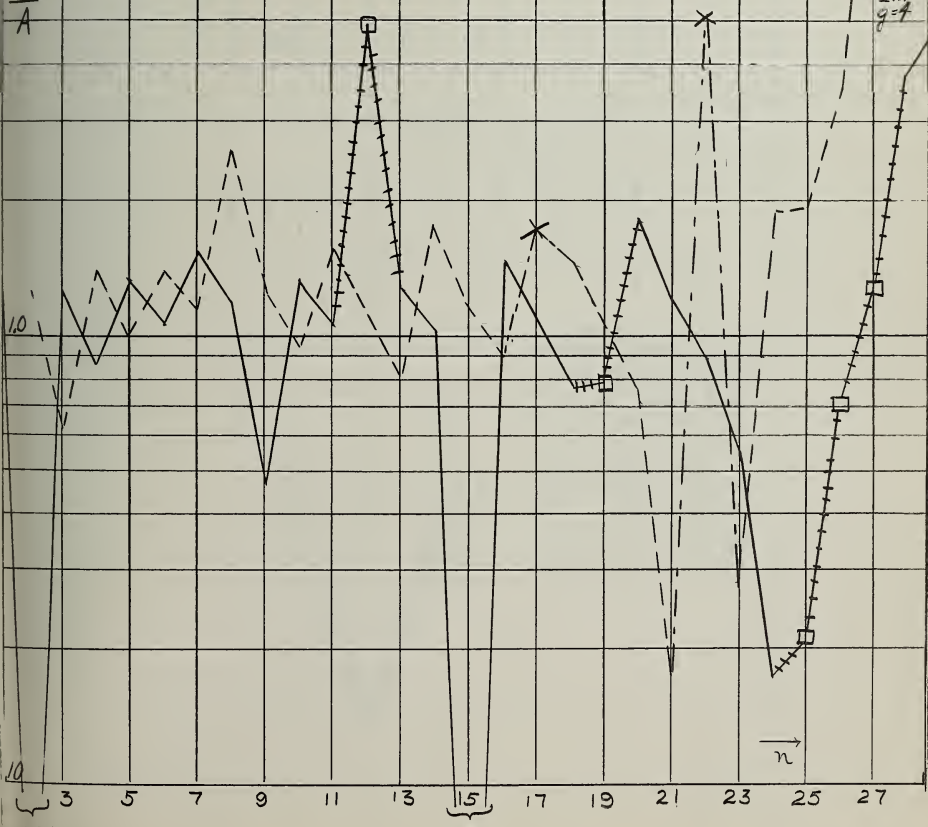
.0340

.042

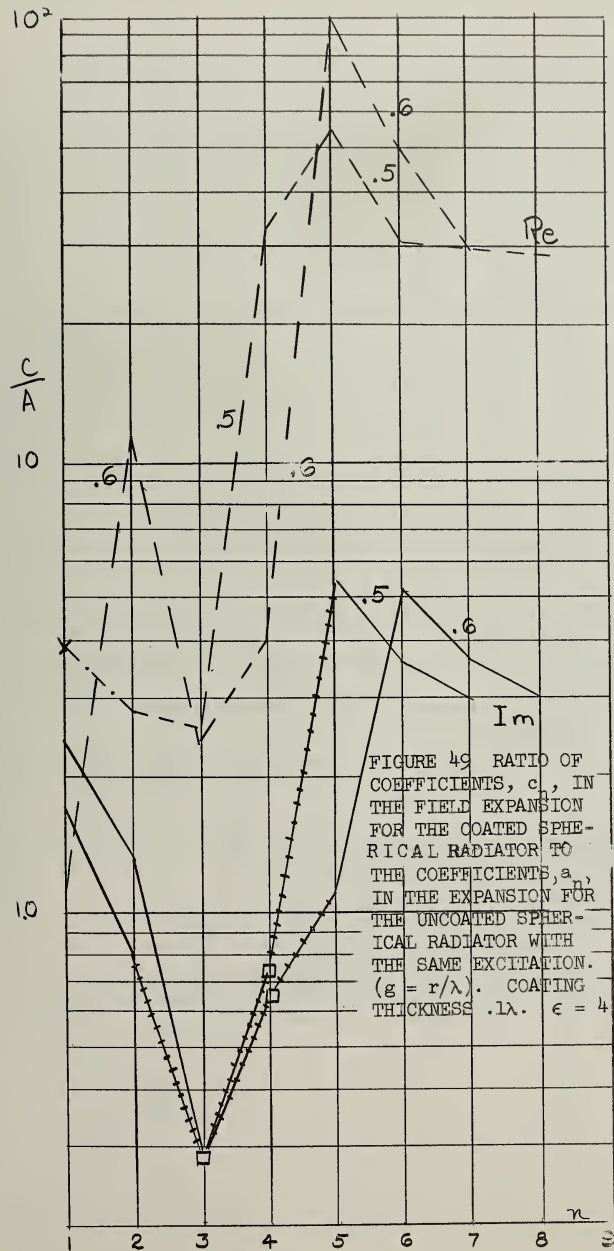
10a

$Re$   
 $g = 4.0$

$Im$   
 $g = 4$

 $n$ 







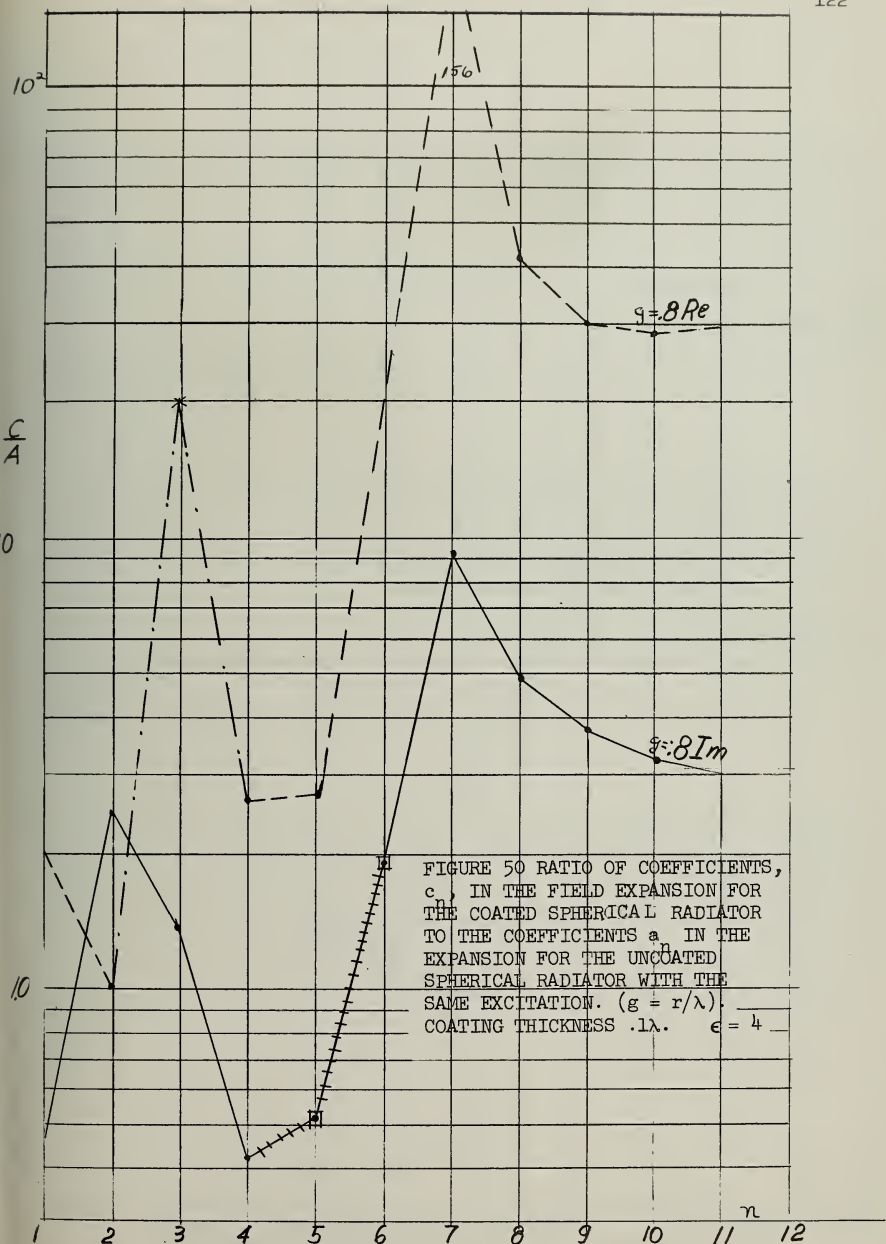


FIGURE 50 RATIO OF COEFFICIENTS,  
 $C_A$  IN THE FIELD EXPANSION FOR  
 THE COATED SPHERICAL RADIATOR  
 TO THE COEFFICIENTS  $a_n$  IN THE  
 EXPANSION FOR THE UNCOATED  
 SPHERICAL RADIATOR WITH THE  
 SAME EXCITATION. ( $g = r/\lambda$ ).  
 COATING THICKNESS  $.1\lambda$ .     $\epsilon = 4$



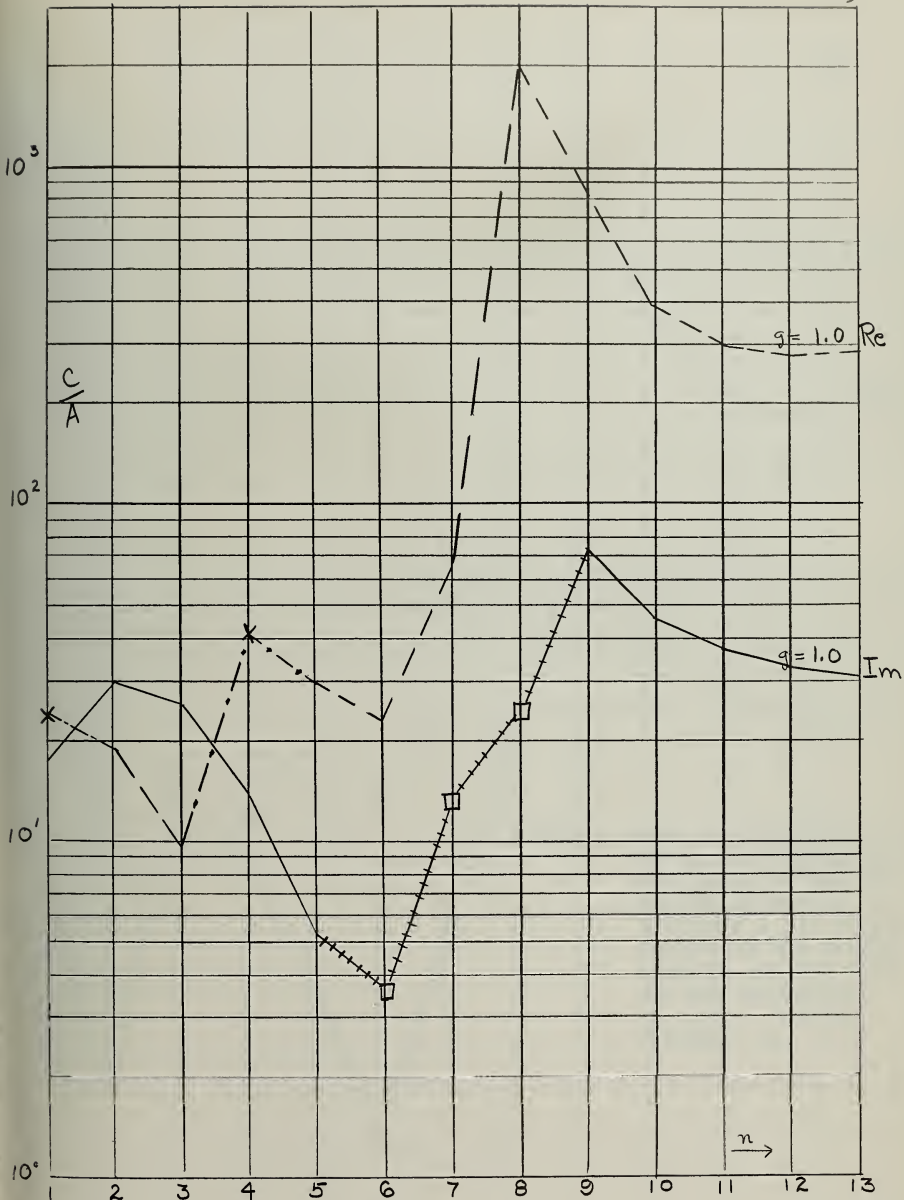


FIGURE 51 RATIO OF COEFFICIENTS,  $c_n$ , IN THE FIELD EXPANSION FOR THE COATED SPHERICAL RADIATOR TO THE COEFFICIENTS,  $a_n$ , IN THE EXPANSION FOR THE UNCOATED SPHERICAL RADIATOR WITH THE SAME EXCITATION.  
 $(g = r/\lambda)$ . COATING THICKNESS  $.1\lambda$ .  $\epsilon = 4$



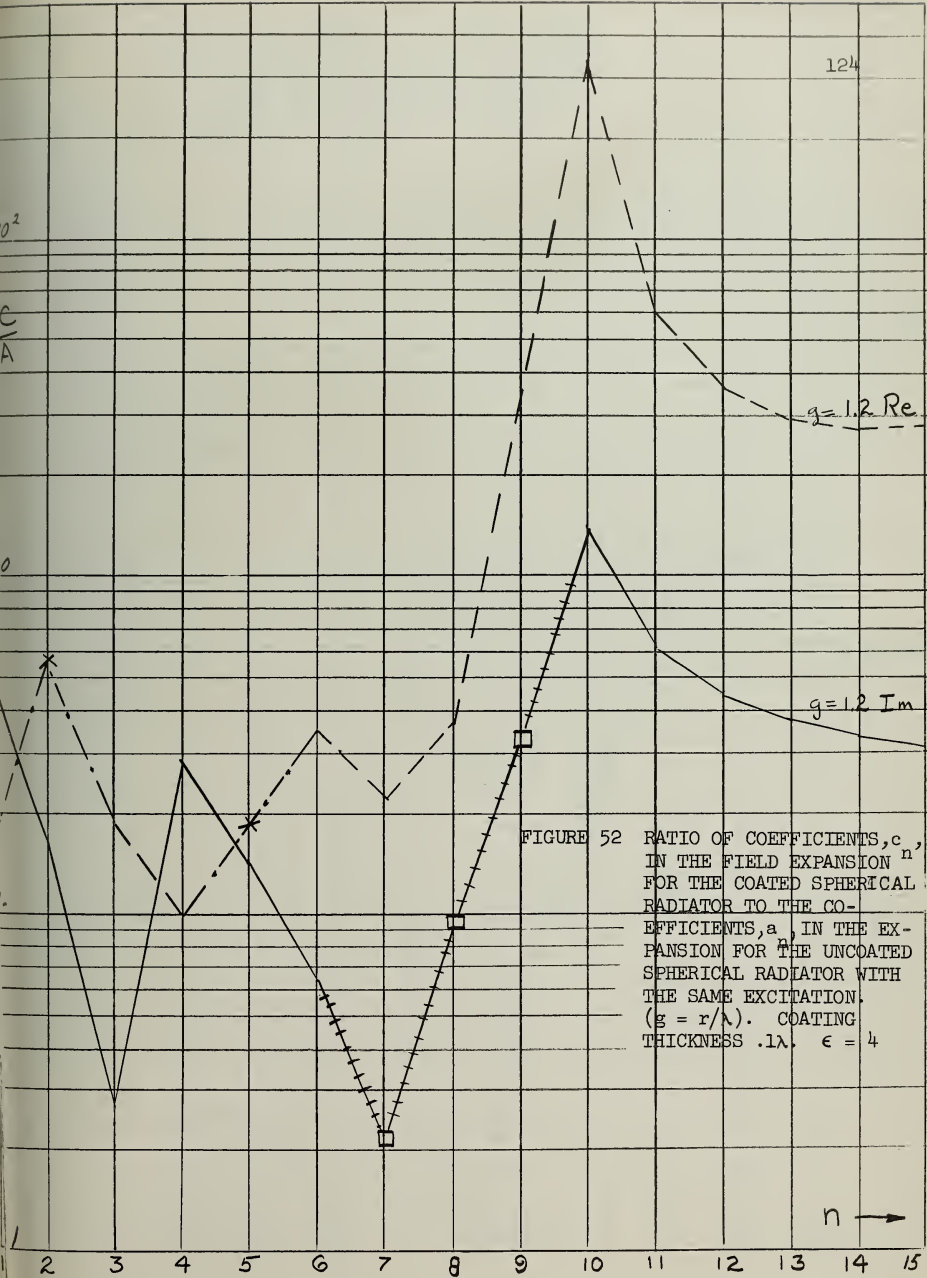
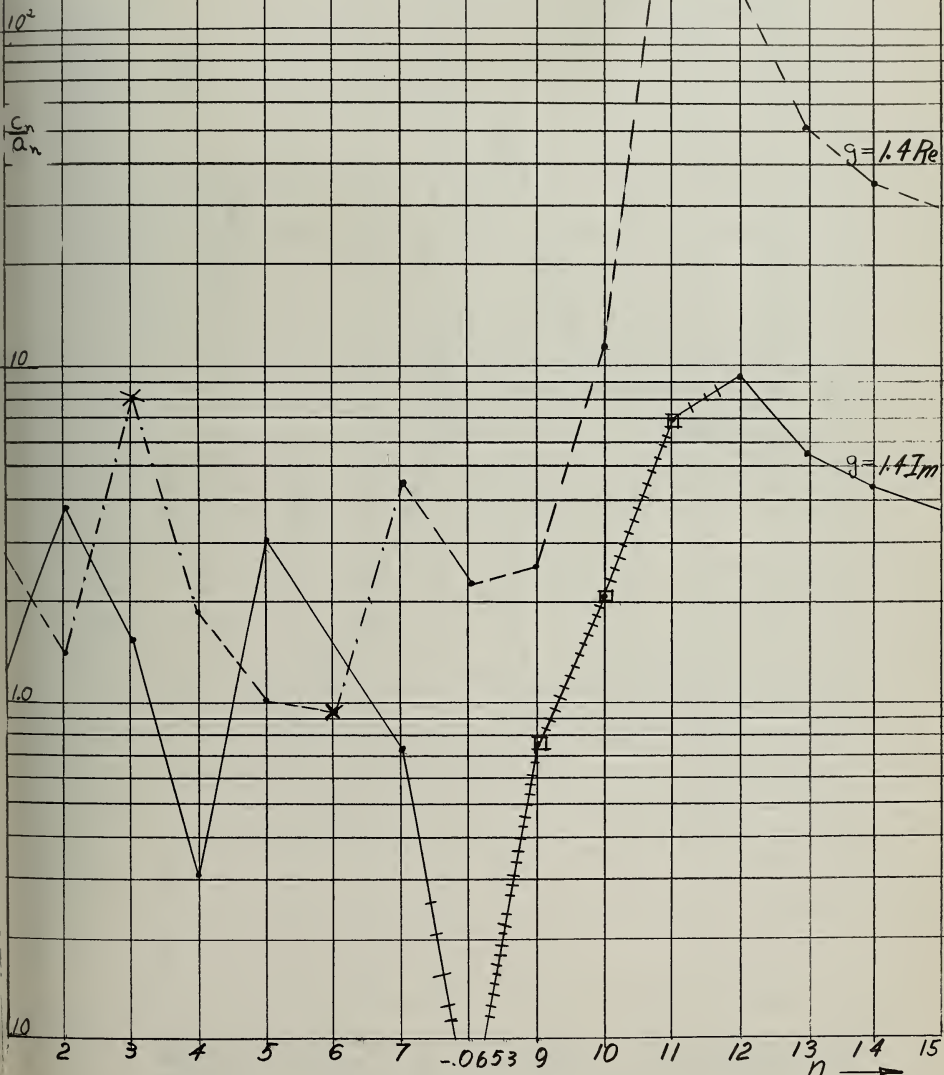


FIGURE 52 RATIO OF COEFFICIENTS,  $c_n$ , IN THE FIELD EXPANSION FOR THE COATED SPHERICAL RADIATOR TO THE COEFFICIENTS,  $a_n$ , IN THE EXPANSION FOR THE UNCOATED SPHERICAL RADIATOR WITH THE SAME EXCITATION. ( $g = r/\lambda$ ). COATING THICKNESS  $.1\lambda$ .  $\epsilon = 4$



FIGURE 53

RADIO OF COEFFICIENTS,  $c_n / a_n$ , IN THE FIELD EXPANSION FOR THE COATED SPHERICAL RADIATOR TO THE COEFFICIENTS,  $a_n$ , IN THE EXPANSION FOR THE UNCOATED SPHERICAL RADIATOR WITH THE SAME EXCITATION. ( $g = r/\lambda$ ). COATING THICKNESS  $.1\lambda$ .  $\epsilon = 4$





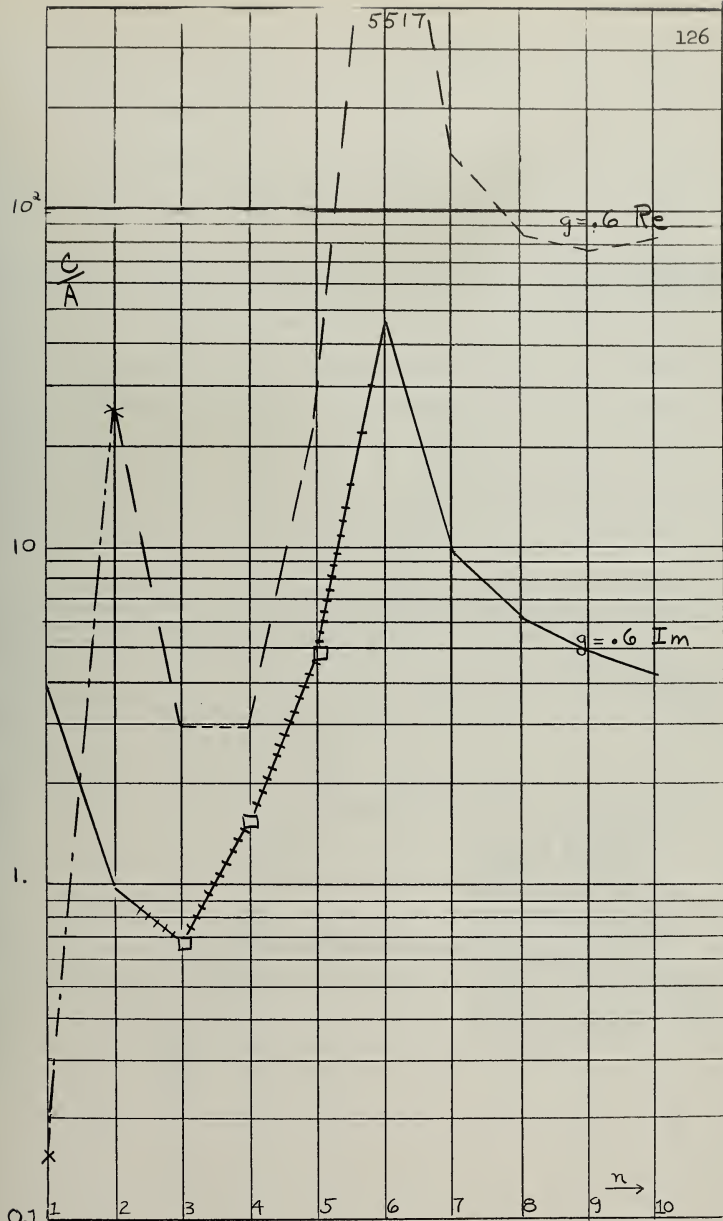
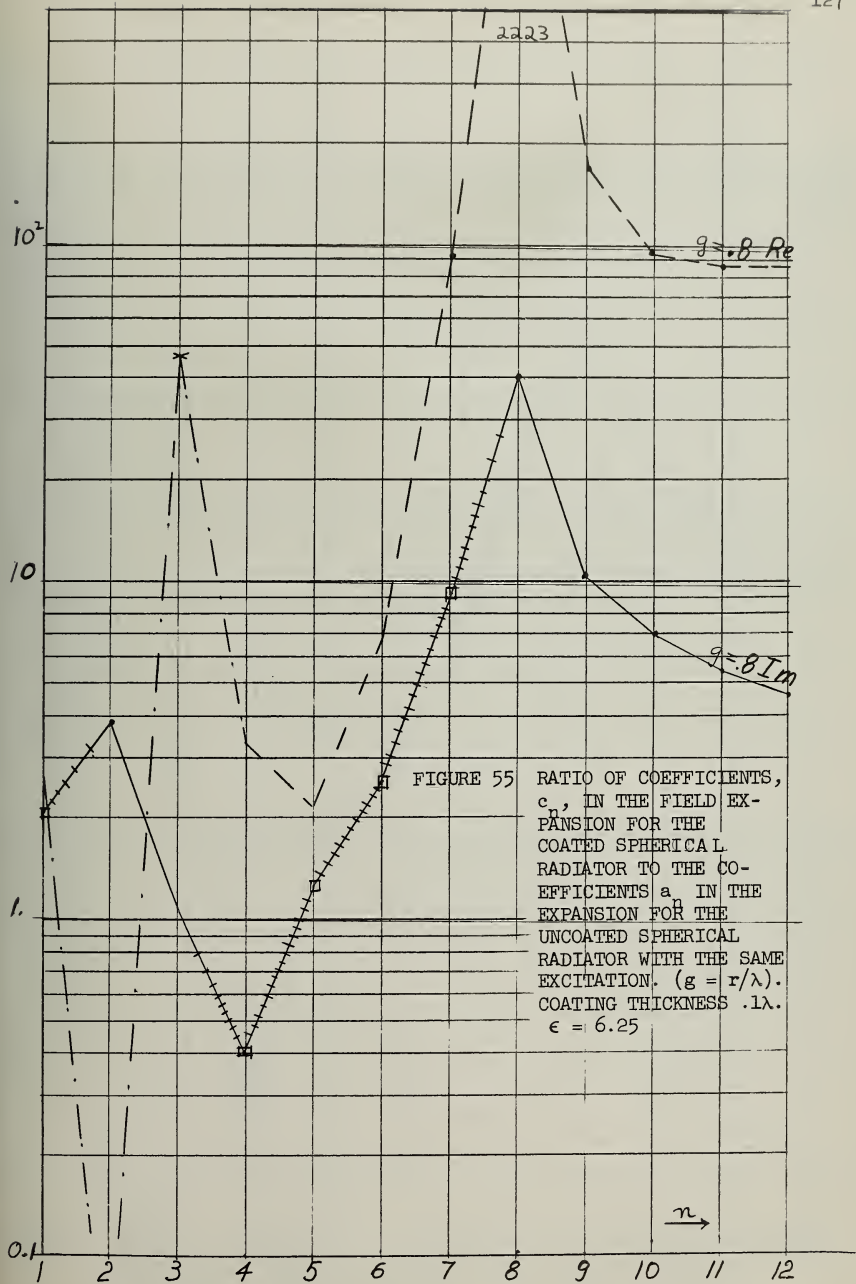


FIGURE 54 RATIO OF COEFFICIENTS,  $c_n$ , IN THE FIELD EXPANSION FOR THE COATED SPHERICAL RADIATOR TO THE COEFFICIENTS  $a_n$  IN THE EXPANSION FOR THE UNCOATED SPHERICAL RADIATOR WITH THE SAME EXCITATION.  
 $(g = r/\lambda)$ . COATING THICKNESS  $.1\lambda$ .  $\epsilon = 6.25$







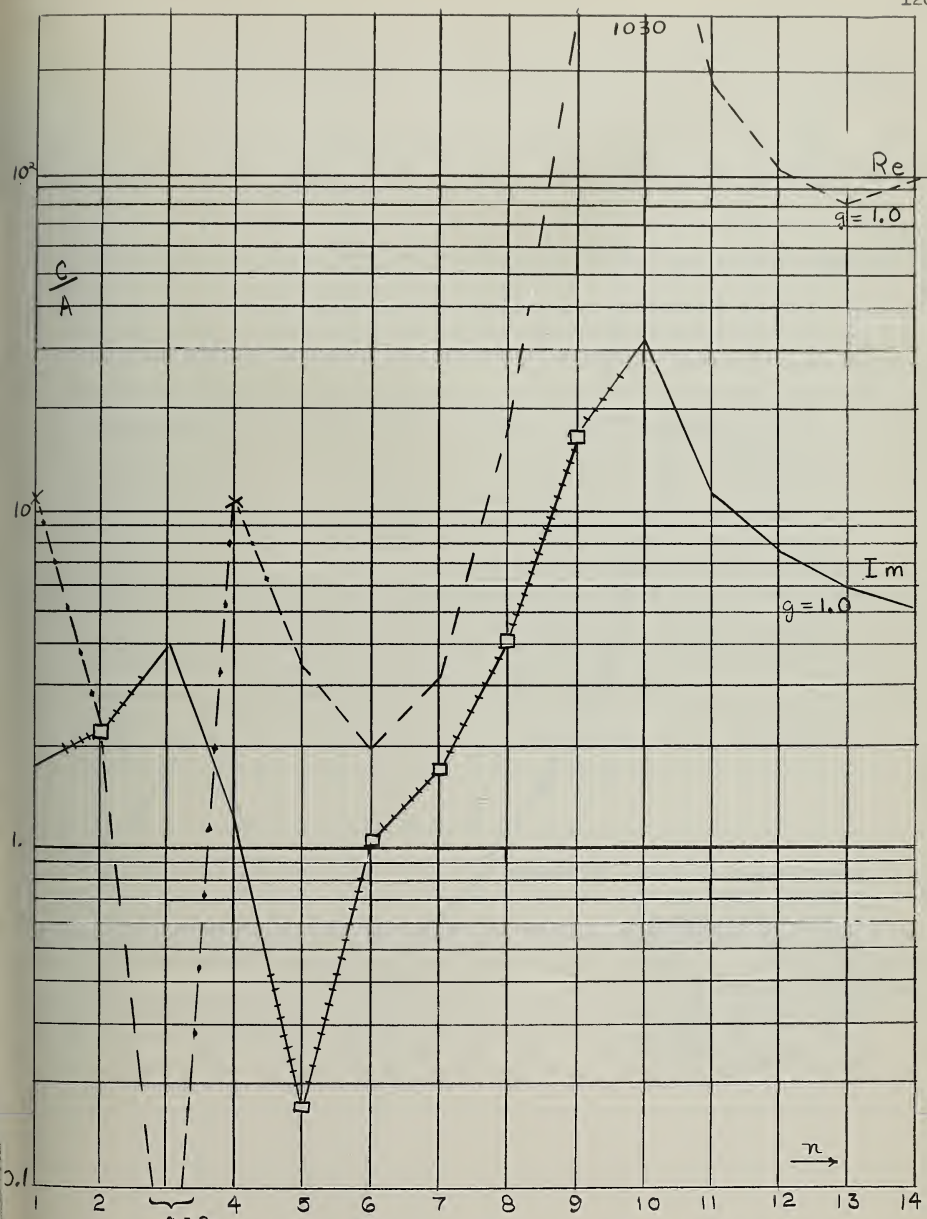


FIGURE 56 RATIO OF COEFFICIENTS,  $c_n$ , IN THE FIELD EXPANSION FOR THE COATED SPHERICAL RADIATOR TO THE COEFFICIENTS  $a_n$  IN THE EXPANSION FOR THE UNCOATED SPHERICAL RADIATOR WITH THE SAME EXCITATION.  
 $(g = r/\lambda)$ . COATING THICKNESS  $.1\lambda$ .  $\epsilon = 6.25$



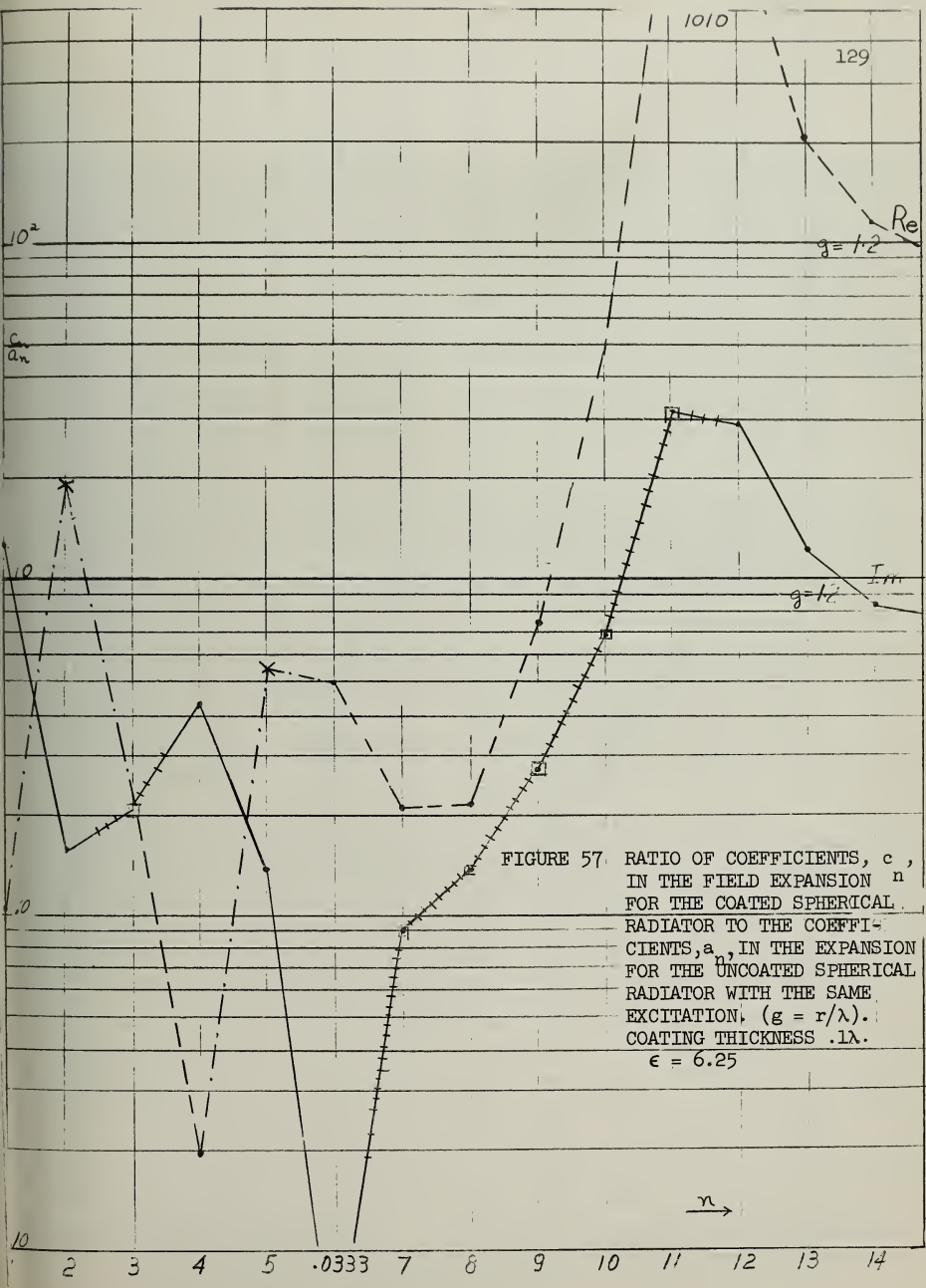


FIGURE 57 RATIO OF COEFFICIENTS,  $c_n$ ,  
 IN THE FIELD EXPANSION FOR THE COATED SPHERICAL  
 RADIATOR TO THE COEFFICIENTS,  $a_n$ , IN THE EXPANSION FOR THE UNCOATED SPHERICAL RADIATOR WITH THE SAME EXCITATION,  $(g = r/\lambda)$ . COATING THICKNESS  $.1\lambda$ .



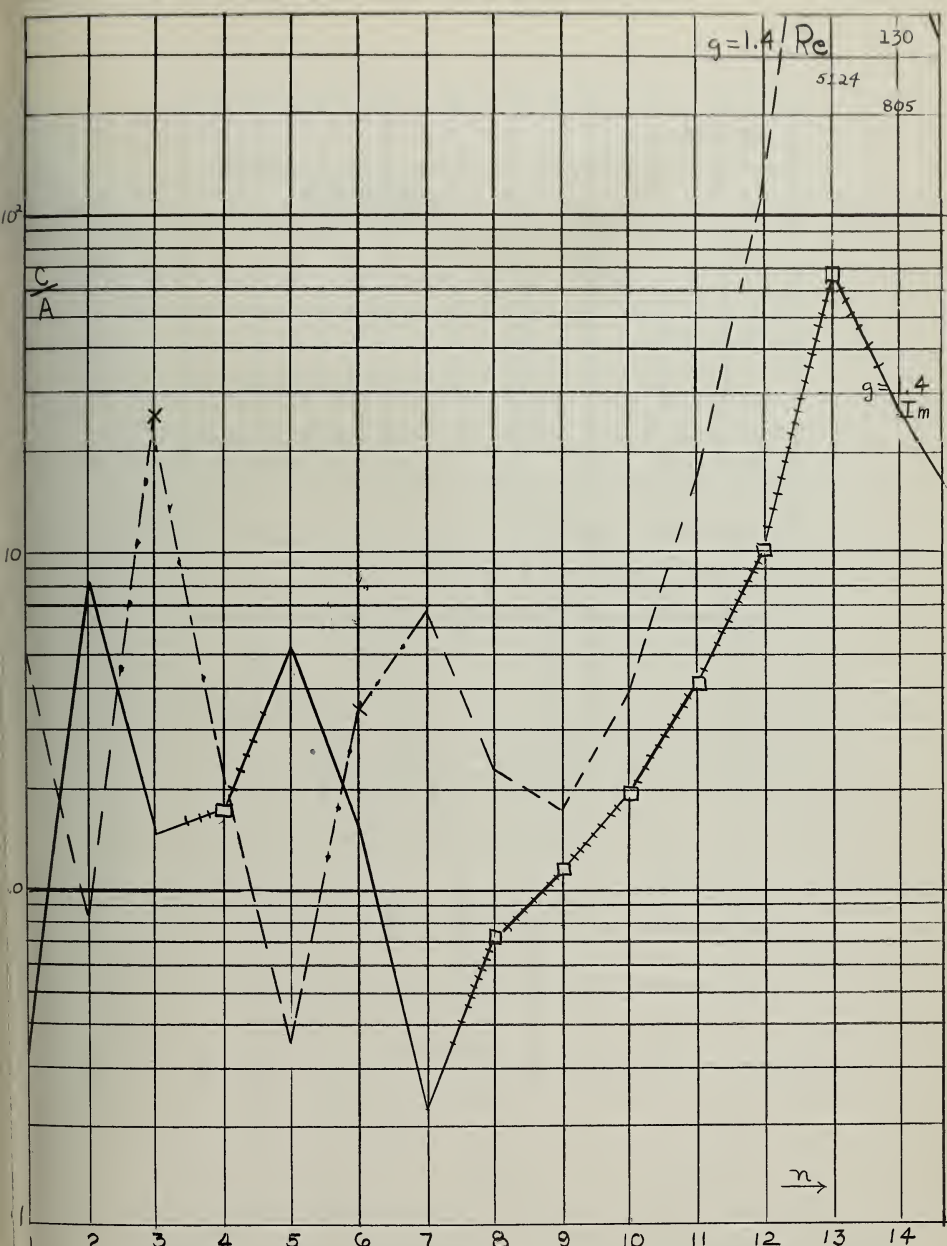


FIGURE 58 RATIO OF COEFFICIENTS,  $\frac{C}{A}$ , IN THE FIELD EXPANSION FOR THE COATED SPHERICAL RADIATOR TO THE COEFFICIENTS  $a_n$  IN THE EXPANSION FOR THE UNCOATED SPHERICAL RADIATOR WITH THE SAME EXCITATION. ( $g = r/\lambda$ ). COATING THICKNESS  $.1\lambda$ .  $\epsilon = 6.25$



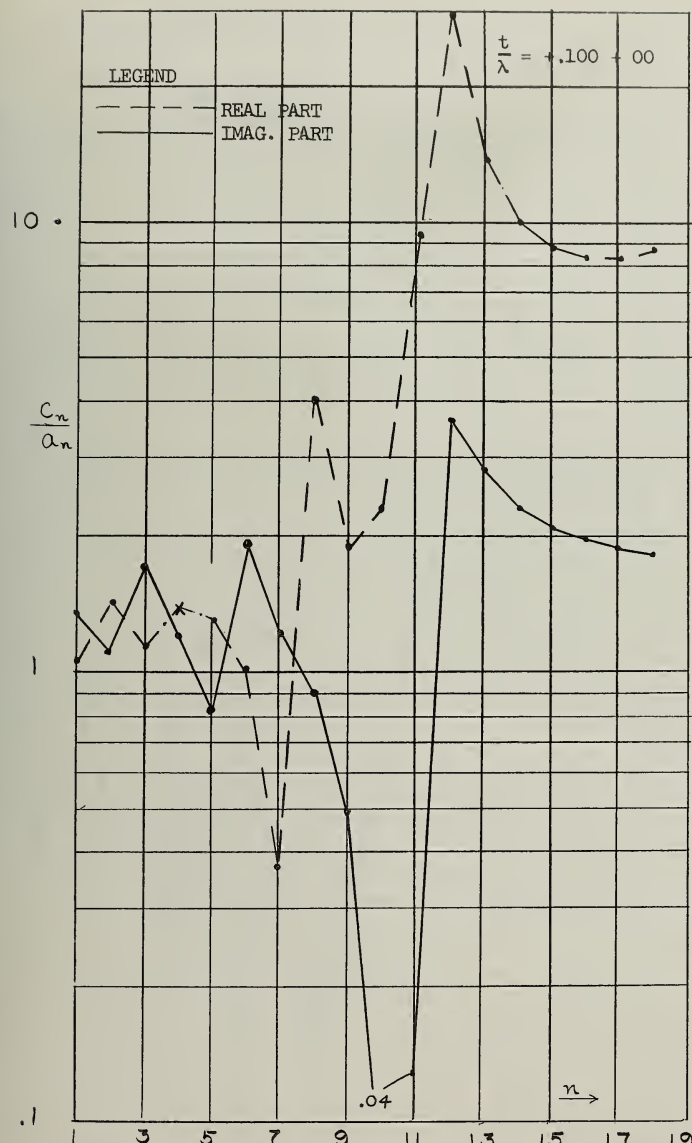


FIGURE 59 RATIO OF COEFFICIENTS,  $c_n$ , IN THE FIELD EXPANSION FOR THE COATED SPHERICAL RADIATOR TO THE COEFFICIENTS,  $a_n$ , IN THE EXPANSION FOR THE UNCOATED SPHERICAL RADIATOR WITH THE SAME EXCITATION.  $\epsilon = 2.25$ ,  $r = 1.6$ . THICKNESS  $t/\lambda$  VARIED IN SUCCESSIVE GRAPHS



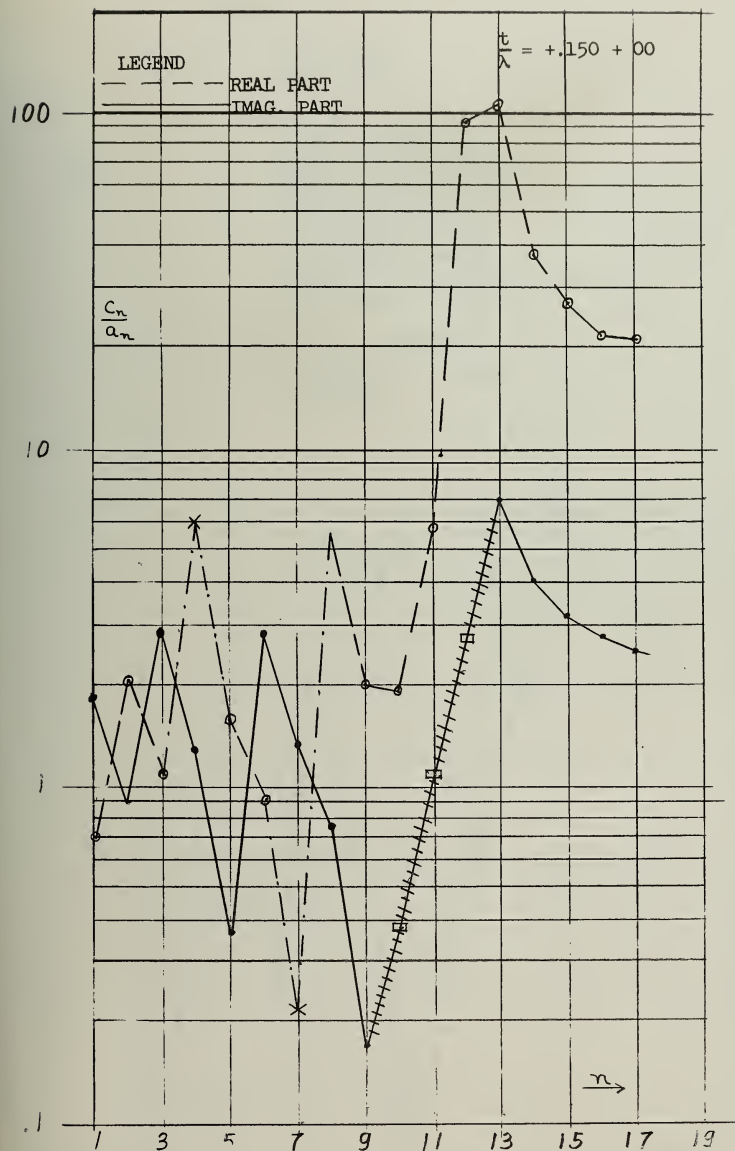


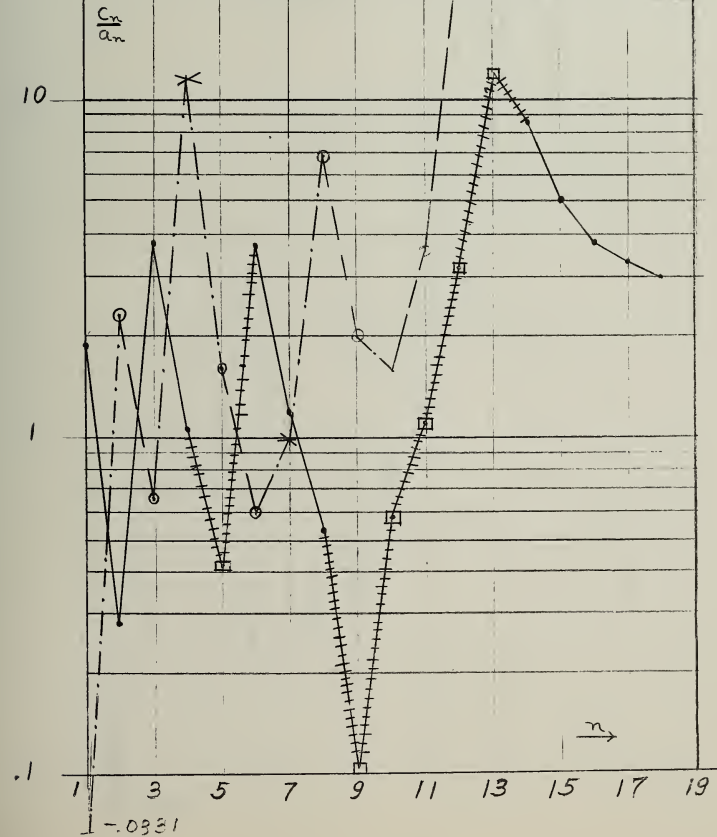
FIGURE 60 RATIO OF COEFFICIENTS,  $c_n$ , IN THE FIELD EXPANSION FOR THE COATED SPHERICAL RADIATOR TO THE COEFFICIENTS,  $a_n$ , IN THE EXPANSION FOR THE UNCOATED SPHERICAL RADIATOR WITH THE SAME EXCITATION.  
 $\epsilon = 2.25$ ,  $\frac{t}{\lambda} = 1.6$ . THICKNESS  $t/\lambda$  VARIED IN SUCCESSIVE GRAPHS



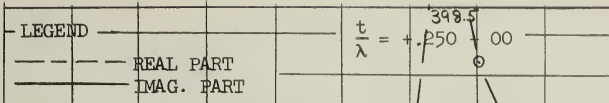
## LEGEND

REAL PART  
IMAG. PART

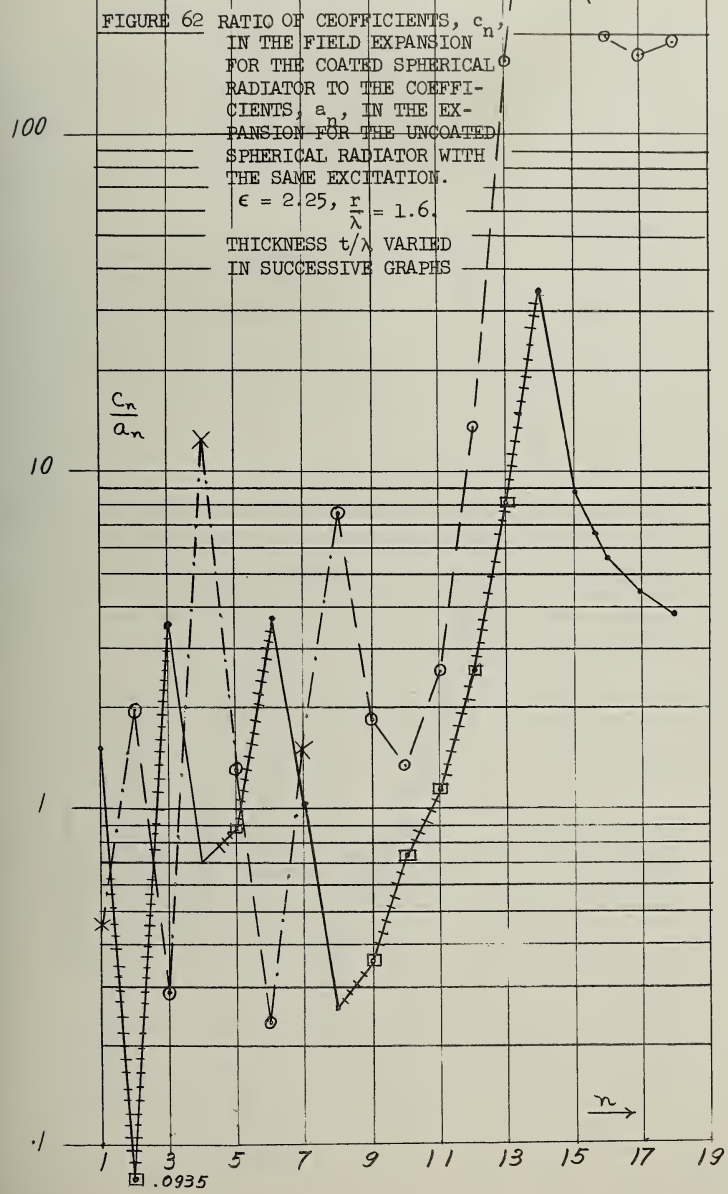
FIGURE 61 RATIO OF COEFFICIENTS,  
 $c_n$ , IN THE FIELD EXPANSION FOR THE COATED SPHERICAL RADIATOR TO THE COEFFICIENTS,  $a_n$ , IN THE EXPANSION FOR THE UNCOATED SPHERICAL RADIATOR WITH THE SAME EXCITATION.  $\epsilon = 2.25$ ,  $r/\lambda = 1.6$ . THICKNESS  $t/\lambda$  VARIED IN SUCCESSIVE GRAPHS







$$\frac{t}{\lambda} = +.250 \quad 00$$





LEGEND		$\frac{t}{\lambda} = .300 + .00$		
	REAL PART			
	IMAG. PART			

FIGURE 63 RATIO OF COEFFICIENTS,  $c_n$ , IN THE FIELD EXPANSION FOR THE COATED SPHERICAL RADIATOR TO THE COEFFICIENTS,  $a_n$ , IN THE EXPANSION FOR THE UNCOATED SPHERICAL RADIATOR WITH THE SAME EXCITATION.

$$\epsilon = 2.25, r = 1.6, \frac{t}{\lambda}$$

THICKNESS  $t/\lambda$  VARIED IN  
SUCCESSIVE GRAPHS

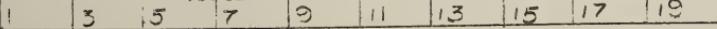
$$\frac{c_n}{a_n}$$

10

1

.0392

.0406

 $n \rightarrow$ 



## REFERENCES

1. Scharfman, H. J.A.P., 25, Nov. 1954.
2. Aden, A.L. and M. Kerker, J.A.P., p. 1242, Oct. 1951.
3. Elliot, R.S. IRE Trans. PGAP, Vol. AP-4, July 1956.
4. Stratton, J.A. Electromagnetic Theory, p. 50, McGraw-Hill Book Co. New York, 1941.
5. Ince, E.L. Ordinary Differential Equations, p. 223ff. Dover Publications, Inc., 1927 (reprint).
6. Churchill, R.V. Fourier Series and Boundary Value Problems, p. 46ff., McGraw-Hill Book Co., 1941.
7. Jahnke, E. and F. Emde, Table of Functions, p. 146, Dover Publications Inc., New York, 1945.
8. Schmid, H.L. Math. Nachr. 1, p. 377-398 (1948); 2, p. 35-44 (1949).
9. Wells, C.P. Mathematical Theory of Antenna Radiation, Final Report OOR Project 1013, Dept. of Mathematics, Michigan State University.
10. Stratton, J.A., P. Morse, L. Chu, J. Little, F. Corbato, Spheroidal Wave Functions, John Wiley and Sons, Inc. New York, 1956.
11. Marcuvitz, N. Waveguide Handbook, McGraw-Hill Book Co., New York, 1951.
12. Felsen, L. Spherical Transmission Line Theory, Report R-253-51 PIB 194, Microwave Research Institute, Polytechnic Institute of Brooklyn, Jan. 1952.

## SUPPLEMENTARY BIBLIOGRAPHY

## BOOKS

1. Flammer, C. Spheroidal Wave Functions, Stanford University Press, Stanford, California, 1957.



2. Morse, P., and H. Feshbach, Methods of Theoretical Physics, Vol. II, McGraw-Hill Book Company, 1953.
3. Schelkunoff, S.A., Advanced Antenna Theory, John Wiley and Sons, New York, 1952.

#### PERIODICALS

1. Page, L. and N. Adams, Phys. Rev. 53, p. 819-31, May 15, 1938.
2. Chu, L. and J.S. Stratton, J.A.P. 12, p. 241-48, March 1941.
3. Ryder, R., J.A.P. 13, 327-343, May 1942.
4. Page, L., Phys. Rev. 65, p. 98-117, Feb. 1944.
5. Bailin, L. and S. Silver, IRE Trans. PGAP Vol. AP-4, p. 5-16, Jan. 1956.
6. Myers, H., IRE Trans. PGAP Vol. AP-4 p. 58-64, Jan. 1956.
7. Andreasen, M. IRE Trans. PGAP Vol. AP-5, p. 267-270, July 1957.
8. Wells, C.P., IRE Trans. PGAP Vol. AP-6, p. 125-129, Jan. 1958.



## APPENDIX A

## Determination of the Eigenvalues of Unfamiliar Eigenfunctions

The purpose of this appendix is to outline a general method for the calculation of the eigenvalues which are associated with a second order differential equation with boundary conditions, in the event that the functions which satisfy the differential equations are unknown. This problem is different from the problem of eigenvalue determination as it is usually encountered in engineering problems in that the functions which represent the solutions are known only in the form of some kind of infinite series, and the dilemma is that the coefficients in the infinite series depend on the eigenvalues (which are as yet unknown).

The method discussed here is essentially a generalization of the method described in Section 2.2.3 for the calculation of the eigenvalues of the spheroidal functions. (It is assumed that the reader is familiar with the idea that orthogonal functions are generated by differential equations. This is discussed briefly by Churchill<sup>6</sup> and thoroughly by Ince<sup>5</sup>.) The method is probably well known to mathematicians, but it is not presented specifically in any of the books into which the engineer ordinarily looks for help in solving his problems.

A.1 Consider a general second order linear differential equation of the Sturm-Liouville type

$$p(x)y'' + q(x)y' + (r(x) + k_k s(x))y = 0 \quad (\text{A1})$$



with the boundary conditions

$$\begin{aligned} \alpha_1 y(a) + \beta_1 y'(a) &= 0 \\ \alpha_2 y(b) + \beta_2 y'(b) &= 0 \end{aligned} \quad (A2)$$

The problem is to find the eigenvalues,  $k_k$ , in the event that the functions  $y_k$  are unfamiliar. To find these, expand the functions  $y_k$  in a series of known functions which form a complete orthogonal set and satisfy the equation

$$p_1(x)\phi_n'' + q_1(x)\phi_n' + (r_1(x) + \lambda_n s_1(x))\phi_n = 0 \quad (A3)$$

and identical boundary conditions (A2). (That is, the eigenvalues of  $\phi_n$  are known or can be readily found.) Thus, assuming that term by term differentiation is possible, the series

$$y_k = \sum_{n=1}^{\infty} c_{kn} \phi_n \quad (A4)$$

is substituted into (A1) with the result

$$p(x) \sum_n c_{kn} \phi_n'' + q(x) \sum_n c_{kn} \phi_n' + (r(x) - k_k s(x)) \sum_n c_{kn} \phi_n = 0. \quad (A5)$$

To generate a system of linear equations having the form

$$\sum_n c_{kn} L_{nm} = 0$$

multiply through by  $\phi_m$  and integrate over the range. The result, after interchanging the order of summation and integration and grouping the coefficients of  $c_{kn}$ , is



$$\sum_n C_{kn} \left[ \int_a^b p(x) \phi_n'' \phi_m dx + \int_a^b q(x) \phi_n' \phi_m dx + \int_a^b r(x) \phi_n \phi_m dx + k_k \int_a^b s(x) \phi_n \phi_m dx \right] = 0 \quad (A6)$$

The quantity in brackets is an array of numbers which will be designated

$L_{nm}$ . The eigenvalues are those numbers which make the determinant of this array equal to zero, since this is the condition for consistency of the set of equations. As is shown in Section A.2, the values obtained from a finite size determinant will be good approximations since the representation has stationary properties.

The determination of the elements of  $L_{nm}$  can be simplified, and the rate of convergence improved, by the judicious choice of the functions  $\phi_n$ . To show this, multiply each member of the set of Eqs. A3 by the corresponding member of the set of constants,  $C_{kn}$ , and add these equations together to form

$$p_1(x) \sum_n C_{kn} \phi_n'' + q_1(x) \sum_n C_{kn} \phi_n' + (r_1(x) + \lambda_n s_1(x)) \sum_n C_{kn} \phi_n = 0 \quad (A7)$$

Now subtract this equation from (A5), multiply successively by the set of functions,  $\phi_m$ , and integrate over the range of orthogonality to obtain the result

$$\begin{aligned} & \sum_n C_{kn} \left[ \int_a^b (p(x) - p_1(x)) \phi_n'' \phi_m dx + \int_a^b (q(x) - q_1(x)) \phi_n' \phi_m dx \right. \\ & \left. + \int_a^b (r(x) - r_1(x)) \phi_n \phi_m dx - \lambda_n N_{nm} + k_k \int_a^b s(x) \phi_n \phi_m dx \right] = 0 \end{aligned} \quad (A8)$$

in which  $N_{nm}$  is the normalization integral of the functions,  $\phi$ , that is



$$N_{nm} = \delta_{nm} \int_a^b s(x) \phi_n \phi_m dx .$$

The elements of  $L_{nm}$  in the brackets of (A8) may be easier to evaluate than those of (A6). In particular, Eq. A8 displays formally the (intuitively obvious) conditions which make  $\phi_n$  a favorable set of functions, namely, they should satisfy a differential equation which is as nearly like the given equation as possible. The best possible condition is that all except one of the following hold:

$$p(x) = p_1(x), q(x) = q_1(x), r(x) = r_1(x), s(x) = s_1(x) .$$

Otherwise,  $\phi_n$  should be selected so as to make the integrations as simple as possible.

We note also from (A8) the condition for symmetry of the matrix

$$(L_{nm} = L_{mn}) :$$

$$\int_a^b (p-p_1) \phi_n'' \phi_m dx + \int_a^b (q-q_1) \phi_n' \phi_m dx = \int_a^b (p-p_1) \phi_m'' \phi_n dx + \int_a^b (q-q_1) \phi_m' \phi_n dx . \quad (A9)$$

Thus, if  $p=p_1$  and  $q=q_1$ , there is no question of the symmetry of the matrix,  $L_{nm}$ . An integration by parts permits (A9) to be replaced by the condition

$$\int_a^b \left[ \frac{d}{dx} (p-p_1) - (q-q_1) \right] \phi_m \phi_n' dx = \int_a^b \left[ \frac{d}{dx} (p-p_1) - (q-q_1) \right] \phi_n \phi_m' dx . \quad (A10)$$

This is a sufficient, but perhaps not a necessary condition.



There are a few more comments which can be made about (A6) and (A8). If the values of the elements so calculated were placed in an infinite determinant, and the condition  $|L_{nm}| = 0$  enforced, then exact eigenvalues would be obtained. But the vital question is whether finite determinants can be employed to obtain usefully accurate values. The use of such a finite determinant can be regarded as equivalent to the replacement of the infinite series (A4) by a finite sum of N terms as follows:

$$y_k \doteq \sum_{n=1}^N c_{kn} \phi_n .$$

The practical questions are: Can the eigenvalues,  $\lambda_k$ , be obtained to arbitrary accuracy with a finite  $N$ , and if so, how large must  $N$  be to obtain a specified accuracy? The answer, of course, is inseparably connected to the matter of how closely the functions  $y_k$  and  $\phi_k$  resemble each other. In any case, however, as is shown in Section A.2, (A6) and (A8) are results which have stationary properties (that is, they are the same results as obtained by the application of a variational procedure). Thus, the end result is insensitive to small differences in the quantities  $y_k$  and  $\sum_{n=1}^N c_{kn} \phi_n$ . Moreover, the assumption of uniform convergence is necessary in order to justify the term by term differentiation to arrive at (A5). Such uniform convergence means exactly that

$$|y_k - \sum_{n=1}^N c_{kn} \phi_n| < \epsilon$$



independent of  $x$ , for some finite  $N$ . This implies that  $c_{km} = 0$ ,  $M > N$ , so that the accuracy of the  $k$ -th eigenvalue can be determined to an accuracy set by the value of  $\epsilon$  selected. In practice, the error analysis is difficult, so that with a high speed computing machine available, the question is perhaps best answered by repeated trials in which the size of the matrix is varied. It is interesting that in the case of the spheroidal functions (Section 2.2.3), even the value  $N = 1$  gives a correction to the eigenvalue of the trial function  $P_1'$  (lowest eigenvalue).

The idea of replacing the infinite sum (A4) by a finite sum suggests one other technique which is useful in practice in the calculation of the higher order eigenvalues. For with the higher order functions, a good approximation may be as follows:

$$y_k \doteq \sum_{n=n_0}^N c_{kn} \phi_n,$$

that is, the lower order coefficients may also be approximately zero. This means that the accuracy of the higher order eigenvalues can be improved, with a given size matrix, by taking a section "out of the middle" of the infinite matrix (that is, dropping out some of the lower order coefficients as well as some of the higher order). (Of course, the coefficients for all orders of the functions satisfy the same set of (infinite) equations, so the solution of a single matrix gives an approximation for as many eigenvalues as coefficients included -- however, the accuracy of the individual eigenvalues so determined



depends primarily on how well the finite sum for each order approximates the function of that order.

A.2 It will now be shown that a variational method leads to Eq. A6 and hence to the same determinant as the one obtained earlier. Consider the differential equation in operational form

$$Ly + \lambda y = 0 .$$

Multiply this equation by a trial function,  $\psi$ , and integrate over the complete range:

$$\int \psi Ly dx + \lambda \int \psi y dx = 0 .$$

Now perform a first variation

$$\int \delta \psi Ly dx + \delta \lambda \int \psi y dx + \lambda \int \delta \psi y dx$$

and set  $\delta \lambda = 0$  to obtain the result

$$\int (Ly + \lambda y) \delta \psi dx = 0 .$$

In the present problem,  $Ly + \lambda y$  is of course just the right hand side of Eq. A1, which implies

$$\int_a^b \left\{ p(x)y'' + q(x)y' + (r(x) + k_k s(x)y) \right\} \delta \psi dx = 0$$

Now assume  $y = \sum_n c_n \phi_n$ , take  $\psi = \sum_m c_m \phi_m$  (so  $\delta \psi = \sum_m \delta c_m \phi_m$ )

and find

$$\int_a^b \left\{ p(x) \sum_n c_n \phi_n'' + q(x) \sum_n c_n \phi_n' + (r(x) + k_k s(x)) \sum_n c_n \phi_n \right\} x \sum_m \delta c_m \phi_m dx = 0$$



$$\text{or } \sum_m \delta c_m \left[ \int_a^b (p(x) \sum_n c_n \phi_n'' + q(x) \sum_n \phi_n' + (r(x) + k_k s(x)) \sum_n c_n \phi_n) \phi_m dx \right] = 0.$$

But the variations in  $c_n$ ,  $\delta c_n$ , must be arbitrary, so

$$\int_a^b (p(x) \sum_n c_n \phi_n'' + q(x) \sum_n c_n \phi_n' + (r(x) + k_k s(x)) \sum_n c_n \phi_n) \phi_m dx = 0$$

or

$$\sum_n c_n \int_a^b \left\{ p(x) \phi_n'' \phi_m + q(x) \phi_n' \phi_m + (r(x) + k_k s(x)) \phi_n \phi_m \right\} dx = 0,$$

which is the result stated in Eq. A6. Thus we have demonstrated that

(A6) has stationary properties.



## APPENDIX B

## Orthogonality Properties of the Vector Functions of Chapter 3

In the problem of the spherical antenna excited by an arbitrary slot configuration, it is convenient to represent the transverse electric field,  $\bar{E}_\tau$ , by means of an expansion in orthogonal functions. In order that this can be done, the following set of orthogonality relations is required:

$$\int_{r=r_1} \bar{e}'_{ie} \cdot \bar{e}'_{je} dS = \delta_{ij} \int \bar{e}'_{ie}^2 dS \quad (B1)$$

$$\int_{r=r_1} \bar{e}'_{io} \cdot \bar{e}'_{jo} dS = \delta_{ij} \int \bar{e}'_{io}^2 dS \quad (B2)$$

$$\int_{r=r_1} \bar{e}'_{ie} \cdot \bar{e}'_{jo} dS = 0 \quad (B3)$$

$$\int_{r=r_1} \bar{e}'_i \cdot \bar{e}''_j dS = 0 \quad (B4)$$

$$\int_{r=r_1} \bar{e}''_{ie} \cdot \bar{e}''_{je} dS = \delta_{ij} \int \bar{e}''_{ie}^2 dS \quad (B5)$$

$$\int_{r=r_1} \bar{e}''_{io} \cdot \bar{e}''_{jo} dS = \delta_{ij} \int \bar{e}''_{io}^2 dS \quad (B6)$$

$$\int_{r=r_1} \bar{e}''_{ie} \cdot \bar{e}''_{io} dS = 0 \quad (B7)$$



in which

$$\bar{e}'_{ie} = \nabla T_{ie},$$

$$\bar{e}''_{ie} = \nabla T_{ie} \times \hat{r}.$$

The relations (B3) and (B7), which involve products of the even and odd vector functions, follow almost immediately since the integrals will all involve the product of a sine function and a cosine function integrated over the range 0 to  $2\pi$ .

The relationship (B4) can be shown in general by employing the divergence theorem and some well known vector identities (listed for example in Stratton, p.604) as follows:

$$\int \nabla \cdot \bar{A} dS = \int \bar{A} \cdot \bar{n} dS$$

put  $\bar{A} = T_i (\hat{r} \times \nabla T_j)$  . Then

$$\nabla \cdot \bar{A} = \nabla T_i \cdot (\hat{r} \times \nabla T_j) \quad \text{and}$$

$$\int \bar{A} \cdot \bar{n} dS = \int T_i (\hat{r} \times \nabla T_j) \cdot \hat{r} dS = 0$$

Thus  $\int \nabla T_i \cdot (\hat{r} \times \nabla T_j) dS = \int \bar{e}'_i \cdot \bar{e}''_j dS = 0$  .

The relation (B1) can be demonstrated as follows: The terms of  $\nabla T_{ie}$  are  $\frac{\partial}{r} \frac{dP_n^m}{d\theta} \cos m\phi - \frac{\partial P_n^m}{r \sin \theta} \frac{1}{\sin \theta} \sin m\phi$ , so that the product of  $\nabla T_{ie} \cdot \nabla T_{je}$  is composed of such terms involving all possible combinations of  $m$  and  $n$ . It is clear therefore that unless the index  $m$  is the same in both  $\nabla T_{ie}$  and  $\nabla T_{je}$ , the  $\phi$ -integration will give zero. Thus the product will be of the form

$$\frac{1}{r^2} \frac{dP_n^m}{d\theta} \frac{dP_l^m}{d\theta} \frac{\cos^2 m\phi + \frac{m^2}{r^2 \sin^2 \theta}}{r^2 \sin^2 \theta} P_n^m P_l^m \sin^2 m\phi.$$



After the  $\phi$  -integration, the results are integrals of the type

$$\int_0^\pi \left( \frac{dP_n^m}{d\theta} \frac{dP_\ell^m}{d\theta} + \frac{m^2}{\sin\theta} P_n^m P_\ell^m \right) \sin\theta d\theta .$$

This integral is zero unless  $n = \ell$ , and constant otherwise  
(Stratton, p. 417).

The demonstration of (B2) is completely analogous. Furthermore, the results (B5) and (B6) follow from the same type of argument since the operation  $\hat{r} \times \nabla T_i e_o$  (which is the operation required to transform  $\hat{e}'_{i\sigma}$  into  $\hat{e}''_{j\sigma}$ ) merely interchanges the  $\theta$  - and  $\phi$  -components.



ERRATA

- | Page    |   |
|---------|---|
| iv      | In title of Fig. 22, 23, replace $\epsilon_r = \sqrt{\frac{8}{3}}$ by $\epsilon_r = \sqrt{\frac{8}{5}}$   |
| iv      | In title of Fig. 28, replace $\frac{1}{\hat{H}'_n(\beta_r)^2}$ by $\frac{1}{ \hat{H}'_n(\beta_r) ^2}$   |
| iv-viii | Add one to the page number for Fig. 29 and beyond. Page 100 is a note explaining the symbols in Fig. 29 and those beyond.   |
| 16      | Line 8 insert (Columbia University Press 1947) after <u>Tables of Spherical Bessel Functions.</u>   |
| 18      | Next to last line; replace (33) by (23).  |
| 23      | All quantities $Z_n$ should read $\hat{Z}_n$ .  |
| 24      | Last line; replace "the lower order ratio" by "the next lower order ratio".   |
| 26      | Subscript n left off $\hat{N}'_n$ in two equations.   |
| 41      | Line 21; replace appreicably by appreciably.<br>Line 22; replace magnitude by magnitudes.   |
| 47      | Line 17; replace $\sum_n d_{kn}^2 \frac{2n(n+1)}{2n+1}$ by $\left[ \sum_n d_{kn}^2 \frac{2n(n+1)}{2n+1} \right]^{1/2}$  |
| 48      | Center block; replace $\sum_{n=1}^{10} d_{kn} p'_n$ by $\sum_{n=1}^{10} d_{kn} p_n^1$<br>Third box from top, on right, replace $\sum_n d_{kn}^2 \frac{2n(n+1)}{2n+1}$ by  |
| 60      | Line 3; replace (62) by (63).   |
| 69      | Equation 89 replace $d_{nm} \hat{e}$ by $d'_{nm} \hat{e}$ .   |
| 93, 94  | First line after equation 89. Insert $\hat{e}_1$ at the end of the line.<br>Fig. 22, 23. Replace $\epsilon_r = \sqrt{\frac{8}{3}}$ by $\epsilon_r = \sqrt{\frac{8}{5}}$ . |
| 112-130 | Ordinate of Figures 40-58 should all be lower case, $\left( \frac{c_n}{a_n} \right)$  |



ERRATA (continued)

143 Line 9. Replace  $P_1'$  by  $P_1^1$ .

144 Next to last line; replace  $\delta = \sum_m \delta C_m \phi_m$  by  $\delta\psi = \sum_m \delta C_m \phi_m$ .

145 First equation; replace  $q(x) \sum \phi'$  by  $q(x) \sum_n C_n \phi'_n$ .



ANTENNA LABORATORY  
TECHNICAL REPORTS AND MEMORANDA ISSUED

Contract AF33(616)-310

"Synthesis of Aperture Antennas," Technical Report No. 1, C.T.A. Johnk, October, 1954.

"A Synthesis Method for Broad-band Antenna Impedance Matching Networks," Technical Report No. 2, Nicholas Yaru, 1 February 1955.

"The Asymmetrically Excited Spherical Antenna," Technical Report No. 3, Robert C. Hansen, 30 April 1955.

"Analysis of an Airborne Homing System," Technical Report No. 4, Paul E. Mayes, 1 June 1955, (CONFIDENTIAL).

"Coupling of Antenna Elements to a Circular Surface Waveguide," Technical Report No. 5, H.E. King and R.H. DuHamel, 30 June 1955.

"Input Impedance of a Spherical Ferrite Antenna with a Latitudinal Current," Technical Report No. 6, W.L. Weeks, 20 August 1955.

"Axially Excited Surface Wave Antennas," Technical Report No. 7, D.E. Royal, 10 October 1955.

"Homing Antennas for the F-86F Aircraft (450-2500 mc)," Technical Report No. 8, P.E. Mayes, R.F. Hyneman, and R.C. Becker, 20 February 1957. (CONFIDENTIAL)

"Ground Screen Pattern Range," Technical Memorandum No. 1, Roger R. Trapp, 10 July 1955.

Contract AF33(616)-3220

"Effective Permeability of Spheroidal Shells," Technical Report No. 9, E.J. Scott and R.H. Duhamel, 16 April 1956.

"An Analytical Study of Spaced Loop ADF Antenna Systems," Technical Report No. 10, D.G. Berry and J.B. Kreer, 10 May 1956.

"A Technique for Controlling the Radiation from Dielectric Rod Waveguides," Technical Report No. 11, J.W. Duncan and R.H. DuHamel, 15 July 1956.

"Directional Characteristics of a U-Shaped Slot Antenna," Technical Report No. 12, Richard C. Becker, 30 September 1956.

"Impedance of Ferrite Loop Antennas," Technical Report No. 13, V.H. Rumsey and W.L. Weeks, 15 October 1956.



"Closely Spaced Transverse Slots in Rectangular Waveguide," Technical Report No. 14, Richard F. Hyneman, 20 December 1956.

"Distributed Coupling to Surface Wave Antennas," Technical Report No. 15, Ralph Richard Hodges, Jr., 5 January 1957.

"The Characteristic Impedance of the Fin Antenna of Infinite Length," Technical Report No. 16, Robert L. Carrel, 15 January 1957.

"On the Estimation of Ferrite Loop Antenna Impedance," Technical Report No. 17, Walter L. Weeks, 10 April 1957.

"A Note Concerning a Mechanical Scanning System for a Flush Mounted Line Source Antenna," Technical Report No. 18, Walter L. Weeks, 20 April 1957.

"Broadband Logarithmically Periodic Antenna Structures," Technical Report No. 19, R.H. DuHamel and D.E. Isbell, 1 May 1957.

"Frequency Independent Antennas," Technical Report No. 20, V.H. Rumsey, 25 October 1957.

"The Equiangular Spiral Antenna," Technical Report No. 21, J.D. Dyson, 15 September 1957.

"Experimental Investigation of the Conical Spiral Antenna," Technical Report No. 22, R.L. Carrel, 25 May 1957.

"Coupling Between a Parallel Plate Waveguide and a Surface Waveguide," Technical Report No. 23, E.J. Scott, 10 August 1957.

"Launching Efficiency of Wires and Slots for a Dielectric Rod Waveguide," Technical Report No. 24, J.W. Duncan and R.H. DuHamel, August 1957.

"The Characteristic Impedance of an Infinite Biconical Antenna of Arbitrary Cross Section," Technical Report No. 25, Robert L. Carrel, August 1957.

"Cavity-Backed Slot Antennas," Technical Report No. 26, R.J. Tector, 30 October 1957.

"Coupled Waveguide Excitation of Traveling Wave Slot Antennas," Technical Report No. 27, W.L. Weeks, 1 December 1957.

"Phase Velocities in Rectangular Waveguide Partially Filled with Dielectric," Technical Report No. 28, W.L. Weeks, 20 December 1957.

"Measuring the Capacitance per Unit Length of Biconical Structures of Arbitrary Cross Section," Technical Report No. 29, J.D. Dyson, 10 January 1958.



"Non-Planar Logarithmically Periodic Antenna Structure," Technical Report No. 30, D.W. Isbell, 20 February 1958.

"Electromagnetic Fields in Rectangular Slots," Technical Report No. 31, N.J. Kuhn and P.E. Mast, 10 March 1958.

"The Efficiency of Excitation of a Surface Wave on a Dielectric Cylinder," Technical Report No. 32, J.W. Duncan, 25 May 1958.

"A Unidirectional Equiangular Spiral Antenna," Technical Report No. 33, J.D. Dyson, 10 July 1958.

"Dielectric Coated Spheroidal Radiators," Technical Report No. 34, W.L. Weeks, 12 September 1958.

"A Theoretical Study of the Equiangular Spiral Antenna," Technical Report No. 35, P.E. Mast, 12 September 1958.



DISTRIBUTION LIST

One copy each unless otherwise indicated

Armed Services Technical Information  
Agency  
Arlington Hall Station  
Arlington 12, Virginia 3 & 1 repro

Commander  
Wright Air Development Center  
Wright-Patterson Air Force Base, Ohio  
Attn: WCLRS-6, Mr. W.J. Portune 3 copies

Commander  
Wright Air Development Center  
Wright-Patterson Air Force Base, Ohio  
Attn: WCLNQ-4, Mr. N. Draganjac

Commander  
Wright Air Development Center  
Wright-Patterson Air Force Base, Ohio  
Attn: WCOSI, Library

Director  
Evans Signal Laboratory  
Belmar, New Jersey  
Attn: Technical Document Center

Commander  
U.S. Naval Air Test Center  
Attn: ET-315  
Antenna Section  
Patuxent River, Maryland

Chief  
Bureau of Ordnance  
Department of the Navy  
Attn: Mr. C.H. Jackson, Code Re 9a  
Washington 25, D.C.

Commander  
Hq. A.F. Cambridge Research Center  
Air Research and Development Command  
Laurence G. Hanscom Field  
Bedford, Massachusetts  
Attn: CRRD, R.E. Hiatt

Commander  
Air Force Missile Test Center  
Patrick Air Force Base, Florida  
Attn: Technical Library

Director  
Ballistics Research Lab.  
Aberdeen Proving Ground, Maryland  
Attn: Ballistics Measurement Lab.  
  
Office of the Chief Signal Officer  
Attn: SIGNET-5  
Eng. & Technical Division  
Washington 25, D.C.

Commander  
Rome Air Development Center  
ATTN: RCERA-1 D. Mather  
Griffiss Air Force Base  
Rome, N.Y.

Airborne Instruments Lab., Inc.  
Attn: Dr. E.G. Fubini  
Antenna Section  
160 Old Country Road  
Mineola, New York  
M/F Contract AF33(616)-2143

Andrew Alford Consulting Engrs.  
Attn: Dr. A. Alford  
299 Atlantic Ave.  
Boston 10, Massachusetts  
M/F Contract AF33(038)-23700

Bell Aircraft Corporation  
Attn: Mr. J.D. Shantz  
Buffalo 5, New York  
M/F Contract W-33(038)-14169

Chief  
Bureau of Ships  
Department of the Navy  
Attn: Code 838D, L.E. Shoemaker  
Washington 25, D.C.



DISTRIBUTION LIST (CONT.)

One copy each unless otherwise indicated

Director  
Naval Research Laboratory  
Attn: Dr. J.I. Bohnert  
Anacostia  
Washington 25, D.C.

National Bureau of Standards  
Department of Commerce  
Attn: Dr. A.G. McNish  
Washington 25, D.C.

Director  
U.S. Navy Electronics Lab.  
Point Loma  
San Diego 52, California

Commander  
USA White Sands Signal Agency  
White Sands Proving Command  
Attn: SIGWS-FC-02  
White Sands, N.M.

Consolidated Vultee Aircraft Corp.  
Fort Worth Division  
Attn: C.R. Curnutt  
Fort Worth, Texas  
M/F Contract AF33(038)-21117

Dorne & Margolin  
29 New York Ave.  
Westbury  
Long Island, New York  
M/F Contract AF33(616)-2037

Douglas Aircraft Company, Inc.  
Long Beach Plant  
Attn: J.C. Buckwalter  
Long Beach 1, California  
M/F Contract AF33(600)-25669

Boeing Airplane Company  
Attn: F. Bushman  
7755 Marginal Way  
Seattle, Washington  
M/F Contract AF33(038)-31096

Chance-Vought Aircraft Division  
United Aircraft Corporation  
Attn: Mr. F.N. Kickerman  
Thru: BuAer Representative  
Dallas, Texas

Consolidated-Vultee Aircraft Corp  
Attn: Mr. R.E. Honer  
P.O. Box 1950  
San Diego 12, California  
M/F Contract AF33(600)-26530

Grumman Aircraft Engineering Corp  
Attn: J.S. Erickson  
Asst, Chief, Avionics Dept.  
Bethpage  
Long Island, New York  
M/F Contract NOa(s) 51-118

Hallicrafters Corporation  
Attn: Norman Foot  
440 W. 5th Avenue  
Chicago, Illinois  
M/F Contract AF33(600)-26117

Hoffman Laboratories Division  
Attn: J.D. Funderburg,  
Counter Measures Section  
Los Angeles, California  
M/F Contract AF33(604)-17231

Hughes Aircraft Corporation  
Division of Hughes Tool Company  
Attn: D. Adcock  
Florence Avenue at Teale  
Culver City, California  
M/F Contract AF33(600)-27615

Illinois, University of  
Head, Department of Elec. Eng.  
Attn: Dr. E.C. Jordan  
Urbana, Illinois



DISTRIBUTION LIST (CONT.)

One copy each unless otherwise indicated

Ohio State Univ. Research Foundation  
Attn: Dr. T.C. Tice  
310 Administration Bldg.  
Ohio State University  
Columbus 10, Ohio  
M/F Contract AF33(616)-3353

Air Force Development Field  
Representative  
Attn: Capt. Carl B. Ausfahl  
Code 1010

Naval Research Laboratory  
Washington 25, D.C.

Chief of Naval Research  
Department of the Navy  
Attn: Mr. Harry Harrison  
Code 427, Room 2604  
Bldg. T-3  
Washington 25, D.C.

Beech Aircraft Corporation  
Attn: Chief Engineer  
6600 E. Central Avenue  
Wichita 1, Kansas  
M/F Contract AF33(600)-20910

Land-Air, Incorporated  
Cheyenne Division  
Attn: Mr. R.J. Klessig  
Chief Engineer  
Cheyenne, Wyoming  
M/F Contract AF33(600)-22964

Director, National Security Agency  
RADE 1GM, Attn: Lt. Manning  
Washington 25, D.C.

Melpar, Incorporated  
3000 Arlington Blvd.  
Falls Church, Virginia  
Attn: K.S. Kelleher

Naval Air Missile Test Center  
Point Mugu, California  
Attn: Antenna Section

Fairchild Engine & Airplane Corp  
Fairchild Airplane Division  
Attn: L. Fahnestock  
Hagerstown, Maryland  
M/F Contract AF33(038)-18499

Federal Telecommunications Lab.  
Attn: Mr. A. Kandoian  
500 Washington Avenue  
Nutley 10, New Jersey  
M/F Contract AF33(616)-3071

Ryan Aeronautical Company  
Lindbergh Drive  
San Diego 12, California  
M/F Contract W-33(038)-ac-21370

Republic Aviation Corporation  
Attn: Mr. Thatcher  
Hicksville, Long Island, New York  
M/F Contract AF18(600)-1602

General Electric Co.  
French Road  
Utica, New York  
Attn: Mr. Grimm, LMEED  
M/F Contract AF33(600)-30632

D.E. Royal  
The Ramo-Wooldridge Corp  
Communications Division  
P.O. Box 45444  
Airport Station  
Los Angeles 45, California

Motorola, Inc.  
Defense Systems Lab.  
Attn: Mr. A.W. Boekelheide  
3102 N. 56th Street  
Phoenix, Arizona  
M/F Contract NOa(s)-53-492-c

Stanford Research Institute  
Southern California Laboratories  
Attn: Document Librarian  
820 Mission Street  
South Pasadena, California  
Contract AF19(604)-1296



DISTRIBUTION LIST (CONT.)

One copy each unless otherwise indicated

Johns Hopkins University  
Radiation Laboratory  
Attn: Librarian  
1315 St. Paul Street  
Baltimore 2, Maryland  
M/F Contract AF33(616)-68

Glen L. Martin Company  
Baltimore 3, Maryland  
M/F Contract AF33(600)-21703

McDonnell Aircraft Corporation  
Attn: Engineering Library  
Lambert Municipal Airport  
St. Louis 21, Missouri  
M/F Contract AF33(600)-8743

Michigan, University of  
Aeronautical Research Center  
Attn: Dr. L. Cutrona  
Willow Run Airport  
Ypsilanti, Michigan  
M/F Contract AF33(038)-21573

Massachusetts Institute of Tech.  
Attn: Prof. H.J. Zimmerman  
Research Lab. of Electronics  
Cambridge, Massachusetts  
M/F Contract AF33(616)-2107

North American Aviation, Inc.  
Los Angeles International Airport  
Attn: Mr. Dave Mason  
Engineering Data Section  
Los Angeles 45, California  
M/F Contract AF33(038)-18319

Northrop Aircraft, Incorporated  
Attn: Northrop Library  
Dept. 2135  
Hawthorne, California  
M/F Contract AF33(600)-22313

Radioplane Company  
Van Nuys, California  
M/F Contract AF33(600)-23893

Lockheed Aircraft Corporation  
Attn: C.L. Johnson  
P.O. Box 55  
Burbank, California  
M/F NOa(s)-52-763

Raytheon Manufacturing Company  
Attn: Robert Borts  
Wayland Laboratory, Wayland, Mass.

Republic Aviation Corporation  
Attn: Engineering Library  
Farmingdale  
Long Island, New York  
M/F Contract AF33(038)-14810

Sperry Gyroscope Company  
Attn: Mr. B. Berkowitz  
Great Neck  
Long Island, New York  
M/F Contract AF33(038)-14524

Temco Aircraft Corp  
Attn: Mr. George Cramer  
Garland, Texas  
Contract AF33(600)-21714

Farnsworth Electronics Co.  
Attn: George Giffin  
Ft. Wayne, Indiana  
M/F Contract AF33(600)-25523

North American Aviation, Inc.  
4300 E. Fifth Ave.  
Columbus, Ohio  
Attn: Mr. James D. Leonard  
Contract NOa(s)-54-323

Westinghouse Electric Corporation  
Air Arm Division  
Attn: Mr. P.D. Newhouser  
Development Engineering  
Friendship Airport, Maryland  
Contract AF33(600)-27852



DISTRIBUTION LIST (CONT.)

One copy each unless otherwise indicated

Prof. J. R. Whinnery  
Dept. of Electrical Engineering  
University of California  
Berkeley, California

Professor Morris Kline  
Mathematics Research Group  
New York University  
45 Astor Place  
New York, N.Y.

Prof. A.A. Oliner  
Microwave Research Institute  
Polytechnic Institute of Brooklyn  
55 Johnson Street - Third Floor  
Brooklyn, New York

Dr. C.H. Papas  
Dept. of Electrical Engineering  
California Institute of Technology  
Pasadena, California

Electronics Research Laboratory  
Stanford University  
Stanford, California  
Attn: Dr. F.E. Terman

Radio Corporation of America  
R.C.A. Laboratories Division  
Princeton, New Jersey

Electrical Engineering Res. Lab.  
University of Texas  
Box 8026, University Station  
Austin, Texas

Dr. Robert Hansen  
8356 Chase Avenue  
Los Angeles 45, California

Technical Library  
Bell Telephone Laboratories  
463 West St.  
New York 14, N.Y.

Dr. R.E. Beam  
Microwave Laboratory  
Northwestern University  
Evanston, Illinois

Department of Electrical Engineering  
Cornell University  
Ithaca, New York  
Attn: Dr. H.G. Booker

Applied Physics Laboratory  
Johns Hopkins University  
8621 Georgia Avenue  
Silver Spring, Maryland

Exchange and Gift Division  
The Library of Congress  
Washington 25, D.C.

Ennis Kuhlman  
c/o McDonnell Aircraft  
P.O. Box 516  
Lambert Municipal Airport  
St. Louis 21, Mo.

Mr. Roger Battie  
Supervisor, Technical Liaison  
Sylvania Electric Products, Inc.  
Electronic Systems Division  
P.O. Box 188  
Mountain View, California

Physical Science Lab.  
New Mexico College of A and MA  
State College, New Mexico  
Attn: R. Dressel

Technical Reports Collection  
303 A Pierce Hall  
Harvard University  
Cambridge 38, Mass.  
Attn: Mrs. E.L. Hufschmidt, Librarian

Dr. R.H. DuHamel  
Collins Radio Company  
Cedar Rapids, Iowa



DISTRIBUTION LIST (CONT.)

One copy each unless otherwise indicated

Dr. R.F. Hyneman  
5116 Marburn Avenue  
Los Angeles 45, California

Chief  
Bureau of Aeronautics  
Department of the Navy  
Attn: Aer-EL-931

Director  
Air University Library  
Attn: AUL-8489  
Maxwell AFB, Alabama

Stanford Research Institute  
Documents Center  
Menlo Park, California  
Attn: Mary Lou Fields, Acquisitions

Dr. Harry Letaw, Jr.  
Research Division  
Raytheon Manufacturing Co.  
Waltham 54, Massachusetts

Canoga Corporation  
5955 Sepulveda Blvd.  
P.O. Box 550  
Van Nuys, California  
M/F Contract AF08(603)-4327

Radiation, Inc.  
Technical Library Section  
Attn: Antenna Department  
Melbourne, Florida  
M/F Contract AF33(600)-36705

Westinghouse Electric Corporation  
Attn: Electronics Division  
Friendship International Airport  
Box 746  
Baltimore 3, Maryland  
M/F Contract AF33(600)-27852

North American Aviation, Inc.  
Aerophysics Laboratory  
Attn: Dr. J.A. Marsh  
12214 Lakewood Blvd  
Downey, California  
M/F Contract AF33(038)-18319













